Hydrolytic and transglycosylation activities of *Serratia proteamaculans* 568 on chitinous substrates

Thesis submitted for the degree of
DOCTOR OF PHILOSOPHY

by

P. Purushotham
(Regd. No. 08LPPH26)

Department of Plant Sciences
School of Life Sciences
University of Hyderabad
Hyderabad – 500 046
INDIA

October 2011

University of Hyderabad
(A Central University established in 1974 by an act of parliament)
HYDERABAD – 500 046, INDIA

–

CERTIFICATE

This is to certify that Mr. P. PURUSHOTHAM has carried out the research work embodied in the present thesis under the supervision and guidance of Prof. Appa Rao Podile for a full period prescribed under the Ph.D. ordinances of this University. We recommend his thesis **"Hydrolytic and transglycosylation activities of *Serratia proteamaculans* 568 on chitinous substrates"** for submission for the degree of Doctor of Philosophy of the University.

Prof. Appa Rao Podile
(Research Supervisor)

Head,
Department of Plant Sciences.

Dean,
School of Life Sciences.

University of Hyderabad
(A Central University established in 1974 by an act of parliament)
HYDERABAD – 500 046, INDIA

DECLARATION

This is to declare that the work embodied in this thesis entitled **"Hydrolytic and transglycosylation activities of *Serratia proteamaculans* 568 on chitinous substrates"** has been carried out by me under the supervision of Prof. Appa Rao Podile. This has not been submitted for any degree or diploma in any other University earlier.

P. Purushotham

Prof. Appa Rao Podile
(Research Supervisor)

ACKNOWLEDGEMENTS

I am immensely grateful to all those individuals who have helped me in making this endeavor possible.

At the outset, I would like to take this opportunity to extend my gratitude to my supervisor Prof. Appa Rao Podile for his unrelenting encouragement and constant support, without whom this endeavor would not have been possible, not to mention his meticulous supervision throughout my doctoral research.

I thank the former Dean, Prof. A.S. Raghavendra, and present Dean, Prof. M. Ramanadham, School of Life Sciences and former Head, Prof. Appa Rao Podile, and the present Head, Prof. A.R. Reddy, Dept. of Plant Sciences, for their support in all possible ways.

My heartful thanks to Dr. Daniel van der Lelie, Brookhaven National Laboratory, USA for providing the Serratia proteamaculan 568 strain. My special thanks to Dr. Dominique Gillete, Mahatani Chitosan Pvt Ltd, Veraval, Gujarat, for chitinous substrates.

I thank my doctoral committee members Prof. Ch. Venkata Ramana and Dr. K.P.M.S.V. Padmasree for their suggestions during my work.

My thanks to Prof. Venkata Ramana's students for the help in carrying out HPLC studies. I specially thank Dr. J.S.S. Prakash and Mr. Sai Arun for helping in molecular modeling and analysis of upstream sequences of S. proteamaculans chitinolytic genes. I acknowledge the help and support from Dr. S. Rajagopal and M. Chandramouli for their help in molecular modeling. I thank Dr. K. Gopinath for allowing me to use his lab facilities. I thank Prof. P. Reddanna, Dept of Animal Sciences, for allowing me to use the sonication facility. I thank Ms. Monica Kannan for help in MALDI-TOF/TOF experiments. I also thank Mr. S. Pavan Kumar, CIL for help in SEM experiments. Thanks are also due to all the faculty members of the School of Life Sciences.

I thank all the research scholars of the School of Life Sciences for their cooperation. The help and cooperation of the non-teaching staff is acknowledged.

I thank AP-NL, EU-NBS, DST & UoH for the research fellowships. I would like to acknowledge the infrastructural support provided by UGC-SAP and DST-FIST and DBT-CREBB to the Dept. of Plant Sciences and School of Life Sciences.

I wish to thank my seniors Dr. B. Sashidhar, Dr. V.L. Vasudev, Dr. Ch. Neeraja and Dr. Debashish Dey for their suggestions and help. I thank all my labmates Dr. Swarnalee Dutta, Dr. K. Anil, Dr. Anil Singh, Ms. K. Suma, Mr. K. Sippy, Mr. P.V.S.R.N. Sharma, Ms. B. Uma, Ms. T. Swaroopa, Mr. Subhanarayan Das, Mr. J. Madhu Prakash, Ms. Manjeet Kaur, Mr. V. Sreenivas, Mr. S. Rambabu, Mr. V. Paparao and Ms. K. Parvathi for their cooperation.

I thank Mr.U. Narasimha, Mr. B. Devaiah and Mr. M. Malla Reddy for their assistance in the lab.

Words fail to express my heartfelt gratitude for my parents and my wife P. Punyavathi, and all my family members to whom I'm forever indebted for their love, endless patience, unconditional support and understanding, without whose cooperation I would not have come so far.

P. Purushotham

Dedicated to my
Beloved Parents and
Maternal Uncle
P. Sudarsanam

CONTENTS

ABBREVIATIONS

AMAC	: 2-aminoacridone
BLAST	: basic local alignment search tool
bp	: base pair
CAZy	: carbohydrate active enzyme
CBM	: carbohydrate binding module
CBP	: chitin binding protein
ChBD	: chitin binding domain
CHOS	: chitooligosaccharides
C-terminal	: carboxy terminal
° C	: degree centigrade/degree Celsius
gDNA	: genomic deoxy ribonucleic acid
DP	: degree of polymerization
EDTA	: ethylene diamine tetra acetic acid
F_A	: fraction of acetylation
Fn3	: fibronectin 3
g	: gram
GH18	: glycosyl hydrolase 18
GlcN	: glucosamine
GlcNAc	: N-acetyl glucosamine
h	: hour(s)
HPLC	: high performance liquid chromatography
IPTG	: isopropyl β-D-thiogalactoside
kb	: kilobase
kDa	: kilo dalton
L	: litre

LB : Luria-Bertani

M : molar

MALD-TOF-TOF : matrix assisted laser disruption –time of flite

mg : milligram

min : minute

mL : milliliter

mM : millimolar

MW : molecular weight

NCBI : national centre for biotechnological information

N-terminal : amino terminal

OD : optical density

P_A : pattern of acetylation

PAGE : polyacrylamide gel electrophoresis

PCR : polymerase chain reaction

PDB : protein data bank

PKD : polycystic kidney disease

rpm : revolutions per minute

SDS : sodium dodecyl sulphate

SEC : size exclusion chromatography

sec : seconds

SEM : scanning electron microscopy

TE : Tris-EDTA

TG : transglycosylation

TIM : triosephosphate isomerise

TLC : thin layer chromatography

µg : microgram

µM : micromolar

LIST OF TABLES

.

LIST OF FIGURES

INTRODUCTION

1.1 Chitin exits at least in two different forms in nature

Chitin, poly β-(1-4)-N-acetyl-D-glucosamine, is a natural polysaccharide derivative of cellulose (Fig.1.1) synthesized by an enormous number of living organisms. Considering the amount of chitin produced annually in the world, it is the most abundant polymer after cellulose. Chitin occurs in nature as ordered crystalline micro-fibrils forming structural components in the exoskeleton of arthropods or in the cell walls of fungi. It is also produced by a number of other living organisms in the lower plant and animal kingdoms, serving in many functions where reinforcement and strength are required. The annual production of cellulose and chitin is around one trillion and 100 billion tons, respectively (Tharanathan and Kittur *et al*., 2003, Kim *et al*., 2006), which makes them an almost unlimited source of raw material for environmentally friendly and biocompatible products, as well as biofuels. Despite the widespread occurrence of chitin, up to now, the main commercial sources of chitin have been crab and shrimp shells. In industrial processing, chitin is extracted from crustaceans by acid treatment to dissolve calcium carbonate followed by alkaline extraction to solubilize proteins. In addition, a decolorization step is often added to remove leftover pigments and obtain a colourless product.

Depending on its source, chitin is extracted as two allomorphs, namely α and β forms (Rinaudo, 2006), which can be differentiated by infrared and solid-state NMR spectroscopy together with X-ray diffraction. A third allomorph γ-chitin has also been described, but from a detailed analysis, it seems that it is a variant of α family (Atkins, 1985). The structures of α- and β forms differ only in that the piles of chains are arranged alternately antiparallel in α-chitin, whereas they are all parallel in β-chitin. The γ-structure shows that two chains run in one direction and another chain runs in the opposite direction. Among the chitin variants, α-chitin is the most abundant biopolymer in the nature; it occurs in fungal and yeast cell walls, in krill, in lobster and crab tendons and shells, and in shrimp shells, as well as in insect cuticle. It is also found in or produced by various marine living organisms. According to the crystalline structure, α-chitin has strong intersheet and intrasheet hydrogen bonding, and β-chitin has weak hydrogen bonding by intrasheets. Therefore, in contrast to α-chitin, β-chitin is characterized by a weak intermolecular force, and it has been confirmed to exhibit higher reactivity and affinity for solvents than α-chitin (Kurita *et al*., 1994).

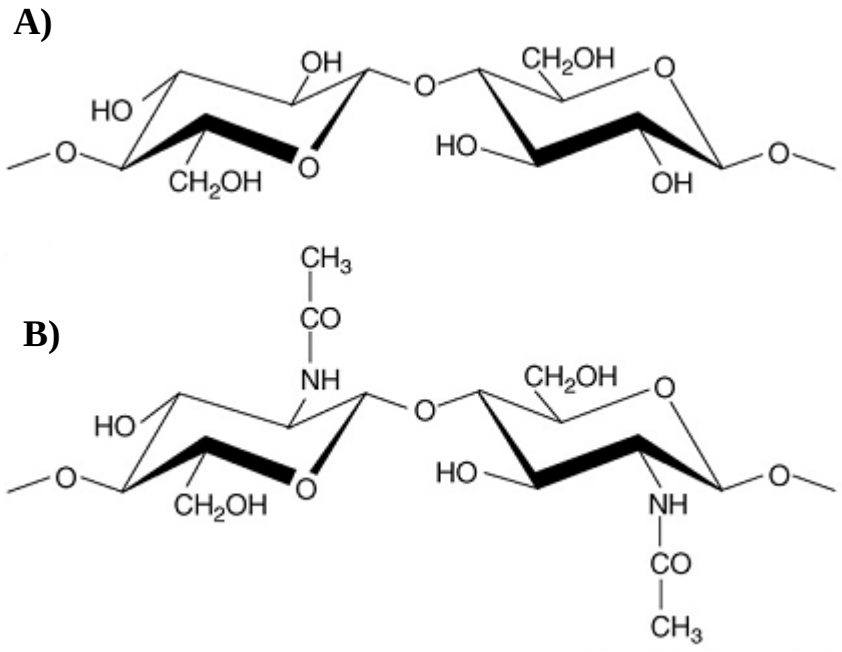

Fig. 1.1: Chemical structures of (A) cellulose and (B) chitin (Eijsink *et al*., 2008)

1.2 Chitosan is the soluble deacetylated form of chitin.

Chitin becomes soluble in aqueous acidic media and is called chitosan when the degree of deacetylation (DDA) of chitin reaches about 50% (depending on the origin of the polymer) (Rinaudo *et al*., 2006). The solubilisation occurs by protonation of the –NH2 function on the C-2 position of the D-glucosamine repeat unit, whereby the polysaccharide is converted to a polyelectrolyte in acidic media. Chitosan was classified according to the fraction of N-acetylated residues (F_A) or degree of N-acetylation (DA), the degree of polymerization (DP) or the molecular weight (MW), the molecular weight distribution (PD, for PolyDispersity), and the pattern of N-acetylation (P_A) or sequence. Chitosan exhibits a variety of interesting physicochemical and biological properties. Chitosan is the only pseudonatural cationic polymer and thus, in combination with its non-toxicity, biocompatibility and biodegradability, finds in numerous applications in agriculture, cosmetics, water treatment and medicine (Neeraja *et al*., 2010).

1.3 Chitinases are wide spread in nature and grouped in to two different families.

The breakdown of chitin is catalyzed by chitinases (EC 3.2.1.14) which hydrolyze chitin to N-acetyl glucosamine, chitobiose or smaller chitooligosaccharide (CHOS) fragments. They are found in a wide range of organisms, including bacteria, fungi, plants and animals. The presence of chitinases in such organisms is closely associated with the physiological roles of their substrates (Bhattacharya *et al*., 2007). For instance, bacteria produce chitinases so that they can use chitin as a source of carbon and nitrogen for growth, whereas chitinases in yeasts and other fungi are important for autolysis, nutritional and morphogenetic functions. Plant chitinases play a role as defensive agents against pathogenic fungi and some parasites by disrupting their cell walls, whereas viral chitinases are involved in the pathogenesis of host cells. Animal chitinases are involved in dietary uptake processes. Human chitinases are particularly associated with anti-inflammatory effects against T-helper-2-driven diseases, such as allergic asthma. Chitinases from bacteria and fungi are extremely important for maintaining a balance between the large amount of carbon and nitrogen trapped in the biomass as insoluble chitin in nature (Li, 2006).

Chitinases can be divided into two major categories: exochitinases and endochitinases (Dahiya *et al*., 2006). Exochitinases can be further divided into two subcategories:

chitobiosidases, which cleave diacetylchitobiose units from the non-reducing end of the chitin chain, β-(1, 4)-N-acetyl-glucosaminidases (NAGase), which cleaves N-acetylglucosamine (NAG) oligomers, generating NAG monomers. Endochitinases cleave glycosidic linkages randomly at internal sites along the chitin chain, eventually providing a variety of low molecular mass NAG oligomers such as diacetylchitobioses and chitotrioses (Dahiya *et al*., 2006) Based on amino acid sequence similarity, chitinases are classified into families 18 and 19 of glycoside hydrolases (GH) [Henrissat and Davies, 1997; described in the Carbohydrate Active enZYme (CAZy) database, http://www.cazy.org/]. The members of the two different families differ in their amino acid sequences, three-dimensional structures, and molecular mechanisms of catalytic reactions (Aronson *et al*., 2003). Family 18 chitinases have catalytic domains of triosephosphate isomerase [TIM barrel $(\beta/\alpha)_8$] fold with a conserved DxDxE motif (Vaaje-Kolstad *et al*., 2004) on the β4-strand and catalyze the hydrolytic reaction by substrate-assisted mechanism (Terwisscha van Scheltinga *et al*., 1996, van Alten *et al*., 2001), whereas family 19 chitinases comprise of high percentage of α-helices with two lobes in the catalytic domain and adopt the single displacement catalytic mechanism (Brameld and Goddard, 1998, Hoell *et al*., 2006). A complete survey of *Trichoderma* chitinases suggested a further family 18 chitinases classification into subgroups A (bacterial⁄ fungal), B (plant⁄ fungal) and C (killer toxin-like chitinases) (Seidl *et al*., 2005). Family 18 chitinases are represented in most living organisms, whereas family 19 enzymes are mostly found in plants, where they contribute to defence against chitinous pathogens.

1.4.1 Chitinases exhibit at least two different modes of catalysis

The hydrolysis of the glycosidic linkage of chitinous substrates like chitin and chitosan is a nucleophilic substitution at the anomeric carbon, and can lead to either retention or inversion of the anomeric configuration. Both hydrolysis reactions take place through general acid catalysis, and require a pair of carboxylic acids at the enzyme's active site (Fig. 1.2). One carboxylic acid is acting as a proton donor, facilitating leaving group departure, and the other acts as a base (inverting mechanism) or as a nucleophile (retaining mechanism). In both the mechanisms, the position of the proton donor is within hydrogen-bonding distance of the glycosidic oxygen. The inverting mechanism (also called the single displacement mechanism) is a "one-step" reaction, where the protonation of the glycosidic oxygen occurs simultaneously with a nucleophilic attack on the anomeric carbon by an activated water molecule. This water molecule is located between a carboxylic group and the anomeric carbon and it is activated by the carboxylic group that acts as a base. Since the water

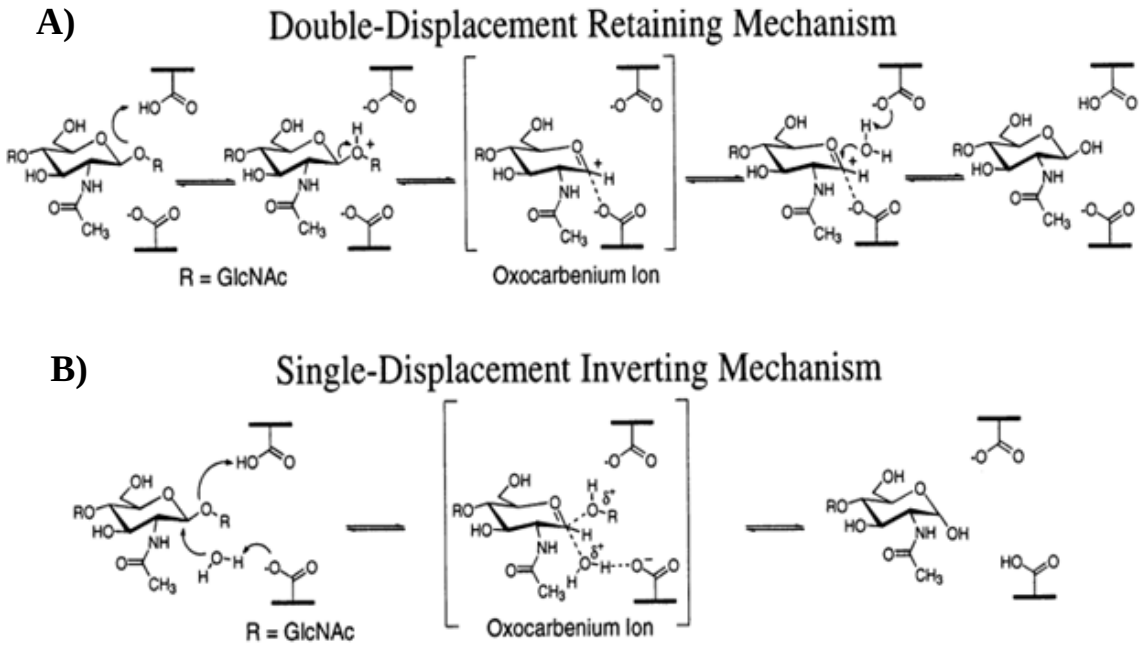

Fig. 1.2: Catalytic mechanism of chitinases (Brameld and Goddard, 1998)

A. The double-displacement hydrolysis mechanism proposed for family 18 chitinases. Protonation of a GlcNAc residue in a boat conformation leads to an oxazoline intermediate, which may be hydrolyzed to form a product with retention of the anomeric configuration.

B. The single-displacement hydrolysis mechanism proposed for family 19 chitinases. Two acidic residues are required in the active site, and the hydrolysis product shows inversion of the anomeric configuration

molecule approaches the anomeric carbon from the side of the catalytic base, this mechanism leads to inversion of the anomeric configuration.

Chitosanases belonging to families GH46, GH75 and GH80 and family 19 chitinases use the inverting mechanism (Davies *et al*., 1995, Fukamizo *et al*., 1995, Iseli *et al*., 1996, Brameld and Goddard, 1998, Adachi *et al*., 2004, Cheng *et al*., 2006, Cantarel *et al*., 2009). The retaining mechanism (also referred to as the double displacement mechanism) is a two-step reaction, where the first step involves the protonation of the glycosidic oxygen (by the catalytic acid) and a congruent nucleophilic attack on the anomeric carbon atom by the nucleophile (the second carboxylic acid). This attack leads to breakage of the glycosidic linkage and the formation of a covalent linkage between the anomeric carbon and the catalytic nucleophile (Vocadlo *et al*., 2001). Subsequently, this intermediate is hydrolyzed by a water molecule that approaches the anomeric carbon from a position close to that of the original glycosidic oxygen, leading to retention of the anomeric carbon configuration. Family 18 chitinases use a special variant of the double displacement mechanism, referred to as the substrate-assisted double displacement mechanism. Here, the carbonyl oxygen atom from the N-acetylgroup of the sugar bound in subsite -1 act as the nucleophile, leading to formation of an oxazolinium ion intermediate. Because of this involvement of the N-acetyl group in catalysis, productive substrate-binding of chitosan and chitosan oligomers to family 18 chitinases requires that a GlcNAc is bound in the -1 subsite (Terwisscha van Scheltinga, *et al*., 1995, Tews *et al*., 1997, Brameld and Goddard., 1998, van Alten *et al*., 2001, Sørbotten *et al*., 2005).

Chitinases and chitosanases can have endo- or exo-activity, where both the endo- and exo-mode of action can be combined with processivity. Processive enzymes will not release the substrate after one cleavage, but remain associated with the substrate so that a new cleavage can take place as the polymer substrate slides through the substrate-binding cleft. Processivity is difficult to analyze when insoluble substrates such as chitin is degraded, but can be studied using chitosan as substrate (Sørbotten *et al*., 2005, Horn *et al*., 2006a, Eijsink *et al*., 2008). Whereas processivity generally is considered to be favourable for the hydrolysis of crystalline substrates, processivity has been shown to reduce enzyme efficiency towards soluble and more accessible polymeric substrates such as chitosan (Horn *et al*., 2006b, Zakariassen *et al*., 2009). Thus, for the industrial production of CHOS, the use of non-processive enzyme variants may be beneficial at least in some cases.

1.4.2 A few family 18 chitinases are transglycosylases

Some of the glycoside hydrolases, besides hydrolysis of glycosidic bonds, are capable of transglycosylation (TG) to form new glycosidic bonds between donor and acceptor saccharides (Fig. 1.3) (Eneyskaya *et al*., 1997, Fujita *et al*., 2007, Umekawa *et al*., 2008). In retaining glycoside hydrolases, the TG reaction occurs through a double-displacement mechanism (Ly and Withers, 1999). In the first step the glycosidic oxygen is protonated by a catalytic acid, and the anomeric carbon is a target for a nucleophilic attack from the catalytic base, leading to cleavage of the glycosidic bond and to formation of a glycosyl-enzyme intermediate. In the second step, the intermediate decomposes with different possible outcomes. Hydrolysis is attained by attack of a water molecule on the glycosyl-enzyme intermediate that is assisted by the conjugated base of the catalytic acid residue and that leads to release of a hydrolyzed sugar. Alternatively, TG may occur if the water molecule is outcompeted by another acceptor such as a carbohydrate or an alcohol.

Since TG is a kinetically controlled reaction, efficient TG requires an enzyme with an active site architecture that disfavours correct positioning of the hydrolytic water molecule and/or favours binding of incoming carbohydrate molecules, through strong interactions in the aglycon subsites (Williams and Withers, 2000). Family 18 chitinases are retaining glycoside hydrolases that are special in the sense that the nucleophilic attack is carried out by the acetamido group of the sugar bound to the -1 subsite. Consequently, the intermediate is not a covalent glycosyl-enzyme intermediate, but a noncovalent oxazolinium ion. The positioning and nucleophilicity of the acetamido group are heavily affected by residues on the enzyme, in particular by a conserved aspartate and tyrosine (van Aalten *et al*., 2001, Bokma *et al*., 2002, Synstad *et al*., 2004). Aspartate is part of the fully conserved diagnostic DxDxE motif that includes the catalytic acid (Glutamate) and another aspartate at a relatively buried position in the core of the $[(\beta/\alpha)_8$ (TIM-barrel) fold], which is considered the catalytic domain in family 18 chitinases.

TG effect of GH 18 was observed in wide range of organisms. These include chitinases from bacteria; *Coccidioides immitis* (Fukamizo *et al*., 2001), chitinase A from *Serratia marcescens* (Aronson *et al*., 2006), chitinase A from *Vibrio harveyi* (Suginta *et al*., 2005), chitianse A1 from *Bacillus circulans* (Sasaki *et al*., 2002) and chitinases from *Bacillus* sp. (Wako Pure Chemical Inc.), Fungi; *Aspergillus fumigatus* (Lü *et al*., 2009), *Mucor hiemalis* (Yamanoi *et al*., 2004), *Trichoderma reesei* (Usui *et al*., 1990), Cycad; *Cycas revoluta* (Taira *et al*.,

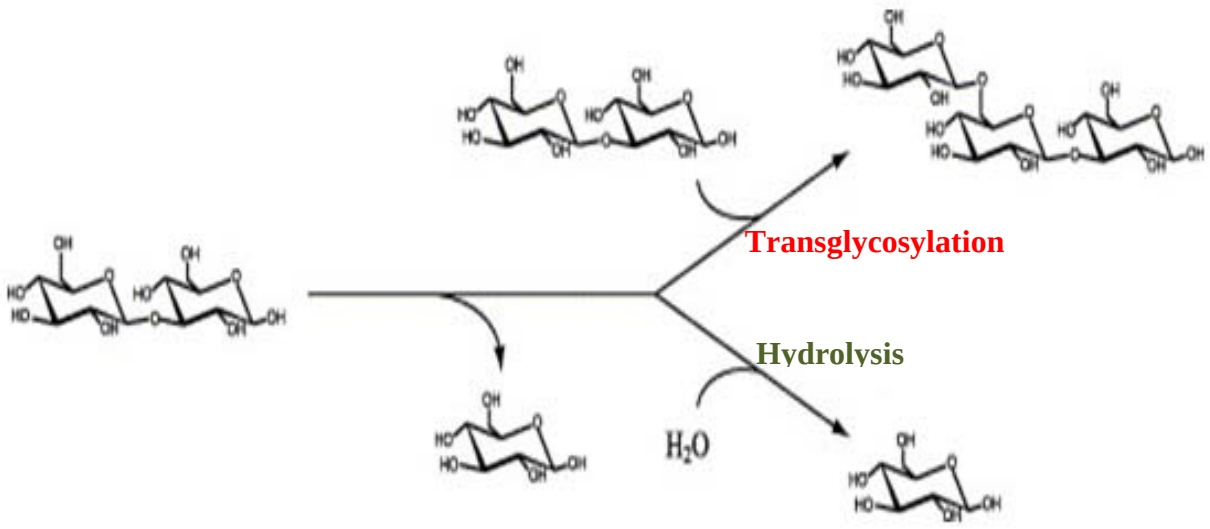

Fig. 1.3: Transglycosylation mechanism of glycoside hydrolases (Kawai *et al*., 2004)

2009), plants; *Nicotiana tabacum* (Ohnuma *et al*., 2011b), *Arabidopsis thalianas* (Ohnuma *et al*., 2011a). The TG activity of these chitinases implicates a great potential for the synthesis of oligosaccharides and polysaccharides of chitin origin.

1.4.3 "Chitin oxidohydrolase" mechanism of action.

Vaaje-Kolstad *et al*. (2010) showed that the CBP21 (chitin binding protein from *S. marcecsens*) is an enzyme that catalyzes cleavage of glycosidic bonds in crystalline chitin, thus opening up the inaccessible polysaccharide material for hydrolysis by normal glycoside hydrolases. This enzymatic activity was first discovered when detected traces of previously unidentified CHOS upon incubation of β-chitin nanowhiskers with CBP21 (Fig. 1.4). The products were identified as CHOS with a normal sugar at the nonreducing end and an oxidized sugar, 2-(acetylamino)-2-deoxy-D-gluconic acid (GlcNAcA), at the other end. Addition of reductants dramatically increased the efficiency of the reaction which enabled the breakdown of large crystalline β-chitin particles by CBP21 alone with the release of a range of oxidized products. The reaction catalyzed by CBP21 comprises of a hydrolytic step and an oxidation step thus Vaaje-Kolstad *et al*. (2010) suggested naming CBP21 a "chitin oxidohydrolase".

1.5 Chitinases are inhibited by wide varieties of natural or synthetic compounds

In addition to general enzyme inhibitors, such as organic compounds and oxidizing/reducing agents, a number of reports are available on the natural chitinase inhibitors (Fig. 1.5). Allosamidin, an antibiotic produced by *Streptomyces* sp., is a known specific inhibitor of chitinases from insects, yeast, fungi, and human serum. Allosamidin is a pseudotrisaccharide that mimics the oxazolinium reaction intermediate. It is similar to GlcNAc but lacks a pyranose ring oxygen and contains an oxazoline ring in which the methyl group is substituted by dimethylamine. Allosamidin is a competitive inhibitor and exerts its inhibitory effect by acting as a nonhydrolyzable analog of the oxazolinium ion intermediate (Tews *et al*., 1997). Allosamidin inhibited the *Bacillus* sp. BG-11 chitinase by 50 and 70% at a concentration of 30 and 50 µg/ml of enzyme solution, respectively, with an IC_{50} value of 40 µM (Bhushan and Hoondal, 1998). Psammaplin A, a brominated tryrosine-derived compound, was found to be a noncompetitive inhibitor of chitinase B from *S. marcescens*, a family 18 chitinase. Crystallographic studies suggest that a disordered Psammaplin A molecule is bound near the

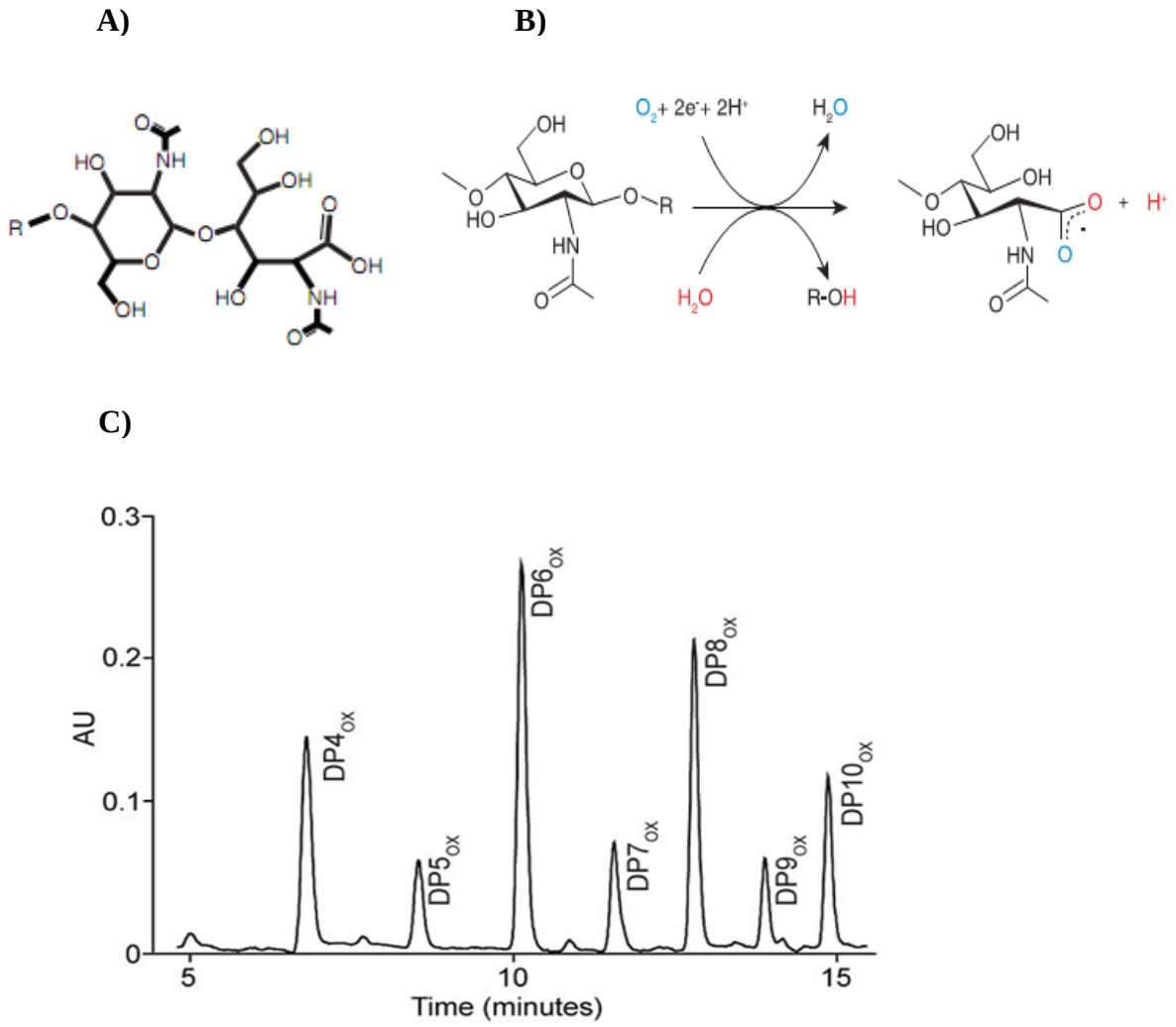

Fig. 1.4: Products from *S. marcescens* CBP21 (Vaaje-Kolstad *et al.*, 2010)

A.Oxidized chitooligosaccharide with a GlcNAcA moiety.

B. Scheme for the enzymatic reaction catalyzed by CBP21. In the final oxidized product, one oxygen comes from molecular oxygen (blue) and one from water (red)

C. UHPLC of oxidized oligosaccharides. A semi-quantitative analysis of products generated by CBP21 was performed by separating the oxidized oligosaccharides by UHPLC. Note that the α- and β-anomers of non-oxidized oligosaccharides would be separated under these chromatographic conditions. The fact that only single peaks are observed confirms the absence of a normal sugar reducing end. Peak identities were determined using MALDI-TOF MS.

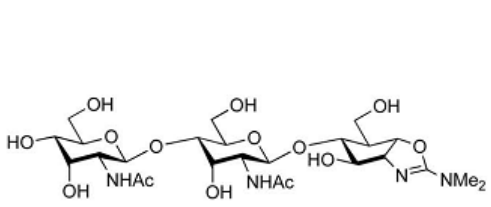

Allosamidin (**1**) (*Streptomyces* sp.)
IC_{50} = 0.05 μM (*Bombyx* chitinase)

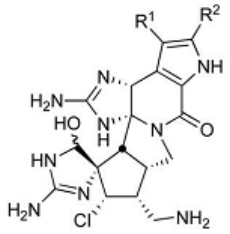

Styloguanidine (**2**); $R^1 = R^2 = H$
[inhibit *Schwanella* chitinase at 2.5 μg/disk]
3-Bromostyloguanidine (**3**); $R^1 = Br$, $R^2 = H$
2,3-dibromostyloguanidine (**4**); $R^1 = R^2 = Br$
(sponge *Stylotella auranthtium*)

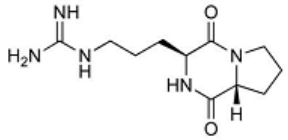

Cl-4 (cyclo-L-Arg-D-Pro) (**5**) (*Pseudomonas* sp.)
IC_{17} = 1 mM (*Bacillus* chitinase)

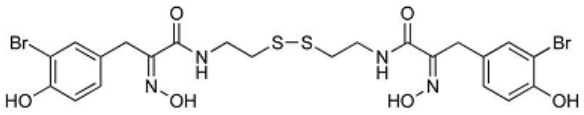

Psammaplin A (**6**) (sponge *Aplysinella rhax*)
IC_{50} = 68 μM (*Bacillus* chitinase)

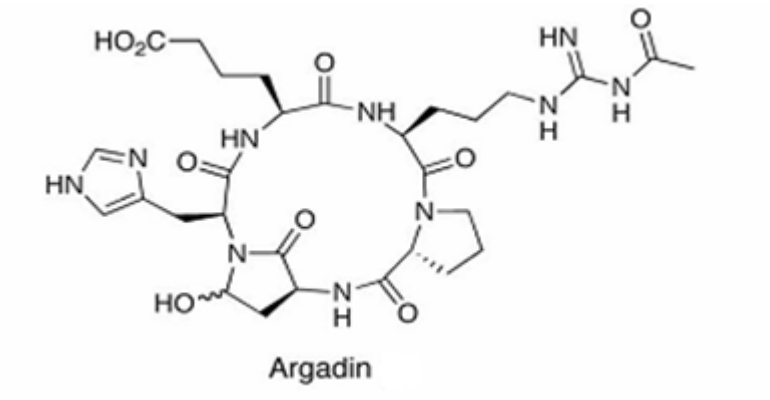

Argadin

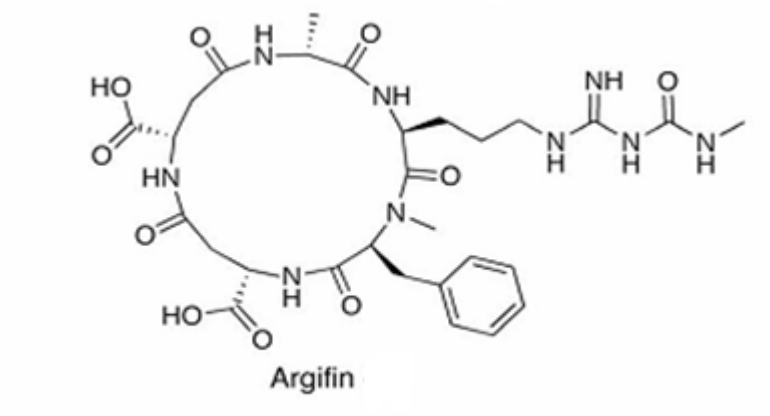

Argifin

Fig. 1.5: Structures of naturally-occurring chitinase inhibitors and their inhibitory activities (Omura *et al*., 2000).

active site (Tabudravu *et al*., 2002). Omura *et al*., (2000) isolated a modified cyclic peptide named argifin from *Gliocladium* sp. FTD 0668. The IC_{50} value of argifin against *Lucilia cuprina* chitinase was 3.7 mM. Another chitinase inhibitor, argadin (modified cyclic pentapeptide), was isolated from *Clonostachy*s sp. FO-7314 by Arai *et al*. (2000). Its IC_{50} value against *L. cuprina* chitinase were 34 nM at 20°C and 150 nM at 37°C. Crystallographic studies of a *S. marcescens* chitinase in complex with argadin/argifin has revealed ordered binding of these cyclic peptides in the active site. A new chitinase inhibitor, CI-4, was isolated from *Pseudomonas* sp. IZ08 by Izumida *et al*. (1996).

Inhibition of family 18 chitinases is emerging as a target for pest and fungal control as well as asthma and inflammatory therapy. To this regard, it is desirable to have access to non-toxic inhibitors that are easy to produce, and have high efficiency and specificity. CHOS that are partially N-acetylated have the potential to fulfill these requirements. The primary cause of the inhibitory effect of CHOS comes from the fact that family 18 chitinases have an absolute preference for an N-acetylglucosamine in the -1 subsite. Therefore, any CHOS that preferably binds to a family 18 chitinase in such a way that a D (Deacetylation) ends up in the crucial -1 subsite will act as an inhibitor (Cederkvist *et al*., 2008).

Unfortunately, all currently available inhibitors have a number of properties that make them unsuitable as inhibitor leads, including high molecular weights (e.g., allosamidin, argifin, argadin). More importantly, there is only limited availability of family 18 chitinase inhibitors with an $IC_{50} < 0.5$ mM, hampering further inhibition studies of these enzymes. Family 18 chitinases play key roles in a range of pathogenic organisms and are over expressed in the asthmatic lung. By screening a library of marketed drug molecules, Rao *et al*., (2005) identified methylxanthine derivatives as possible inhibitor leads. These derivatives, theophylline, caffeine, and pentoxifylline, are used therapeutically as anti inflammatory agents, with pleiotropic mechanisms of action. It was shown that they are also competitive inhibitors against a fungal family 18 chitinase, with pentoxifylline being the most potent (Ki of 37 μM). GH 18 chitinases are inhibited by these xanthine derivatives by forming extensive π-π stacking interactions with conserved tryptophans in the active site of this protein.

1.6 Chitin binding proteins (CBPs) potentiate chitinases activity by increasing the substrate accessibility

Efficient chitin degradation also depends on the action of a small family 33 chitin binding proteins (CBPs), which bind to the insoluble crystalline substrate, leading to structural changes in the substrate and increased substrate accessibility. The function of family 33 CBPs was first demonstrated for CBP21 from *S. marcescens* (Vaaje-Kolstad *et al*., 2005a), and a second example has been described in a study on carbohydrate binding proteins, domains from *T. fusca* (Moser *et al*., 2008) and *Ll*CBP33A from *Lactococcus lactis* ssp *lactis* IL1403 (Vaaje-Kolstad *et al*., 2009) and Cbp50 from *B. thuringiensis* serovar *konkukian* (Mehmood *et al*., 2011).

Genome analyses indicate that secreted family 33 CBPs are produced by most chitin-degrading microorganisms (Vaaje-Kolstad *et al*., 2005a), but only a few have been characterized biochemically. Binding studies of family 33 CBPs have been conducted for CBP21 from *S. marcescens* (Vaaje-Kolstad *et al*., 2005b, Suzuki *et al*., 1998), ChbB (Chu *et al*., 2001) and Chb3 (Saito *et al*., 2001) from *Streptomyces coelicolor*, CHB1 from *Streptomyces olivaceoviridis* (Schnellmann *et al*., 1994), CHB2 from *Streptomyces reticuli* (Kolbe *et al*., 1998), CbpD from *Pseudomonas aeruginosa* (Folders *et al*., 2000), proteins E7 and E8 from *Thermobifdia fusca* (Moser *et al*., 2008) and *Ll*CBP33A from *Lactococcus lactis* ssp *lactis* IL1403 (Vaaje-Kolstad *et al*., 2009) and Cbp50 from *B. thuringiensis* serovar *konkukian* (Mehmood *et al*., 2011) showing a large diversity of binding preferences. Some family 33 CBPs bind to a broad selection of insoluble carbohydrates [e.g. ChbB and *Ll*CBP33A, which bind both α- and β-chitin (Chu *et al*., 2001, Vaaje-Kolstad *et al*., 2009), and Chb3 from *St. coelicolor*, which binds α-chitin, β-chitin, colloidal chitin and chitosan (Saito *et al*., 2001), whereas others bind only to a specific substrate variant [e.g. CBP21 from *S. marcescens* which strictly binds to β-chitin (Suzuki *et al*., 1998) and CHB1 from *St. olivaceoviridis* (Schnellmann *et al*., 1994) and CHB2 from *St. reticuli* (Kolbe *et al*., 1998) which strictly bind to α-chitin and finally and Cbp50 from *B. thuringiensis* serovar *konkukian* (Mehmood *et al*., 2011) bind to α-chitin, β-chitin and colloidal chitin substrates. A common property is that binding is influenced by pH (e.g. CBP21 from *S. marcescens* does not bind at pH < 4.5 (Suzuki *et al*., 1998). X-ray crystallographic and mutational studies of CBP21 revealed that the protein has a "budded" fibronectin type III fold consisting of two β-sheets, arranged as a compact β-sheet sandwich fold surface having a flat conserved region that binds

chitin through interactions mediated by mainly polar amino acids (Vaaje-Kolstad *et al*., 2005a, b). Remarkably, conserved aromatic residues that have been suggested previously to play a role in chitin binding (Perrakis *et al*., 1994, van Aalten *et al*., 2000, Uchiyama *et al*., 2001, Chang *et al*., 2004) were mainly found in the interior of the protein, seemingly incapable of interacting with chitin. CBP21 also contains a solvent accessible metal binding motif consisting of the amino group of the N-terminus and two histidines that is conserved in family 33 CBMs. An oxidohydrolase activity was elegantly demonstrated for CBP21 of *S. marcescens* as described in 1.4.3.

Two important features stand out in CBP21 catalysis. First, the cleavage of glycosidic bonds by CBP21 includes an oxidative step. Second, the products released by CBP21 are dominated by even-numbered oligosaccharides. CBP21 catalysis was found to be inhibited by EDTA, and activity could be restored by adding divalent cations such as Mg^{2+} or Zn^{2+}, which may bind to the conserved histidine motif. As CBP21 is a redox enzyme, it is remarkable that the metal ions activating CBP21 are not redox active. Perhaps the metal ion's primary role lies in stabilization of the active site structure and/or positioning of a hydrolytic water molecule.

CBP21 activity is strongly inhibited by cyanide, a known O_2 mimic, but not by azide, a known inhibitor of heme proteins. Superoxide dismutase did not inhibit CBP21 activity, whereas catalase had only a minor inhibitory effect. Several reductants capable of functioning as electron donors boosted the activity of CBP21. The oxidation step catalyzed by CBP21 is cofactor independent and depends on an external electron donor. The insensitivity for superoxide dismutase indicates that oxygen is activated on the enzyme, where it would be shielded from the solvent. The strong inhibition by cyanide supports the crucial role of the oxidative step. CBP21 binds to the flat, solid, well ordered surface of crystalline material and catalyzes chain breaks by a mechanism that results in oxidation of one of the new chain ends. The chain break will result in disruption of crystalline packing and increased substrate accessibility, an effect that may be enhanced by the oxidation of the new chain end that disrupts the normal chair conformation of the sugar ring and introduces a charge.

1.7 Bacterial chitinolytic cascade is regulated by consensus sequence

Production of chitinolytic enzymes in bacteria is normally induced by the presence of chitin in the culture medium. Since chitin is insoluble, the microorganisms are unable to utilize it

unless it has been hydrolysed to soluble oligomers of N-acetyl-glucosamine. Several proposals have been made to explain how induction may occur in this situation. The most probable inducers of *S. marcescens* chitinolytic enzymes are soluble oligomers derived from chitin. Such soluble oligomers could be produced by the action of trace amounts of chitinolytic enzymes that are present because of constitutive low level expression of the chitinase genes. Alternatively, the signal for induction of synthesis of chitinases could result from physical contact between the cell and the insoluble substrate. However, it has been shown that production of chitinolytic enzymes could indeed be induced by adding only $(GlcNAc)_2$ or $(GlcNAc)_{3-4}$ to the growth medium of *S. marcescens* (Monreal and Reese, 1969, Watanabe *et al*., 1997, Suzuki *et al*., 1998). Whether all the chitinases in *S. marcescens* are induced with oligomers remains to be tested. The production of chitinase by *S. marcescens* growing on chitin is inhibited by addition of glucose and GlcNAc (Monreal and Reese, 1969, Watanabe *et al*., 1997). A glucose effect has also been demonstrated for other bacteria (Ni and Westpheling, 1997, Saito *et al*., 2000), indicating that catabolic repression is generally involved in regulating the chitinolytic system of bacteria.

Studies in other microorganisms have provided some links as to how regulation may be achieved. In *Streptomyces plicatus* a 12-basepair direct repeat sequence (A.TGGTCTAGACCA.T) overlapping with the putative RNA polymerase binding sites of two chitinase genes was shown to be involved in the induction by chitin and the repression of glucose (Ni and Westpheling, 1997, Delic *et al*., 1992). The same direct repeat was found in the promoter regions of eight chitinase genes scattered on the *Streptomyces coelicolor* chromosome (Saito *et al*., 2000). Orikoshi *et al*. (2005) studied the expression of the four chitinases (*chiA*, *chiB*, *chiC*, and *chiD*) of *Alteromonas* sp. strain O-7 at the gene and protein level in the presence of chitin. An alignment of the nucleotide sequences of *Alteromonas* sp. strain O-7 *chiA*, *chiB*, *chiC*, and *chiD* near the promoter regions revealed the presence of a conserved 8-bp sequence, 5´-ACAACATG- 3´. Therefore, these chitinase genes might be coordinately controlled by the same regulatory protein(s).

Long insoluble molecules of chitin cannot enter the cell. They are degraded prior to their assimilation into CHOS and N, N-diacetylchitobiose $(GlcNAc)_2$ as major products, and, less abundantly, into GlcNAc by microorganisms that possess the appropriate enzymatic arsenal. *Streptomycetes* are high-GC Gram-positive soil bacteria and known as major decomposers of chitin in soil, that have a selective advantage in colonizing different types of chitin-containing substrates due to their large pattern of chitinases, β-N-acetyl glucosaminidases and other

chitin-targeting proteins (Schrempf, 2001, Saito *et al*., 2003). This genetic predisposition is accompanied by a performing regulatory system that triggers induction of chitin (chi) genes in the presence of major chitin degradation products - like $(GlcNAc)_2$ - and that triggers repression when more readily assimilated sugars (like glucose) are available (Miyashita *et al*., 2000, Saito *et al*., 1998, 2000).

1.8 Chitooligosaccharides can be assayed with chromatography and MALDI-TOF-TOF.

1.8.3 Purification and characterization of chitooligosaccharides (CHOS)

CHOS produced enzymatically or chemically normally consist of a mixture of oligomers differing in DP, F_A and P_A. Several techniques for separation and purification of CHOS have been reported, like gel filtration (Sørbotten *et al*., 2005), ultrafiltration (Lopatin *et al*., 2009), and ion exchange (Haebel *et al*., 2007) and metal affinity (Le Dévédec *et al*., 2008) chromatography. Often, such techniques need to be applied in combination to obtain homogeneous CHOS fractions. Despite some successful studies, the production of pure CHOS fractions are generally a time consuming and challenging task. Preparative separation of CHOS is most commonly based on size through size exclusion chromatography (SEC). Good methods for the separation of oligomers up to DP40 (individual oligomers up to DP20) have been described (Sørbotten *et al*., 2005). This system allows separation of CHOS with similar DP values ranging from approximately DP2 to DP20, independently of F_A and P_A (Sørbotten *et al*., 2005). Further separation of CHOS can be achieved using cation-exchange chromatography, because protonated amino groups on the deacetylated sugars interact with the ion-exchange material. With this method CHOS of identical DP will be separated based on the number of deacetylated units (Haebel *et al*., 2007). A further partial separation of isobaric CHOS (identical F_A, different P_A) may be achieved using strong cation exchange chromatography. Although, the latter separations are promising and useful, baseline separation of isobaric CHOS has so far not been achieved (Haebel *et al*., 2007). In an alternative strategy, metal affinity chromatography has been successfully used for separation of shorter CHOS. CHOS have a strong affinity for Cu^{2+}. Copper as a chelating agent gave separation up to 90% of fully deacetylated CHOS of DP3 and higher (Le Dévédec *et al*., 2008). This has not been reported for N-acetylated mixtures of CHOS. In order to characterize CHOS in terms of DP, F_A and P_A, several techniques have been applied, primarily nuclear magnetic resonance (NMR) and mass spectrometry. Using NMR, it is

possible to determine FA in a chitosan or CHOS sample and to (partially) identify the P_A in shorter CHOS depending on the complexity of the oligomer mixture. Resonances detected using NMR reveal that the H-1 resonance of a reducing unit is sensitive to its nearest neighbor, making it possible to (partially) determine the P_A of an oligomer (Sørbotten *et al*., 2005). In addition, the P_A of dimers and trimers can be determined using NMR. The identity of the non-reducing end unit of an oligomer can be determined using ^{13}C NMR, which in some instances also may reveal the identity of its nearest neighbor (Vårum *et al*., 1996). Mass spectrometry provides excellent tools for the identification of the DP and F_A of CHOS (Bahrke *et al*., 2002, Cederkvist *et al*., 2006). In Okafo *et al*. (1997) reported a reductive amination of CHOS using 2-aminoacridone (AMAC), which is useful for tagging of the reducing end. Building on this labelling technique, Bahrke *et al*. (2002) developed a method for sequencing of CHOS up to DP12 using reducing end derivatization with AMAC. Starting with CHOS fractions of homogeneous DP they used matrixassisted laser desorption ionization (MALDI) time-of-flight (TOF) post-source decay (PSD) mass spectrometry (MS) for sequence determination. Reducing end derivatization of CHOS using AMAC favours formation of Y-type ions, meaning that sugars are only cleaved after the oxygen in the β-(1→4) linkage from the reducing end. Consequently, interpretation of the resulting mass spectra is quite straightforward. It should be noted though that the method has limitations when applied to mixtures. In a later study from the same group (Haebel *et al*., 2007), a second method for reductive amination, using 3-(acetylamino)-6-aminoacridine, was adopted. Combined detection and fragmentation of isobaric CHOS using MALDI iontrap MS^n was reported. The described technique makes it possible to simultaneously determine sequence and quantity of CHOS of identical DP but different F_A and P_A in an isobaric CHOS mixture.

The MALDI-TOF MS-based assay described by Price and Naumann. (2011) requires 2 µL total volume, containing only 1 ng of enzyme and 2 µg of oligosaccharide substrate. The 60 laser shots used to acquire a mass spectrum takes approximately two minutes, as opposed to typically 30-40 minutes for a single HPLC run. Moreover, by using the standard multiple-place MALDI MS targets up to 100 assays could be run in about 2-3 hours without needing to remove the target from the instrument. This assay is readily applicable to different sized chitin substrates (up to DP6), or structural analogs of chitomers, and to time course estimates. In addition, because the substrate and product chitomers are simultaneously visualized in the TOF spectrum this gives immediate information about the cleavage site and mechanism of the enzyme under study. However, because of the intrinsic semi-quantitative response of

MALDI-TOF MS the assay is not recommended for classical enzyme kinetic studies in its present form.

1.9 Chitin/chitooligosccharides have potential applications in medicine, agriculture and environment.

1.9.1 Applications for chitin/chitosan

The key property of chitin-derived products for use in various biomedical applications is the immuno-modulating effect (Aam *et al*., 2010, Muzzarelli *et al*., 2010). Various mechanisms of immuno-enhancement activity of chitin and its derivatives have been reported. Chitin and chitosan affected C3 and C5 components of complement system and concluded that complement system is activated by chitin and chitosan through the alternative pathway. The intensity of complement and macrophage activation of chitin is less than chitosan; therefore, chitin is more biocompatible (Minami *et al*., 1998).

Hemostasis through blood coagulation is an important step for wound healing. The main cellular components in blood coagulation are platelets. Okamoto *et al*. (2003) reported that chitin is an effective agent for hemostasis maintenance through aggregating platelets, and suggested that the effect of chitin and chitosan is due to both physical and chemical properties of these biopolymers, especially their amino groups (Okamoto *et al*. 2003).

Chitin and chitosan are among the candidates to battle obesity and hypercholesterolemia, as they could reduce the amount of cholesterol in rats (Razdan and Pettersson, 1994). Chitin derivatives such as N-succinyl-chitosan (Kamiyama *et al*., 1999), carboxymethyl chitin (Dev *et al*., 2010), chitosan hydrogel (Ishihara *et al*., 2006), and hydroxyethyl chitin (Zhao *et al*., 2006) possess essential features for drug delivery carrier.

Chitin and its derivatives have antioxidant properties (Ngo *et al*., 2009), hence preventive effects on various diseases. Chitin that was chemically modified to obtain aminoethyl-chitin, showed antioxidant activity against free radicals such as 1,1-diphenyl-2-picrylhydrazyl (DPPH), hydroxyl, superoxide, and peroxyl (Je and Kim, 2006).

The wide usage of heavy metals in industry continues to cause serious and widespread health problems. It is important to remove these metals from the environment. Chitin phosphate could absorb uranium in the presence of sodium carbonate solution (Sakaguchi *et al*., 1981). Chitin and chitosan have been shown to have copper removal capability, which could help to

obtain more stable diesel oil (Peiselt da Silva and Pais da silva, 2004). They also have been successfully tested for the adsorption of organic pollutants (Aksu, 2005).

Chitin has also been utilized by *Clostridium paraputrificum* M-21 to produce hydrogen gas. This gas is considered to be a potential source of alternative energy (Evvyernie *et al*., 2000, Morimoto *et al*., 2005).

1.9.2 Applications for chitooligosaccharides

N-acetylchitooligosaccharide and chitooligosaccharide (CHOS) originate from chitin and chitosan, respectively. Oligomers of chitin and chtitosan can be obtained both chemically and enzymatically (Aam *et al*., 2010). Their degree of polymerization (DP) is usually < 20. The CHOS accelerates the wound healing effects of poly vinyl alcohol if it is used in the early stages of the healing process (You *et al*., 2004). It could inhibit the growth of *Actinobacillus*, indicating that it has antimicrobial activity (Choi *et al*., 2001). The CHOS causes an increase in biophotons emission from suspension-cultured rice cells. Photon emissions from rice cells elicited by N-acetylchitohexaose are closely associated with the ROS-generating system, and are regulated by Ca^{2+} signaling and protein phosphorylation *via* phosphatidic acid (PA), an intermediate of phospholipid signaling (Kageyama, 2006). CHOS play an important role in defense mechanisms of plants against microbial invasion (Day *et al*., 2001). They could also promote carrot somatic embryos survival (De Jong *et al*., 1993). Chitin fragments can desensitize the perception system of tomato, which can lead to improvement of the defense mechanism in tomato cells (Felix *et al*., 1998). Chitin in the form of lipo-chitin can induce the formation of nodule in soybean root (Minami *et al*., 1996). Rice is another important plant in which chitin fragments have been shown to boost the defense system (Ito *et al*., 1997, Okada *et al*., 2001).

CHOS have shown inhibitory effects on tumor growth and metastasis of lung cancer in mice (Shen *et al*., 2009). N-acetylchitohexaose (chitin derivertive) and chitohexaose (chitosan derivertive) also induce production of interleukins 1 and 2 and, consequently, help to improve the function of macrophages, natural killers, cytotoxic T cells, and polymorphonuclear leukocytes, in defense mechanisms. The anti-metastatic activity of acetylchitohexaose against Lewis lung carcinoma in mice (Tsukada *et al*., 1990) has been demonstrated. There are many reports indicating antitumor activity of chito-oligosaccharides (Wang *et al*., 2008). The oligosaccharides that contain N-acetylglucosamine play an important role in the interaction between HIV and T-helper during pathogenesis of this virus (Mizuochi and Nakata, 1999).

CHOS was used as analogue to study lysozyme (Chipman *et al*., 1968). Thus, these materials can be used to study protein-carbohydrate interaction and associated enzymatic activities.

Production of specific oligosaccharides by chemical methods is challenging due to the need to selectively protect and manipulate chemically quite similar saccharide donors and acceptors. For this reason, development of methods for enzymatic synthesis of oligosaccharides is desirable. The transglycosylation activity of family 18 chitinases (Fukamizo *et al*., 2001, Aguilera *et al*., 2003, Boer *et al*., 2004, Chou *et al*., 2006, Taira *et al*., 2010) is of special interest because there are potential applications for CHOS [i.e., homo- or hetero-oligomers of glucosamine (GlcN) and N-acetylated glucosamine (GlcNAc)], especially in the food, medical, and agriculture fields (Tharanathan and Kittur *et al*., 2003, Rinaudo, 2006). The bioactivities of CHOS are thought to depend on a combination of oligomer length, DA and P_A (sequence) (Aam *et al*., 2010). Transglycosylating chitinases have the potential to play a central role in the development of new well-defined mixtures of CHOS with new or improved biological activity, by coupling smaller CHOS building blocks to each other or to other functional groups (Zakariassen *et al*., 2011).

1.10 Objectives of present study

S. proteamaculans 568, belongs to family *Enterobacteriaceae*, was isolated as a root endophyte from *Populus trichocarpa* (Taghavi *et al*., 2009). It is a Gram-negative, rod shape, facultative anaerobe. The CAZy data base shows eight genes from the genome sequence of *S. proteamaculans* 568 potentially involved in chitin turnover, coding for the following: four family 18 chitinase (*Sp* ChiA, *Sp* ChiB, *Sp* ChiC and *Sp* ChiD); three family 33 CBP (*Sp* CBP21, *Sp* CBP28 and *Sp* CBP50); and a family 20 N-acetylhexosaminidase (*Sp* CHB). The objective of this study was to characterize the hydrolytic and transglycosylation properties of the heterogeneously expressed chitinases and chitin-binding proteins of *S. proteamaculans* 568.

MATERIALS & METHODS

2. 1. 1 Bacterial culture

Serratia proteamaculans strain 568 (Kindly gifted by Dr. Daniel vander lilie, USA)

Escherichia coli Rosetta-gami 2 (DE3) (Novagen, USA)

2. 1. 2 Media used

2.1.2.1 Luria Bertani medium (LB medium)

LB medium – To 900 mL of water, 10 g tryptone, 10 g NaCl, 5 g yeast extract and 15 g agar was added. The pH was adjusted to 7.2 and volume was made up to 1 litre.

2.1.2.2 Chitin agar medium

Colloidal chitin-10 g, Na_2HPO_4-0.065 g, KH_2PO_4-1.5 g, NaCl-0.25 g, NH_4Cl-0.5 g, $MgSO_4$-0.12 g, $CaCl_2$-0.005 g and agar -15 g. The pH was adjusted to 7.5 and the volume was made up to 1 litre.

2. 1. 3 Chemicals

Isopropyl-β-D-thiogalactoside (IPTG), X-Gal, phenol solution Tris equilibrated, GeneElute HP Plasmid miniprep kit and Agarose were purchased from Sigma-Aldrich (USA). Antibiotics were purchased from Calbiochem. All other chemicals, and routine media components for bacterial culture were of analytical grade and obtained from Merck, HiMedia laboratories (India) unless otherwise stated. The polymeric substrates α- chitin, β-chitin and chitosan substrates were kindly provided by Dr. Dominique Gillete, Mahtani Chitosan Pvt., Ltd. (Veraval, India). Chito-oligosaccharides with different degrees of polymerization (DP) were purchased from Seikagaku Corporation (Tokyo, Japan).

2. 1. 4 Kits

Plasmid isolation kit and *Taq* DNA polymerase were from Simga-Aldrich, while Gel extraction kit, DNeasy Blood & Tissue Kit for genomic DNA isolation were from Qiagen.

2. 1. 5 Enzymes

Pfu DNA polymerase, T4 DNA ligase and all restriction enzymes from MBI Fermentas (Germany), *Taq* DNA polymerase from Simga-Aldrich. All the enzymes were used as per the manufacturer's instructions.

2. 2 Plasmids

The brief details of the vectors used and the constructs generated in this study are given in Table 2.1

2. 3 Primers used for PCR

The primers used in this study (Table 2.1) were procured from MWG Biotech Pvt. Ltd.

2.4 Identification and selection of *S. proteamaculans* 568 for chitinolysis

2.4.1 Phylogenetic analysis of *S. proteamaculans* 568 based on 16S rDNA

The 16S rRNA gene sequence was amplified from isolate KCK genomic DNA, isolated using of a genomic DNA purification kit, with the two bacterial universal primers (Table 2.1) using thermocycler (Eppendorf Mastercycler Gradient, Germany) at 50°C annealing temperature. The PCR product was analyzed on 1% agarose gel and eluted for sequencing at MWG Pvt. Ltd., Bangalore, India. The partial sequences were matched with the nucleotide database available at GenBank, using BLAST tool in NCBI (National Centre for Biotechnology Information). A phylogenetic tree was constructed by using MEGA (Molecular Evolutionary Genetics Analysis) version 4 (Kumar *et al*. 2008).

2.4.2 Chitinolysis by *S. proteamaculans* 568 on the chitin-containing agar plate

Single colony of *S. proteamaculans* strain 568, which was grown on LB plate overnight, was spotted on to the chitin-agar medium plate and incubated at 30°C for 4-5 days to observe the zone of clearance around the bacterial colony.

2.5 Cloning and characterization of chitinases from *S. proteamaculans* 568 (*Sp chi*s)

2.5.1 Amplification and cloning of chitinase from *S. proteamaculans* 568

The molecular biology protocols including PCR, restriction digestion, agarose gel electrophoresis, ligation, competent cell preparation and transformation were done following Sambrook and Russell, (2001). Oligonucleotide primers synthesis and sequencing of the amplicons was done by MWG Biotech. Proof reading DNA polymerase (*pfu*) was used for the amplification of the target genes.

S.No	GeneBank I.D	Gene name	Primer name	Primer sequence 5' ⟶ 3'	Restriction site	Name of the clone	Amplicon Size (kb)	Expected protein size (kDa)
1.	CP000826.1	16S rDNA	27F	GTTTGATCCTGGCTCAG	-	-	1.5	-
			1489R	TACCTTGTTACGACTTCA	-			
1.	ABV39247.1	*Sp chiA*	Sp chiA FP	CAA TAA CCA TGG CCG TAC CGG GTA AGC CTA C	*Nco* I	pET 28a-*Sp* chiA	1.62	58
			Sp chiA RP	AAT AAC TCG AGT TGC GTG CCG GCG CTG TTG	*Xho* I			
2.	ABV40327.1	*Sp chiB*	Sp chiB FP	CAT AAC CAT GGT GTC CGA ACG TAA AGC CGT TAT TG	*Nco* I	pET 28a-*Sp* chiB	1.49	55
			Sp chiB RP	AAT AAC TCG AGT GCC ACG CGG CCC ACT TTC	*Xho* I			
3.	ABV42574.1	*Sp chiC*	Sp chiC FP	GCT CAC CAT GGT GAG CAC CAA TAA TAT TAT CAA TGC	*Nco* I	pET 28a-*Sp* chiC	1.45	54
			Sp chiC RP	AAT AAC TCG AGG GCG GTC AAC TGC CAC AG	*Xho* I			
4.	ABV41826.1	*Sp chiD*	Sp chiD FP	TAA TAC CAT GGG TGC CGG CAT GGC TCA TG	*Nco* I	pET 22b-*Sp* chiD	1.22	44.75
			Sp chiD RP	AAT AAC TCG AGC TGT TTC CCG TTA ATC C	*Xho* I			
5.	ABV42205.1	*Sp cbp21*	Sp cbp21 FP	AAT AAC CAT GGT TCA CGG CTA TGT CGA AAC	*Nco* I	pET 22b-*Sp* cbp21	0.51	18.6
			Sp cbp21 RP	GCA TAC TCG AGT TTA GTC AAA TTA ACG TC	*Xho* I			
6.	ABV42576.1	*Sp cbp28*	Sp cbp21 FP	ATA CAC CAT GGT TCA GGA GCA AGT TTC CAC TAC	*Nco* I	pET 22b-*Sp* cbp28	0.762	28.0
			Sp cbp21 RP	AAT CAC TCG AGG CCT TTG ATA TTG ACG TCA C	*Xho* I			
7.	ABV43333.1	*Sp cbp50*	Sp cbp50 FP	TCA AGA ATT CCA TGG TTA TGT TGA ATC GCC G	*Eco* RI	pET 22b-*Sp* cbp50	1.350	50.0
			Sp cbp50 RP	ATA AAC TCG AGT CAG TTT TTT AAT ATC CAG GCT TGT TGC C	*Xho* I			

Table 2.1: Details of *Sp* chitinolytic genes cloning. Sequences underlined represent restriction sites.

2.5.2 Genomic DNA isolation from *S. proteamaculans*

Genomic DNA (gDNA) was isolated using DNeasy kit (Qiagen, Germany) from *S. proteamaculans* 568.

2.5.3 PCR amplification and cloning of *S. proteamaculans* chitinases

Based on ORF sequences available in *S. proteamaculans* 568 genomic data base (http://genome.jgi-psf.org/finished_microbes/serpr/serpr.home.htmL), primers were designed for the amplification of four chitinase encoding genes from the gDNA of *S. proteamaculans* 568. The genes encoding for *Sp chiA*, *Sp chiB*, *Sp chiC* and *Sp chiD* were PCR amplified from *S. proteamaculans* 568 genomic DNA by referring the annotated sequence (GenBank accession no. ABV39247.1, ABV40327.1, ABV42574.1 and ABV41826.1). The respective genes were amplified with gene-specific forwad and reverse primers using *Pfu* DNA polymerase at 58°C annealing temperature with 4 min polymerization time. Amplicons were gel extracted using Qiagen Gel Clean up kit. Bacterial expression vectors pET- 28a(+), pET 22b(+) and the amplicons were double digested with *Nco* I and *Xho* I, gel purified both the amplicons and vectors were ligated in to pET- 28a(+) [*Sp chiA*, *Sp chiB*, *Sp chiC*] and pET 22b(+) [*Sp* ChiD] using T4 DNA ligase at 16°C for 16 h. The resultant plasmids were designated as pET 28a-*Sp chiA*, pET 28a-*Sp chiB*, pET 28a-*Sp chiC* and pET 22b-*Sp chiD* to express *Sp* ChiA, *Sp* ChiB, *Sp* ChiC and *Sp* ChiD, respectively in *E.coli*.

2.5.4 Protein expression and purification of *Sp* chitinases

2.5.4.1 Protein expression

E.coli Rosette-gami 2 (DE3) (Invitrogen) was transformed with pET 28a-*Sp chiA*, pET 28a-*Sp chiB*, pET 28a-*Sp chiC* and pET 22b-*Sp chiD* and transformants were selected on LB plates containing 50 µg/mL kanamycin and 25 µg/mL chloramphenicol for pET28a- *Sp chiA*, pET28a-*Sp chiB* and pET28a-*Sp chiC* and 100 µg/mL ampicillin, 25 µg/mL chloramphenicol for pET22b-*Sp chiD*. Bacterial cells harboring recombinant plasmids were stored at -80°C as glycerol stocks. Overnight cultures grown from -80°C stocks of *E.coli* Rosette-gami 2 (DE3) cells containing pET 28a-*Sp chiA*, pET 28a-*Sp chiB*, pET 28a-*Sp chiC* and pET 22b-*Sp chiD* were inoculated in LB medium containing 50 µg/mL kanamycin, 25 µg/mL chloramphenicol and 100 µg/mL amplicillin, 25 µg/mL chloramphenicol, respectively. The cultures were incubated at 37°C and 200 rpm. When the cell density reached 0.6 ($O.D_{600}$), IPTG was added

to a final concentration of 0.5 mM, and the cultures were further incubated for 24 h at 18°C and 200 rpm, followed by centrifugation at 9,000 g for 10 min at 4°C for harvesting of cells. The expressed recombinant proteins from plasmids pET 28a-*Sp chiA*, pET 28a-*Sp chiB*, pET 28a-*Sp chiC* and pET 22b-*Sp chiD* were designated as *Sp* ChiA, *Sp* ChiB, *Sp* ChiC and *Sp* ChiD, respectively.

2.5.4.2 Protein purification

The expressed proteins of *Sp* ChiA, *Sp* ChiB and *Sp* ChiC were isolated from respective cell pellets by whole cell lysate using sonicator, while *Sp* ChiD was isolated from the periplasmic fraction. The cell pellets of expressed *Sp* ChiA, *Sp* ChiB and *Sp* ChiC were resuspended in Ni-NTA equilibration buffer (50 mM NaH_2PO_4, 100 mM NaCl and 10 mM imidazole pH 8.0), and the cells were lysed by sonication at 20% amplitude with 30 x 15 s pulses (with 20 s delay between pulses) on ice, with a Vibra cell Ultrasonic Processor, converter model CV33, equipped with a 3 mm probe (Sonics, Newtown, CT, USA). The sonicated material was centrifuged at 15,200 g for 10 min at 4°C in order to pellet the insoluble cell debris. Periplasmic fraction was prepared according to the protocol (pET manual, Novagen). Cell pellet was resuspended in 30 mL of buffer containing 30 mM TrisCl pH 8.0, 20% sucrose and 1 mM EDTA) with slow stirring for 10 min on ice, followed by centrifugation at 4°C for 10 min at 9,000 g. The supernatant was discarded and pellet was further resuspended in 30 mL of 5 mM $MgSO_4$ followed by slow stirring at 4°C for 10 min, centrifuged at 4°C for 10 min at 9,000 g. At this stage, *Sp* ChiA, *Sp* ChiB, *Sp* ChiC, and *Sp* ChiD were found in the soluble fraction. The cleared lysate was applied to a Ni-NTA column (Sigma,USA) equilibrated with running buffer (50 mM NaH_2PO_4, 100 mM NaCl and 10 mM imidazole pH 8.0). *Sp* chitinases were eluted by running four column volumes of elution buffer (50 mM NaH_2PO_4, 100 mM NaCl and 250 mM imidazole) through the column. The pure fraction containing chitinase was collected, concentrated and buffer exchanged with 50 mM sodium acetate buffer pH 6.0 using Macrosep Centrifugal Devices (Pall Corporation, USA).

2.5.5 SDS-PAGE analysis

The protein samples were separated by SDS-PAGE on vertical slab gels according to Laemmli (1970). The stacking gel contained 4.5 % polyacrylamide in 0.125 M Tris-HCl, pH 6.8 and the resolving gel contained 12% polyacrylamide in 0.375 M Tris-HCl, pH 8.8.

Electrode buffer contained 0.025 M Tris-HCl, 0.192 M glycine and 0.1% (w/v) SDS of pH 8.5. The samples were boiled at 100°C for 5 min in sample buffer [1% SDS (w/v) and 12% glycerol (v/v), in 0.063 M Tris-HCl, pH 6.8] and electrophoresis was carried out at 50V in stacking gel and at 100V in resolving gel. The gels were stained in a solution containing 0.5% (w/v) Coomassie brilliant blue G-250, 30% (v/v) methanol and 10% (v/v) glacial acetic acid, and destained in a solution containing 30% (v/v) methanol and 10% (v/v) glacial acetic acid till the protein bands were visible.

2.5.6 Zymogram analysis for *Sp* chitinases

A simple dot blot assay was performed to detect the activity of purified recombinant chitinases. A composite gel supplemented with 0.1% glycol chitin was prepared. Five µg of *Sp* chitinases were spotted on to the gel and placed in humid chamber at 37°C for overnight. After incubation, the gel was stained with 0.01% calcofluor white M2R in 0.5 M Tris-HCl pH 8.9 for 10 min at 4°C. Finally, the brightener solution was removed, and the gel was washed with distilled water for 10 min at 4°C. Lytic zones were visualized by placing the gels on a UV transilluminator.

2.5.7 Characterization of *Sp* chitinases

2.5.7.1.1 Chitinase enzyme assay

Chitinase activity was determined by a modified Schales' procedure (standard assay) using colloidal chitin as the substrate (Imoto and Yagishita, 1971). The reaction mixture (200 µL) consisting of recombinant *Sp* chitinase (*Sp* ChiA-ChiC: 5 µg and *Sp* ChiD: 27 µg) and colloidal chitin (*Sp* ChiA-ChiC: 4 mg/mL and *Sp* ChiD: 25 mg/mL) in 50 mM buffer (*Sp* ChiA: sodium phosphate pH 7.0, *Sp* ChiC: sodium phosphate pH 6.0, *Sp* ChiB and *Sp* ChiD: sodium acetate pH 6.0) at 40°C for 1 h with constant shaking at 190 rpm. After incubation, 1.5 mL of color reagent (0.5 M sodium carbonate, 0.05% potassium ferricyanide) was added and boiled for 15 min in dark and centrifuged at 16,100 g at room temperature (30°C) for 10 min. Then the supernatant containing reducing sugars were separated and triplicate samples were loaded in 96 well microtiter plates. OD was measured at 420 nm using microtitre plate reader (Multiscan, Labsystems, Finland). One unit was defined as the amount of enzyme that liberated 1 µmol of reducing sugar per minute.

2.5.7.1.2 Kinetics analysis of *Sp* chitinases

Chitinase activity of the *Sp* chitinases was measured by incubating the recombinant enzymes (*Sp* ChiA-ChiC: 5 µg and *Sp* ChiD: 27 µg) with different concentration of colloidal chitin (*Sp* ChiA-ChiC: 0-15 mg/mL and *Sp* ChiD: 0-50 mg/mL) in 50 mM buffer (*Sp* ChiA: sodium phosphate pH 7.0, *Sp* ChiC: sodium phosphate pH 6.0, *Sp* ChiB and *Sp* ChiD: sodium acetate pH 6.0) with respective controls in triplicates at 40°C for 1 h at 190 rpm and chitinase assay was done as described in 2.5.7.1.1. Enzyme activity was defined as the release of one micromole of N-acetyl-glucosamine (NAG) per sec under standard experimental conditions. Specific activity in µM/sec/mg of protein was calculated and kinetic values were evaluated from three independent sets of data fitting to the Michaelis-Menten equation by nonlinear regression function available in GraphPad Prism version 5.0 (GraphPad Software Inc., San Diego, CA).

2.5.7.1.3 Optimum temperature

The optimum temperatures of *Sp* chitinases was determined by incubating the enzymes (*Sp* ChiA-ChiC: 5 µg and *Sp* ChiD: 27 µg) with colloidal chitin (*Sp* ChiA-ChiC: 4 mg/mL and *Sp* ChiD: 25 mg/mL) in 50 mM buffers (*Sp* ChiA: sodium phosphate pH 7.0, *Sp* ChiC: sodium phosphate pH 6.0, *Sp* ChiB and *Sp* ChiD: sodium acetate pH 6.0) for 1 h at different temperatures of 20, 30, 40, 50, 60, 70, 80, 90 and 100°C. Relative activity (%) was determined under standard assay condition.

2.5.7.1.4 Optimum pH

The optimum pH of *Sp* chitinases was determined by incubation of enzymes (*Sp* ChiA-ChiC: 5 µg and *Sp* ChiD: 27 µg) in a buffer at different pHs (2.0-12.0) for 1 h at 37°C under standard assay conditions using colloidal chitin (*Sp* ChiA-ChiC: 4 mg/mL and *Sp* ChiD: 25 mg/mL) as a substrate. The buffers used were 50 mM sodium citrate buffer (pH 2.0-5.0), 50 mM sodium acetate buffer (pH 5.0-6.0), 50 mM sodium phosphate buffer (pH 6.0-8.0), and 50 mM glycine-NaOH buffer (pH 8.0-10.0) and 50 mM NaH_2PO_4-NaOH (pH 10.0-12.0). The relative activity (%) was determined under standard assay conditions.

2.5.7.1.5 Substrate specificity determination of *Sp* chitinases

The substrate specificity of purified *Sp* chitinases on chitin and non-chitin derived substrates were tested. The substrates used were α-chitin, β-chitin, colloidal chitin, glycol chitin,

chitosan with 90% DDA, water soluble chitosan with 90% DDA and Avicel (microcrystalline cellulose) (sigma). The reaction mixture contained of *Sp* chitinases (*Sp* ChiA-ChiC: 5 µg and *Sp* ChiD: 27 µg) and polymeric insoluble and soluble substrates (*Sp* ChiA-ChiC: 0.4%, w/v and *Sp* ChiD: 2.5 %, w/v) were incubated in 50 mM buffer (*Sp* ChiA: sodium phosphate pH 7.0, *Sp* ChiC: sodium phosphate pH 6.0, *Sp* ChiB and *Sp* ChiD: sodium acetate pH 6.0) at 40°C for 1 h. Enzyme assay was done under standard chitinase assay conditions.

2.5.7.2 Binding of recombinant *Sp* chitinases

2.5.7.2.1 The insoluble polymeric substrates.

Binding studies were performed using α-chitin, β-chitin, colloidal chitin, chitosan with 90% DDA and Avicel as substrates. The insoluble substrates were suspended in 50 mM buffer (*Sp* ChiA: sodium phosphate pH 7.0, *Sp* ChiC: sodium phosphate pH 6.0, *Sp* ChiB and *Sp* ChiD: sodium acetate pH 6.0) to yield 20 mg/mL stock suspensions that were continuously stirred with a magnetic stirrer in order to obtain consistent amounts when pipetting. The standard 1 mL binding assay mixture contained 1.0 mM of protein and 1.0 mg of substrates in 50 mM buffer (*Sp* ChiA: sodium phosphate pH 7.0, *Sp* ChiC: sodium phosphate pH 6.0, *Sp* ChiB and *Sp* ChiD: sodium acetate pH 6.0). All assays were performed in triplicate and with blanks (buffer + 1.0 mg/mL chitin) and controls for a specific binding of the protein (buffer +*Sp* chitinases) and non-specific adsorption (buffer + bovine serum albumin). To minimize enzyme-mediated hydrolysis of the bound substrate, the binding assay mixture was maintained at 4°C. After the mixture was incubated for 1 h with rotary shaking at 1300 rpm in an thermomixer (Eppendorf Thermomixer comfort, Eppendorf, Germany), the supernatant containing unadsorbed protein was separated from the insoluble polysaccharides by centrifugation at 16,100 g for 15 min at 4°C. Protein concentration in the supernatant was estimated from the absorbance at 280 nm using the molar extinction coefficients calculated from the amino acid compositions of the proteins as described by Pace *et al*. (1995).

2.5.7.2.2 The soluble polymeric substrates

The capacity of *Sp* chitinases to bind different insoluble polysaccharides was evaluated by affinity electrophoresis under non-denaturing conditions. Affinity electrophoresis was carried out by preparing continuous polyacrylamide gels consisting of 8.0% (w/v) acrylamide. Appropriate 0.1% of soluble polysaccharides [glycol chitin, laminarin and carboxymethyl-

cellulose (CM-cellulose)] were copolymerized in one of the gels. The control gel without polysaccharide was prepared and run simultaneously. Samples of 10 µg *Sp* chitinases and non-interacting control BSA were mixed with bromophenol blue, glycerol and subjected to electrophoresis at 4°C at a constant current of 80 V. After electrophoresis, proteins were visualized by staining with Coomassie blue G-250.

2.5.7.3 Analysis of products of *Sp* chitinases on chitooligosaccharides (CHOS) and chitin

2.5.7.3.1 Thin layer chromatography (TLC)

In a 150 µL reaction mixture, containing 2 mM of substrate (CHOS; DP2-DP6) and 5 µg of purified *Sp* chitinases in 50 mM buffer (*Sp* ChiA: sodium phosphate pH 7.0, *Sp* ChiC: sodium phosphate pH 6.0, *Sp* ChiB and *Sp* ChiD: sodium acetate pH 6.0). Reaction mixtures were incubated at 37°C and each time period starting from 0 (just after addition of enzyme), 1, 2, 3, 5, 15, 30, 45, 60, 120,180 and 720 min, 10 µL of the reaction mixture was transferred to an eppendorf tube containing 10 µL of 0.1N NaOH, to stop the reaction and samples were stored at -20°C until analysis. Aliquots (20 µL) of the reaction mixtures were chromatographed on a silica gel plate (TLC Silica gel 60, Merck Co., Germany) with a solvent system containing n-butanol, methanol, 25% ammonia solution-water (5:4:2:1[v:v:v:v]), and the products were detected by spraying the plate with aniline-diphenylamine reagent (400 µL aniline, 400 mg of diphenylamine, 20 mL of acetone, and 3 mL of 85% phosphoric acid) and baking it at 180°C using hot air gun (Black & Decker, Germany) for 3 min.

2.5.7.3.2 High performance liquid chromatography (HPLC)

2.5.7.3.2.1 Time-course of colloidal chitin hydrolysis

Analyses of the hydrolysis of colloidal chitin by *Sp* chitinases were conducted by incubating recombinant enzymes (*Sp* ChiA-ChiC: 0.3 µM and *Sp* ChiD: 3 µM) with colloidal chitin (*Sp* ChiA-ChiC: 4 mg/mL and *Sp* ChiD: 25 mg/mL) in 50 mM buffer (*Sp* ChiA: sodium phosphate pH 7.0, *Sp* ChiC: sodium phosphate pH 6.0, *Sp* ChiB and *Sp* ChiD: sodium acetate pH 6.0). Reaction mixtures were incubated at 40°C and 1300 rpm in a thermomixer, during time points starting from 0, 1, 2, 3, 5, 15, 30, 45, 60, 90, 120 and 720 min; 75 µL of the reaction mixture was transferred to an eppendorf tube containing 75 µL of 70% acetonitrile, to stop the reaction. The reaction mixtures were centrifuged at 16,100 g for 10 min at 4°C to remove the undigested colloidal chitin. The supernatant was further concentrated in concentrator (Eppendorf concentrator, Germany) till the complete evaporation of the solvent

without heating. The residue was dissolved in 20 µL of 35% acetonitrile and reaction mixtures were stored at -20°C until analysed by isocratic HPLC at 25°C using a Shimadzu 10ATvp UV/VIS HPLC system (Shimadzu corporation, Tokyo, Japan) equipped with a Shodex Asahipack NH2P-50 4E column (4.6 ID x 250 mm) (Showa Denko K.K,USA). Twenty microliter of the reaction mixture was injected in to the HPLC using Hamilton syringe (HAMILTON Bonaduz, Switzerland). The liquid phase consisted of 67% acetonitrile: 33% MilliQ H_2O and flow rate was set to 0.70 mL/min, eluted CHOS were monitored by recording absorption at 210 nm. Based on the peak areas obtained from HPLC profiles, CHOS concentrations were calculated using authentic oligosaccharide solutions. CHOS HPLC mixture, which contains the equal weights of oligomer ranging from DP1-DP6 were used for standard graph preparation. Standard calibration curves of CHOS moieties were constructed separately for each oligosaccharide. These data points yielded a linear curve for each amino standard sugar with the R^2 values of 0.997-1.0, thus allowing molar concentrations of CHOS to be determined with a confidence.

2.5.7.3.2.2 Reaction time-course of DP3-DP6 substrates hydrolysis/transglycosylation (TG) catalyzed by *Sp* ChiD.

To detect the range of products (especially TG products) generated by *Sp* ChiD from DP3-DP6 substrates, isocratic HPLC was performed according to the method mentioned in 2.5.7.3.2.1 by combining 560 nM *Sp* ChiD and 3.5 mM of each individual substrate ranging from DP3-DP6 in a reaction solution (800 µL) containing 50 mM sodium acetate buffer pH 6.0.

2.5.7.3.3 MALDI-TOF-MS

After HPLC analysis, the remaining reaction mixtures (15^{th} min sample for DP3, DP5 and 30^{th} min sample for DP4, DP6) were analyzed by MALDI-TOF-MS to determine the mass dependent product identity. A portion of reaction mixture (40 µL) was concentrated in a concentrator till the complete evaporation of the solvent and dissolved in 4 µL of HPLC grade MilliQ water. Two microliter of a 9 mg/mL mixture of 2,5- dihydroxybenzoic acid (DHB) in 30% acetonitrile was applied to a MTP 384 target plate ground steel TF (Bruker Daltonics). To this, 2 µL sample was then mixed into the DHB droplet and dried under a stream of air. Then the samples were analyzed with an Ultraflex MALDI-TOF/TOF instrument (Bruker Daltonics GmbH, Germany) with a autoflex 123 smart beam. The instrument was operated in positive acquisition mode and controlled by the FlexControl 3.0

software package. All spectra were obtained in the reflectron mode with an acceleration voltage of 25kV, a reflector voltage of 26, and pulsed ion extraction of 40 ns in the positive ion mode. The acquisition range used was from m/z 50 to 4000. The data were collected from averaging 500 laser shots, with the lowest laser energy necessary to obtain sufficient signal to noise ratios. Peak lists were generated from the MS spectra using Bruker FlexAnalysis software (Version 3.0).

2.5.7.3.4 Effect of enzyme and substrate concentrations on hydrolysis/TG activities of *Sp* ChiD

To study the influence of substrate and enzyme concentrations on the hydrolytic/TG activity of *Sp* ChiD, enzymatic reaction was performed according to the method mentioned in 2.5.7.3.2.1 using DP6 as a substrate by altering the enzyme and substrate concentrations. Different concentrations of substrate (0.35 and 1.75 mM) and enzyme (56 and 5600 nM) were incubated by keeping each time one component concentration constant and altering the other component.

2.5.7.4 A structural based sequence alignment and homology modelling of *Sp* ChiA, *Sp* ChiB and *Sp* ChiD

Catalytic domains of *Sp* ChiA - *Sp* ChiD and Heva (hevamine from *Hevea brasiliensis*) were aligned using clustalw2 (www.ebi.ac.uk/Tools/msa/clustalw2/). The models of *Sp* ChiA, *Sp* ChiB and *Sp* ChiD were generated by Modeller9v8 (http://www.salilab.org/modeller/) using templates of *S. marcescens* ChiA (PDB ID: 2WLY), ChiB (PDB ID: 1E15) and chitinase II (PDB ID: 3QOK) from *Klebsiella pneumoniae*, respectively as structural templates and the figures were prepared using PyMOL (http://www.pymol.org/).

2.6 Cloning and characterization of *S. proteamaculans* 568 chitin binding proteins (*Sp* CBPs)

2.6.1 Amplification and cloning

Three genes encoding chitin binding proteins (*Sp cbp21*, *Sp cbp28* and *Sp cbp50)* were amplified from the gDNA by referring the annotated sequences of *S. proteamaculans* 568 (GenBank accession no. ABV42576.1, ABV42205.1 and ABV43333.1) at 55°C annealing temperature using gene specific forward and reverse primers (Table 2.1). Expression vectors, and the amplicons were double digested with *Nco* I and *Xho* I [pET 22b(+), *Sp cbp21* and

Sp cbp28] and *Eco* RI and *Xho* I [pET 28a(+) and *Sp cbp50*], gel purified and ligated using T4 DNA ligase at 16°C for 16 h. The resultant plasmids were designated as pET 28a-*Sp cbp21*, pET 28a-*Sp cbp28* and pET 22b-*Sp cbp50* to express *Sp* CBP21, *Sp* CBP28 and *Sp* CBP50, respectively in *E.coli*.

2.6.2 Expression and purification of *Sp* CBPs were as described in 2.5.4.1 and 2.5.4.1.2, respectively

2.6.3 Characterization

2.6.3.1 Insoluble substrate binding specificity

Insoluble substrate binding of *Sp* CBPs was conducted by using 100 µg of proteins in 50 mM sodium phosphate buffer pH 7.0 with 1.0 mg/mL of substrates (α-chitin, β-chitin, colloidal chitin and Avicel) for 24 h at 37°C with vigorous shaking at 1300 rpm on thermomixer. Further procedures were according to the method described in 2.5.7.2.1.

2.6.3.1.1 Time course binding of *Sp* CBP21 and *Sp* CBP50 towards α and β-chitin

To study the time at which the binding of *Sp* CBP21 and *Sp* CBP50 are getting saturated with natural chitin variants (α and β-chitin), time dependent binding of *Sp* CBP21 and *Sp* CBP50 were assessed at different time points from 0 to 24 h as described in 2.5.7.2.1.

2.6.3.1.2 Absorption isotherms of *Sp* CBP21 and CBP50 towards α and β-chitin

Absorption isotherms of *Sp* CBP21 and *Sp* CBP50 towards α and β-chitin was done according to the method described in 2.5.7.2.1 with minor modification; varied concentrations of proteins from 0 to 10.0 µM were used and reaction mixtures were incubated with substrates for different saturation periods with respect to the substrates; *Sp* CBP21 with α-chitin the incubation time was 12 h and *Sp* CBP21 with β-chitin the incubation time was 3 h where as for the *Sp* CBP50 with α-chitin and β-chitin the incubation time was 12 h.

2.6.3.2 Soluble substrate binding specificity

The *Sp* CBPs binding to soluble polysaccharides (glycol chitin, laminarin, CM cellulose) was evaluated by affinity electrophoresis as described in 2.5.7.2.2.

2.6.4 Scanning electron microscopy

A 0.1 mg/mL of α-chitin suspension in 50 mM sodium phosphate buffer, pH 7.0, was pre incubated for 24 h at 37 °C in 1.5 mL reaction tubes with either 0.1 mg/mL bovine serum albumin (BSA) or 0.1 mg/mL BSA and 0.1 mg/mL *Sp* CBP21 and S*p* CBP50 applied onto cover slips (10 µL drops), and dried at 37 °C to fix the sample. The cover slips containing the samples were glued onto scanning electron microscopy aluminum studs with carbon tape and sputter-coated (JEOL FC 1100) with gold-palladium. Scanning was performed in a Philips scanning electron microscope at 20 kV.

2.6.5 Synergistic effect of *Sp* CBP21 and *Sp* CBP50 with *Sp* chitinases in chitin degradation

A standard 200 µL reaction mixture containing 1mg/mL of chitin substrates (α-, β-chitin) and 1 µM of *Sp* chitinase with varying concentrations of *Sp* CBPs; 5.3 µM and 2.2 µM of *Sp* CBP21 was used for the degradation of α and β-chitin respectively, 9.4 µM and 2.3 µM of *Sp* CBP50 was used for the degradation of α and β-chitin, respectively. Reaction mixtures were incubated at 37°C for 24 h. No agitation was used since the insoluble substrate adheres to the dry inner walls of the tubes (which would affect the substrate concentration). Products were quantified by standard chitinase assay described in 2.5.7.1.

2.6.6 A sequence alignment for *Sp* CBPs and homology modelling of *Sp* CBP21

All three *Sp* CBPs from *S. proteamaculans* were aligned with CBP21 from *S. marcescens* using clustalw2 (www.ebi.ac.uk/Tools/msa/clustalw2/) and *Sp* CBP21 model was generated using the template structure of CBP21 (PDB ID: 2BEM) from *S. marcescens* as described in 2.5.7.4.

RESULTS

3.1 Identity confirmation and screening for chitinolytic potential of *S. proteamaculans* 568

The 16S rRNA gene sequence of *S. proteamaculans* 568 was amplified, sequenced and submitted for BLAST search in NCBI, showed 100% homology to *S. proteamaculans* 568. The nearly complete 16S rRNA gene sequence was determined, and a phylogenic tree was constructed (Fig. 3.1). A BLAST search of the GenBank database was used to identify the closest neighbour, which was *S. plymuthica* (AJ233433.1) with 97% homology.

Actively growing *S. proteamaculans* 568 was spotted on agar plate containing colloidal chitin as the sole carbon and nitrogen source. After 4 days of incubation at 28^{o}C, the wide zone of clearance around the colony indicated the strong chitinolytic potential of *S. proteamaculans* 568 (Fig. 3.2).

3.2 Cloning and characterization of *S. proteamaculans* 568 chitinases

3.2.1 Amplification and cloning of chitinases

Sp chitinases (*Sp* ChiA, *Sp* ChiB, *Sp* ChiC and *Sp* ChiD) were amplified using gene specific primers with gDNA as template. The genes, *Sp* ChiA and *Sp* ChiD were predicted (http://www.cbs.dtu.dk/services/SignalP/) to contain N-terminal leader peptides directing sec-dependent secretion. Both these genes were cloned without the signal peptide-encoding nucleotides (*Sp chiA*: 69 bp and *Sp chiD*: 57 bp). The amplicons, 1.62 kb of *Sp chiA*, 1.49 kb of *Sp chiB*, 1.45 kb of *Sp chiC* and 1.22 kb of *Sp chiD* were cloned in the *Nco* I and *Xho* I sites of pET- 28a (+) and pET 22b (+), respectively (Fig. 3.3A-D). The clones were confirmed by double digestion with *Nco* I and *Xho* I enzymes (Fig. 3.3E-H) and the insert sequence was confirmed by automated DNA sequencing (Europhins, India).

3.2.2 Expression and purification of *Sp* chitinases

All the four *Sp* chitinase genes were over expressed with C-terminal His-tag in *E. coli*. The expressed chitinases, either extracted from whole cell lysate (*Sp* ChiA-ChiC) or periplasmic fraction (*Sp* ChiD), were obtained in soluble form. The extracted proteins were purified using Ni-NTA agarose chromatography. SDS-PAGE analysis (Fig. 3.4) of purified chitinases revealed a molecular weight of 58, 55, 54 and 44 kDa which correspond to *Sp* ChiA, *Sp* ChiB, *Sp* ChiC and *Sp* ChiD, respectively.

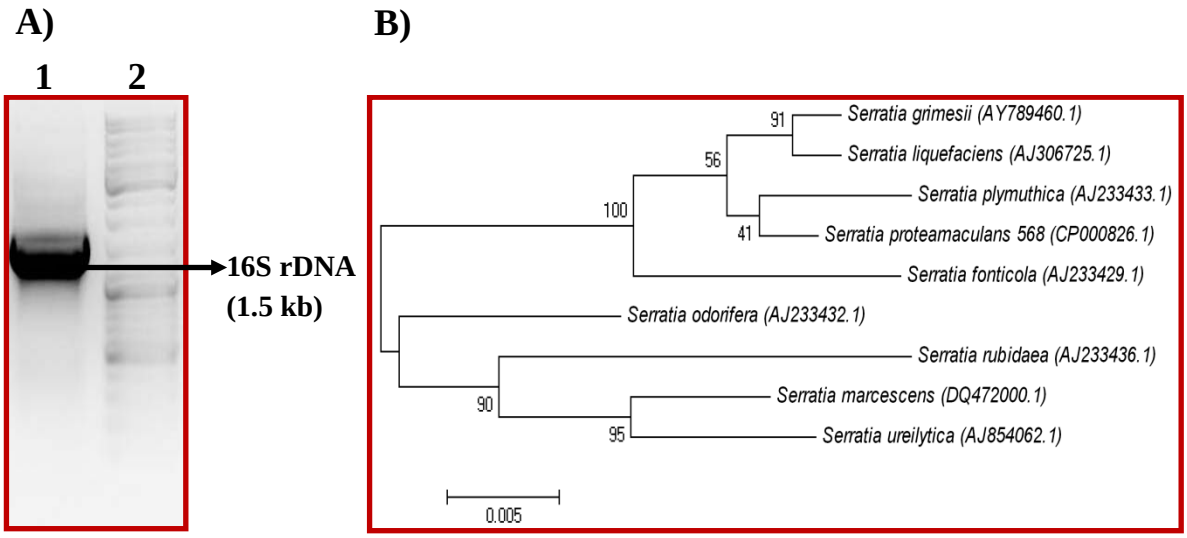

Fig. 3.1: Phylogenetic analysis of *S. proteamaculans* 568

A) *S. proteamaculans* 16S rDNA was PCR amplified using bacterial universal primers. Lane 1: Amplified 16S rDNA, Lane 2: DNA ladder mix (100 bp - 10 kb).

B) Amplified *S. proteamaculans* 16S rDNA was gel extracted and sequenced. A non-rooted phylogenetic tree of 16S rDNA sequence from *S. proteamaculans* 568 (CP000826.1) with the other representatives of the species of *Serratia* with validly published names were used for the phylogenetic analysis. The numbers on the tree are the percentages of bootstrap replicates in which the cluster was found. The scale bar indicates the amount of genetic change measured as the number of nucleotide substitutions per site.

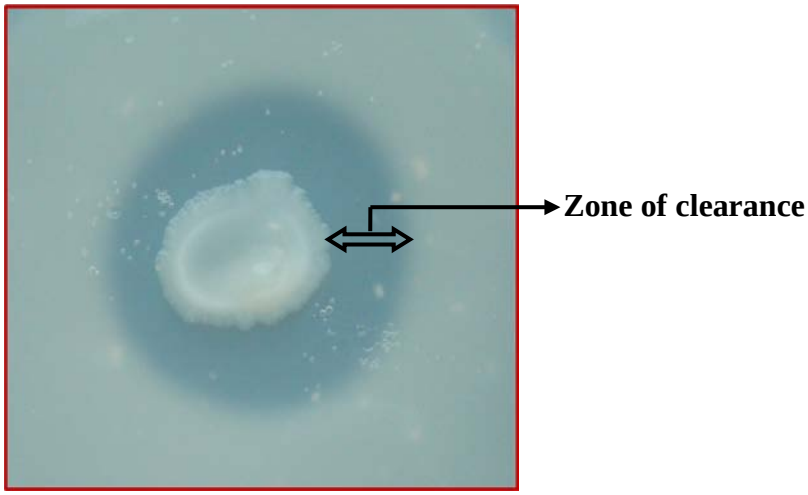

Fig. 3.2: *S. proteamaculans* 568 on chitin containing agar

S. proteamaculans 568 was spotted on colloidal chitin containing M9 minimal medium and incubated for 4 days at 28°C.

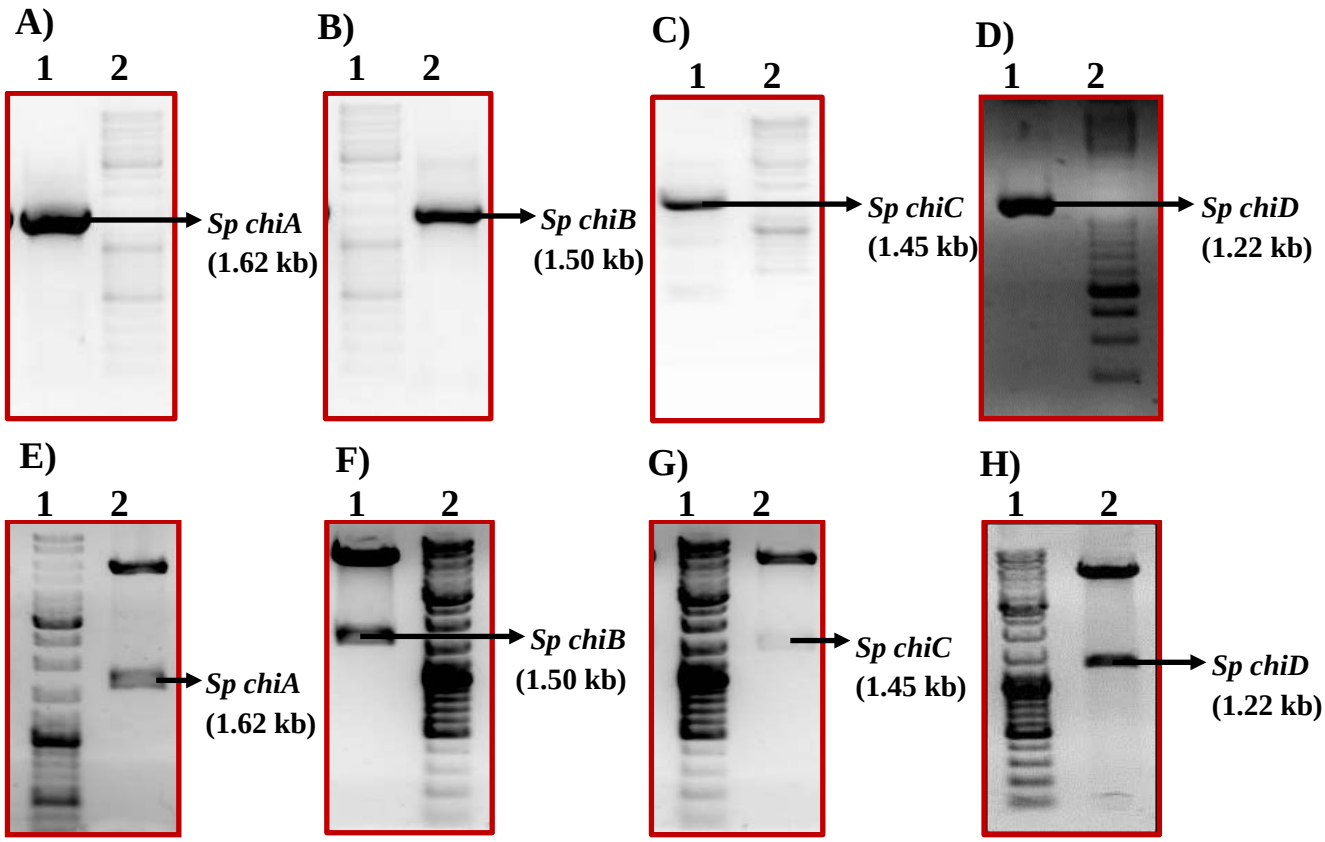

Fig. 3.3: Amplification and cloning of chitinases from *S. proteamaculans* 568

A-D. Chitinases from *S. proteamaculans* 568, *Sp chiA* (Lane A1), *Sp chiB* (Lane B2), *Sp chiC* (Lane C1), *Sp chiD* (Lane D1) were PCR-amplified with gene specific primers using gDNA as template and resolved on a 1% agarose gel. The molecular weight marker was DNA ladder mix (100 bp - 10 kb; lanes A2, B1, C2, and D2).

E-H. The amplicons were ligated to *Nco* I and *Xho* I sites of pET- 28a (+) [*Sp chiA*, *Sp chiB* and *Sp chiC*] and pET 22b (+) [*Sp chiD*]. The presence of insert was confirmed by double digestion with *Nco* I and *Xho* I. Lane E2: *Sp chiA* (1.62 kb), Lane F1: *Sp chiB* (1.50 kb), Lane G2: *Sp chiC* (1.45 kb), Lane H2: *Sp chiD* (1.221 kb). The molecular weight marker was DNA ladder mix (100 bp -10 kb; lanes E1, F2, G1, and H1).

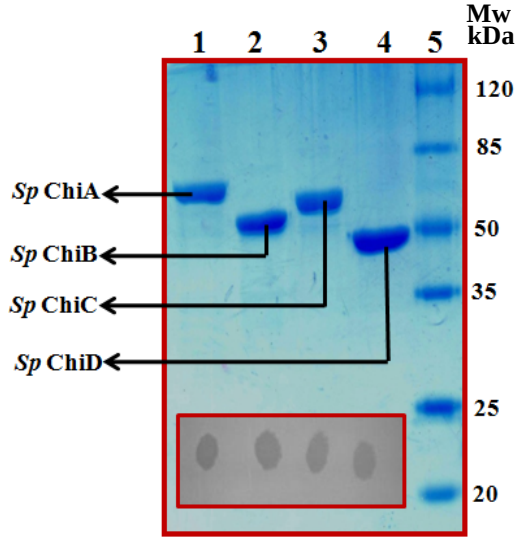

Fig. 3.4: Purification and activity analysis of of *S. proteamaculans* chitinases

Recombinant *Sp* ChiA, *Sp* ChiB, *Sp* ChiC and *Sp* ChiD were purified using Ni-NTA agarose chromatography. Elution buffer containing 250 mM imidazole was used to elute chitinases from the column and loaded on 12% SDS-PAGE followed by staining with Coomassie brilliant blue G-250. The molecular weight (Mw) of the standards is indicated in kDa. Lane 1-4: Purified *Sp* ChiA, *Sp* ChiB, *Sp* ChiC and *Sp* ChiD; lane 5: Protein standards.

Inset showing the activity of purified *Sp* chitinases. Purified chitinases were spotted (5 µg) on glycol chitin substrate containing polyacrylamide gel chamber and incubated overnight at 37°C in humid chamber. After incubation, the gel was stained with 0.01% Calcofluor white M2R for 10 min at 4°C. Finally, the brightener solution was removed and the gel was washed with distilled water for 10 min at 4°C. The gel was placed on UV transilluminator to visualize lysis zones. Lanes 1-4: *Sp* ChiA, *Sp* ChiB, *Sp* ChiC and *Sp* ChD enzymes.

3.2.3 Dot blot activity assay of *Sp* chitinases

The purified recombinant *Sp* chitinases were spotted on glycol chitin substrate containing polyacrylamide gel to detect the activity. All the four recombinant *Sp* chitinases showed activity zones on substrate containing gel (Fig. 3.4).

3.2.4 Charachterization

3.2.4.1 Steady state kinetics analysis

The kinetic values of the enzyme were determined with colloidal chitin as substrate using reducing end assay. Specific activity (µmoles/sec/mg of protein) and substrate concentration (mg/ml) data were directly fitted to the Michaelis–Menten equation by nonlinear regression function of (Fig. 3.5 and Table 3.1) GraphPad Prism version 5.0 software. The curve fitting for the enzymes showed highest V_{max} value for *Sp* chiA (4.317×10^{-2}) followed by *Sp* ChiB (3.559×10^{-2}), *Sp* ChiC (2.244×10^{-2}) and *Sp* ChiD (0.663×10^{-2}). The K_m for ChiA (2.625) was lower than those of *Sp* ChiB (5.556), *Sp* ChiC (5.164) and *Sp* ChiD (70.00) indicating the substrate-binding affinity of *Sp* ChiA was highest than the other three chitinases (*Sp* ChiA, *Sp* ChiB and *Sp* ChiC). Among the *Sp* chitinases, catalytic activity (k_{cat}) of *Sp* ChiA had highest value (1.013×10^{-2}) followed by *Sp* ChiB (0.079×10^{-2}), *Sp* ChiC (0.046×10^{-2}) and *Sp* ChiD (0.021×10^{-2}). *Sp* ChiA (0.385×10^{-2}) displayed the highest overall catalytic efficiency (k_{cat}/K_m) when compared to *Sp* ChiB (0.14×10^{-2}), *Sp* ChiC (0.09×10^{-2}) and *Sp* ChiD (0.003×10^{-2}). V_{max}, k_{cat} and k_{cat}/K_m decreased from *Sp* ChiA-ChiD while K_m increased from *Sp* ChiA-ChiD except that the *Sp* ChiC affinity towards substrate was slightly lower than the *Sp* ChiB.

3.2.4.2 Effect of pH

Enzyme assay with different pH range buffers revealed that *Sp* ChiA and *Sp* ChiC showed opimum activity in sodium phosphate buffer pH 7 and 6, respectively, while *Sp* ChiB and *Sp* ChiD had optimum activity in sodium acetate buffer pH 6 (Fig. 3.6). *Sp* ChiA was active over a broad pH range between pH 5.0 – 11.0, and the activity was less than half maximum below pH 5.0. *Sp* ChiB maintained 80% of its maximum activity between pH 5.0-8.0 and steadily lost activity below pH 2.0. *Sp* ChiC had a narrow pH activity profile with only 40% of its maximum activity between pH 4 and 8 and negligible activity at pH 3.0 and 12.0. *Sp* ChiD showed 70% of its maximum activity between pH 5.0 and 9.0 and completely lost activity at pH 2.0 and 12.0.

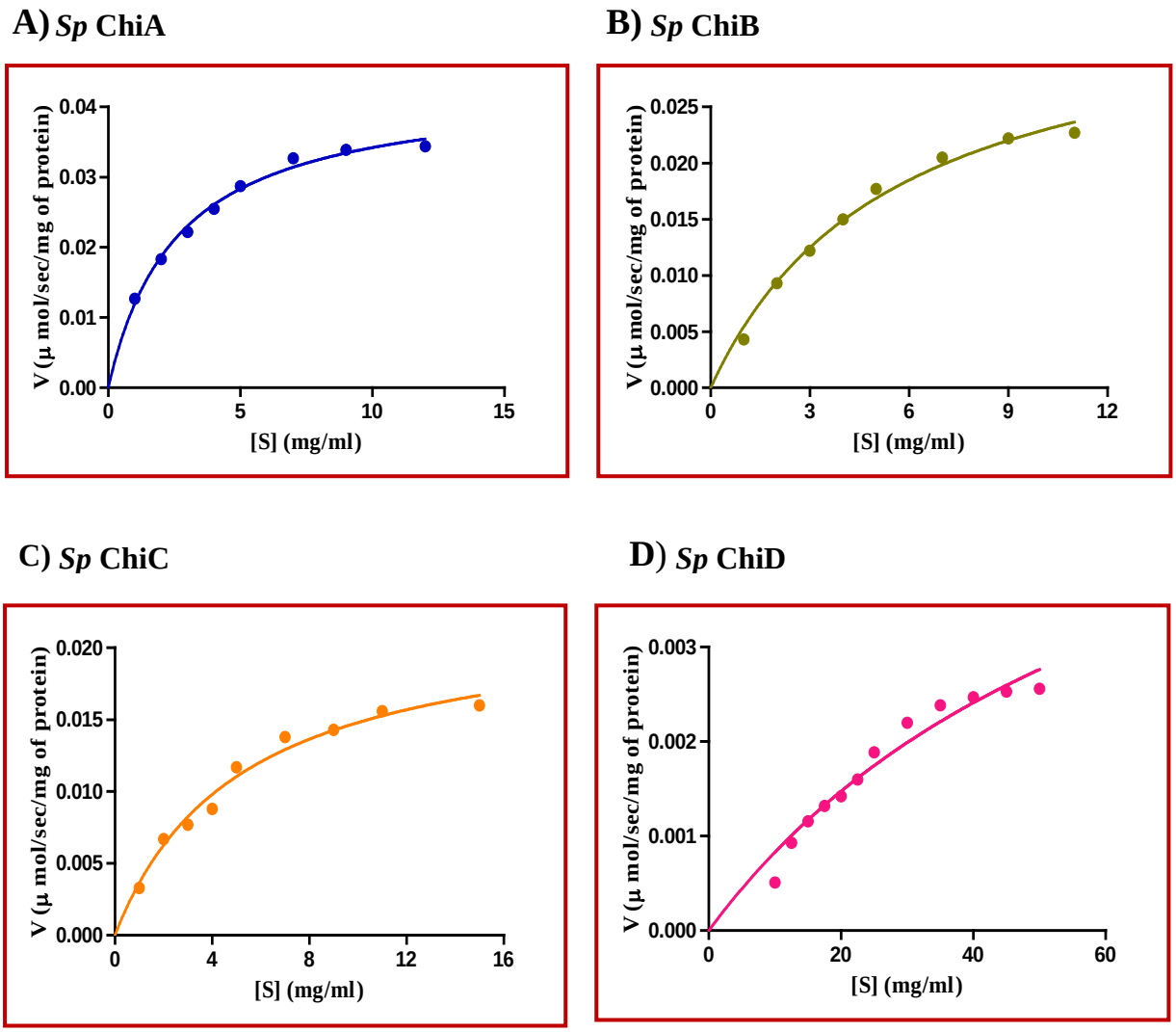

Fig. 3.5: Kinetic analyses of *Sp* chitinases on colloidal chitin substrate

Kinetic analyses of *Sp* chitinases were done by reducing end assay using colloidal chitin as a substrate. Varying concentration of substrate (*Sp* ChiA-ChiC: 0-15 mg/mL and *Sp* ChiD: 0-50 mg/mL) was incubated with *Sp* chitinases (*Sp* ChiA-ChiC: 5 µg and *Sp* ChiD: 27 µg) in 50 mM buffer with respective controls in triplicates at 40°C for 1 h at 190 rpm. Specific activity in µmoles/sec/mg of protein was calculated and plotted against substrate concentration. The data was fitted to the Michaelis–Menten equation by nonlinear regression function using GraphPad Prism software version 5.0, to construct the kinetics graph and derive kinetic parameters.

A-D. Kinetic graphs of *Sp* ChiA-ChiD.

Enzyme	V_{max} (µmol sec^{-1} mg^{-1} of protein)	K_m (mg ml^{-1})	k_{cat} (s^{-1})	k_{cat}/K_m ($mg^{-1}ml\ s^{-1}$)
Sp ChiA	4.317×10^{-2}	2.625	1.013×10^{-2}	0.385×10^{-2}
Sp ChiB	3.559×10^{-2}	5.556	0.079×10^{-2}	0.14×10^{-2}
Sp ChiC	2.244×10^{-2}	5.164	0.046×10^{-2}	0.09×10^{-2}
Sp ChiD	0.663×10^{-2}	70.00	0.021×10^{-2}	0.003×10^{-2}

Table 3.1: Kinetic parameters of colloidal chitin hydrolysis by *Sp* chitinase

GraphPad Prism software version 5.0 was used to calculate V_{max}, K_m, k_{cat} and K_m/k_{cat}.

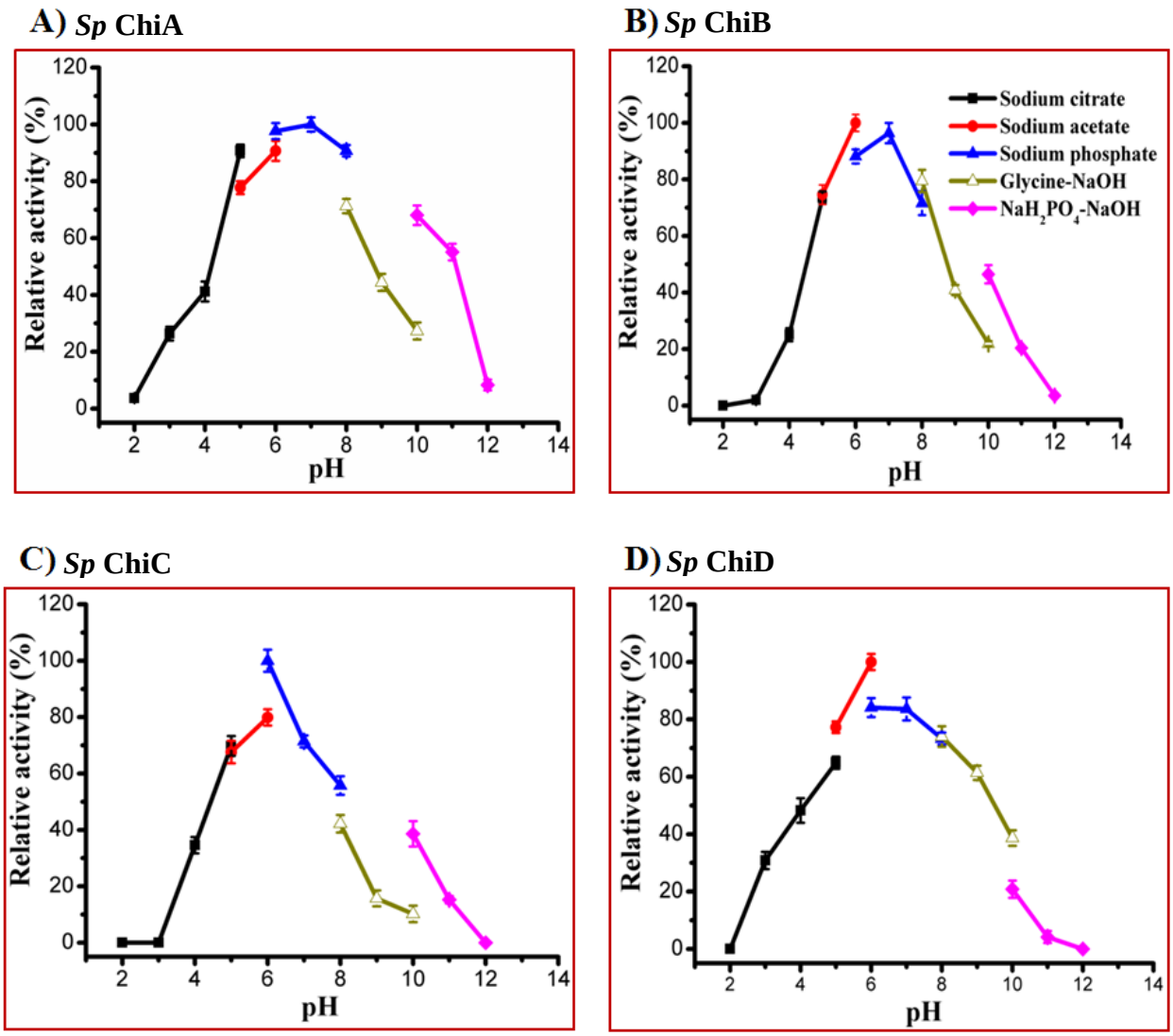

Fig. 3.6: Optimum pH for activity of *Sp* chitinases

The optimal pH of *Sp* chitinases was determined by incubating the enzymes (*Sp* ChiA-ChiC: 5 µg and *Sp* ChiD: 27 µg) with colloidal chitin (*Sp* ChiA-ChiC: 4 mg/mL and *Sp* ChiD: 25 mg/mL) at 40°C for 1 h in 50 mM of different buffers pH ranging from 2-12 and the relative activity (%) was determined under standard assay condition. Vertical bars represent standard deviation of triplicate experiments.

A-D. *Sp* ChiA-ChiD

3.2.4.3 Effect of temperature

The *Sp* chitinases were incubated with colloidal chitin, at different temperatures (20-100^{o}C) to study the optimum temperature for the four chitinases. All four *Sp* chitinases had temperature optimum as 40^{o}C (Fig. 3.7). The enzymes, *Sp* ChiA, *Sp* ChiB, and *Sp* ChiD showed ~80% activity at 20^{o}C. The activity of these three enzymes significantly decreased above 40^{o}C; only 40% activity was detectable at 60^{o}C. *Sp* ChiC activity was affected below 40^{o}C, with a ~40% decrease in activity at 20^{o}C. *Sp* ChiB, *Sp* ChiC and *Sp* ChiD had no activity at 100^{o}C, where as *Sp* ChiA showed at least 10% of activity at 100^{o}C.

3.2.4.4 Hydrolyzing activities against various polymeric substrates

To understand the substrate specificities of *Sp* chitinases, the hydrolytic activities of the *Sp* chitinases with different insoluble and soluble polymeric substrates was compared. The purified *Sp* ChiA, *Sp* ChiB and *Sp* ChiC enzymes hydrolyzed β-chitin more efficiently among the other polymeric substrates, while *Sp* ChiD is having highest activity on water soluble chitosan with 90% DDA (Fig. 3.8). The *Sp* ChiB and *Sp* ChiA preferred colloidal chitin as substrate, after β-chitin, while *Sp* ChiC showed preference to glycol chitin. Avicel and CM-cellulose were least preferred by the four *Sp* chitinases.

With α-chitin, *Sp* ChiA had highest activity followed by *Sp* ChiB, *Sp* ChiC and *Sp* ChiD. In β-chitin substrate, *Sp* ChiA and *Sp* ChiB displayed almost equal amount of activity, while *Sp* ChiC, *Sp* ChiD showed lower activity with respect to *Sp* ChiA and ChiB. *Sp* ChiA and *Sp* ChiB had similar preference for colloidal chitin, where as *Sp* ChiC preferred glycol chitin. Colloidal chitin was not a preferred substrate for *Sp* ChiD. When soluble chitin (glycol chitin) was used as a substrate, *Sp* ChiC displayed highest activity among the four chitinases, *Sp* ChiA and *Sp* ChiB had equal activity, while *Sp* ChiD showed the lowest activity. In chitosan with 90% DDA substrate, *Sp* ChiA had highest activity and *Sp* ChiB showed slightly low activity and *Sp* ChiC had half the activity of *Sp* ChiA where as *Sp* ChiD, like with other substrates showed lower activity. Water soluble chitosan with 90% DDA was the preferred substrate for *Sp* ChiA. *Sp* ChiB had slightly low activity, whereas the activities of the *Sp* ChiC and *Sp* ChiD were significantly low in comparison with *Sp* ChiA. Only *Sp* ChiA was active on Avicel among the other *Sp* chitinases. In the soluble cellulose substrate (CM-cellulose), *Sp* ChiA, *Sp* ChiB, *Sp* ChiC showed relatively very low activity compared to other substrates, while *Sp* ChiD displayed no activity. The order of the substrate preference of the all four *Sp* chitinases was as below:

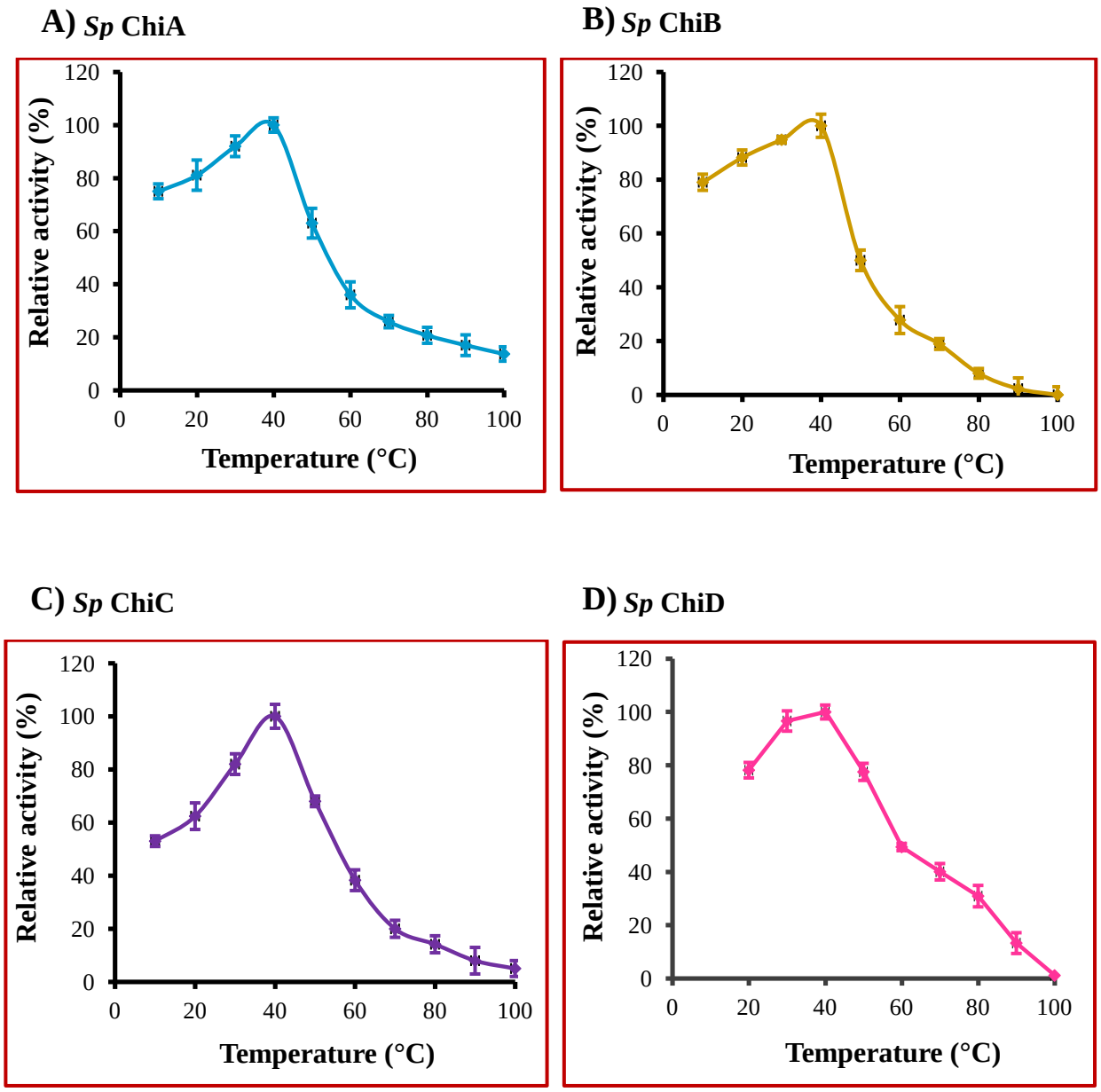

Fig. 3.7: Optimum temperature for activity of *Sp* chitinases

The Optimum temperature for *Sp* chitinases was determined by incubating the chitinases (*Sp* ChiA-ChiC: 5 µg and *Sp* ChiD: 27 µg) with colloidal chitin (*Sp* ChiA-ChiC: 4 mg/mL and *Sp* ChiD: 25 mg/mL) in 50 mM buffers for 1 h at different temperatures ranging from 20-100°C. Relative activity (%) was determined under standard assay condition. Vertical bars represent standard deviation of triplicate experiments.

A-D. *Sp* ChiA-ChiD

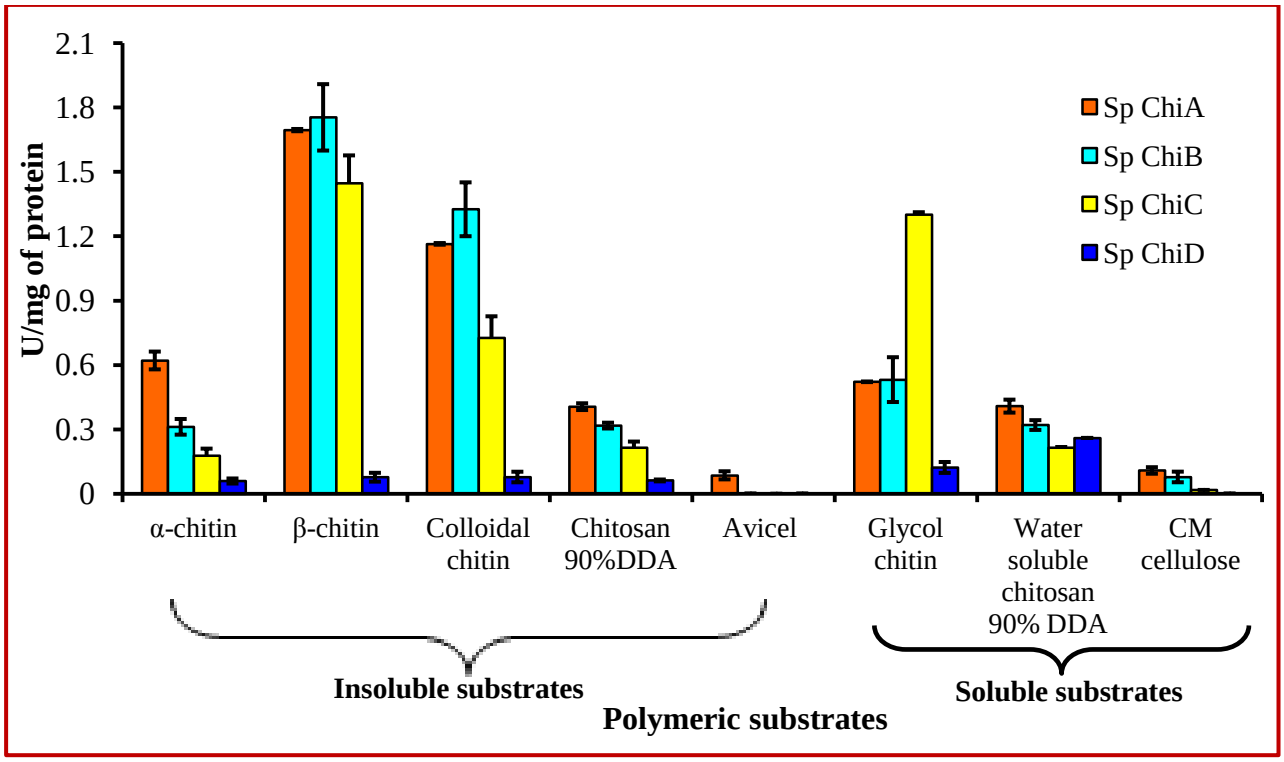

Fig. 3.8: Substrate specificity of *Sp* chitinases

The reaction mixture contained *Sp* chitinases (*Sp* ChiA-ChiC: 5 µg and *Sp* ChiD: 27 µg) and indicated polymeric insoluble and soluble substrates (*Sp* ChiA-ChiC: 0.4%, w/v and *Sp* ChiD: 2.5 %, w/v) were incubated in 50 mM buffer at 40°C for 1 h. The reaction was monitored by reducing sugar determination. One unit of chitinase activity was defined as the amount of enzyme that produces 1 µmol of reducing sugar per minute. Vertical bars represent standard deviation of triplicate experiments.

1. *Sp* ChiA: β-chitin > colloidal chitin > α-chitin > glycol chitin > water soluble chitosan with 90%DDA > chitosan with 90% DDA > CM-cellulose > Avicel.

2. *Sp* ChiB: β-chitin > colloidal chitin > α-chitin > glycol chitin > water soluble chitosan with 90%DDA ≅ chitosan with 90%DDA > CM-cellulose.

3. *Sp* ChiC: β-chitin > glycol chitin > colloidal chitin > water soluble chitosan with 90% DDA > chitosan with 90% DDA > α-chitin > CM-cellulose.

4. *Sp* ChiD: Water soluble chitosan with 90% DDA > glycol chitin > colloidal chitin ≅ β-chitin > chitosan with 90%DDA > α-chitin.

3.2.4.5 Binding of *Sp* chitinases towards insoluble and soluble polymeric substrates

3.2.4.5.1 Insoluble substrates binding

The binding ability of *Sp* chitinases to the insoluble substrates was investigated at 4^{o}C, to minimize enzyme-mediated hydrolysis of the bound substrate. All *Sp* chitinases displayed more than 65% binding to β-chitin and colloidal chitin substrates (Fig. 3.9). Among the *Sp* chitinases, *Sp* ChiA (73.4%) and *Sp* ChiD (68.8%) showed maximum binding to α-chitin where as *Sp* ChiB (56.4%) and *Sp* ChiC (36.9%) had lower binding ability. To the β-chitin, *Sp* ChiC (96.1%) displayed highest binding activity followed by *Sp* ChiA (84.2%), *Sp* ChiD (78.7%) and *Sp* ChiB (63.9%). When colloidal chitin was used as a binding substrate, *Sp* ChiB (93.1%) showed highest binding ability, *Sp* ChiC (86.6%) had slightly low binding activity, where as *Sp* ChiA (76.3%) and *Sp* ChiD (68.9%) showed significantly lower binding. *Sp* ChiB (65.9%) showed maximum binding activity with Avicel. Binding was slightly lower for *Sp* ChiD (50.2%) where as *Sp* ChiC (30.5%) had less than half the binding activity of *Sp* ChiB, while *Sp* ChiA (8.6 %) showed very less binding and displayed only 13.0% of binding to that of *Sp* ChiB.

3.2.4.5.2 Soluble substrates binding

Binding of *Sp* chitinases to soluble polysaccharides was investigated by affinity electrophoresis in a native PAGE with and without polysaccharides. Comparison of electrophoretic pattern of proteins in the presence or absence of the substrates revealed that *Sp* chitinases were not affected by the presence of CM-cellulose, laminarin, or without substrate. The mobility of *Sp* chitinases in the presence of glycol chitin decreased indicating that these enzymes bind to glycol chitin substrate (Fig. 3.10).

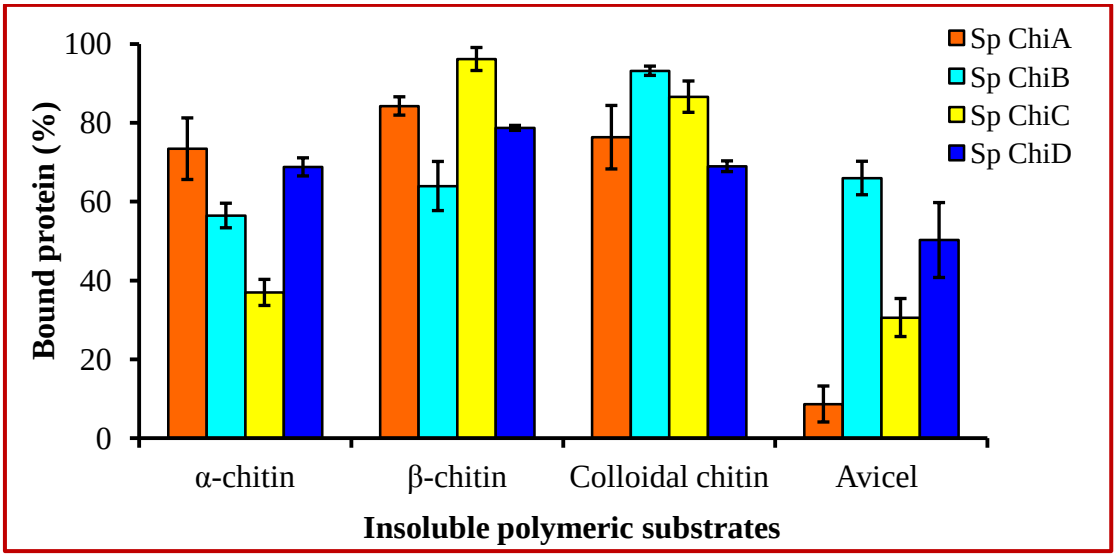

Fig. 3.9: Binding of *Sp* chitinases towards insoluble polymeric substrates

The reaction mixture (1 mL) containing 1 µM *Sp* ChiA/ChiB/ChiC/ChiD and 1 mg of substrate (α-chitin/β-chitin/colloidal chitin/Avicel) was incubated in 50 mM buffer. After incubation at 4°C for 1 h, with constant shaking at 16100 g, the mixtures were centrifuged, unbound protein in the supernatant was estimated. The amount of protein bound was calculated as the difference unbound and initial concentration of protein. Vertical bars represent standard deviation of triplicate experiments.

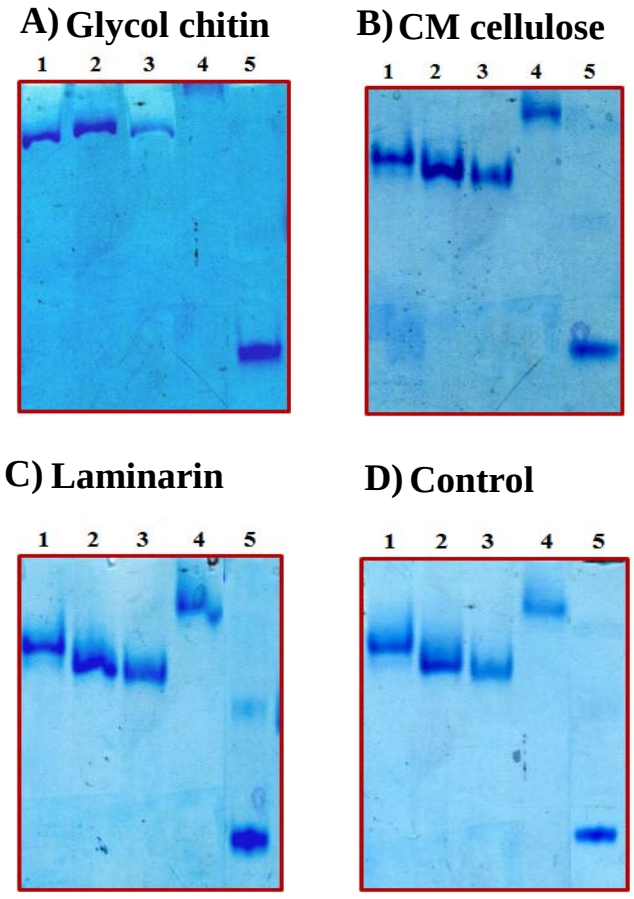

Fig. 3.10: Binding of *Sp* chitinases towards soluble polymeric substrates

Affinity non-denaturing gel electrophoresis was performed at 4°C by preparing 8% polyacrylamide gels. Ten µg of *Sp* chitinases and BSA were electrophoresed without (D) or with 0.1% (w/v) substrates incorporated with glycol chitin (A), CM-cellulose (B) and laminarin (C). Proteins were visualized by Coomassie blue G-250 staining after electrophoresis. Lane 1-4: *Sp* ChiA-ChiD, lane 5: BSA.

3.2.4.6 Hydrolytic activities of *Sp* chitinases on CHOS and colloidal chitin

3.2.4.6.1 Product analysis by thin-layer chromatography

To assess the ability and efficiency of the isolated enzymes to degrade their natural substrates, the hydrolytic products formed in the course of their action on CHOS was analyzed using TLC.

Up to 720 min of incubation, there was no hydrolytic product detected in reaction mixtures containing DP2 substrate with *Sp* ChiA, *Sp* ChiB and *Sp* ChiC, while *Sp* ChiD was able to hydrolyze DP2 to DP1 starting from 15 min of the reaction. The hydrolysis of DP2 by *Sp* ChiD was slow. Complete hydrolysis of DP2 was attained by 720 min (Fig. 3.11A-D).

When DP3 was used as a substrate, *Sp* ChiA, *Sp* ChiB and *Sp* ChiC released DP2 and DP1 end product, while *Sp* ChiD released DP1 as major product by 720 min (Fig. 3.11E-H). *Sp* ChiD also released intermediate, lower chain length DP2 product (hydrolysis) along with higher chain length DP4-DP6 transglycosylation (TG) products. The TG products (DP4-DP6) formation was detectable from 0-5 min, and after that these products were hydrolysed, finally resulting formation of DP1 as end product by 720 min. Substrate hydrolysis rate was slow for *Sp* ChiA-ChiC as they required 180 min to hydrolyze completely, where as the *Sp* ChiD had rapid degradation rate and hydrolyzed the substrate completely within 5 min.

With DP4 substrate, DP2 was detected as major end product from *Sp* ChiA-ChiC enzymes along with DP3 intermediate product, while *Sp* ChiD yielded DP1(Fig. 3.12A-D). *Sp* ChiA and *Sp* ChiB hydrolyzed DP4 directly into DP2 without formation of other intermediate products. The *Sp* ChiC yielded DP3 as intermediate product till 15 min of reaction, which was further hydrolyzed to DP1 and DP2. *Sp* ChiD also released intermediate hydrolysis (DP2 and DP3) and TG (DP5 and DP6) products. TG products formation was visible till 45 min of the reaction. Substrate degradation rate was high for *Sp* ChiA, *Sp* ChiB and *Sp* ChiC. Complete hydrolysis was observed within 3, 1, 5 min, respectively. *Sp* ChiD displayed slower hydrolysis and complete utilization of DP4 and TG products was achieved by 45 min.

When DP5 was used as substrate, *Sp* ChiA-ChiC released DP2 as major end product while *Sp* ChiD released DP1 (Fig. 3.12E-H). *Sp* ChiA, *Sp* ChiB and *Sp* ChiC released DP3 as intermediate product, which was present 180, 15 and 5 min, respectively and further hydrolyzed into DP2 and DP1. On the other hand, *Sp* ChiD also released intermediate hydrolysis (DP2-DP4) and TG (DP6) products. DP5 hydrolysis was rapid for *Sp* ChiA,

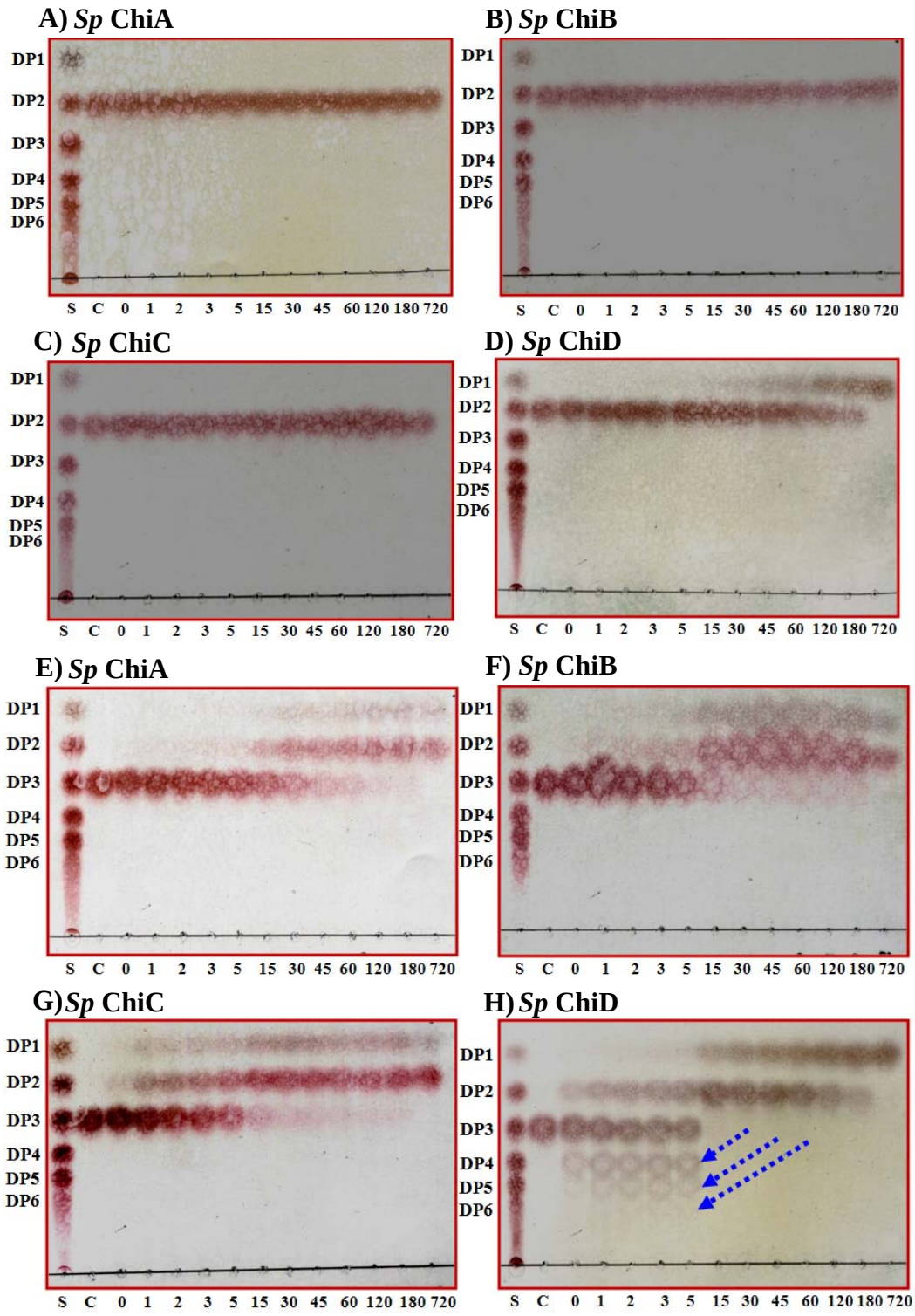

Fig. 3.11: Time course of DP2 and DP3 hydrolysis of *Sp* chitinases as analyzed by TLC

A reaction mixture, containing 5 µg *Sp* chitinases (*Sp* ChiA/*Sp* ChiB/*Sp* ChiC/*Sp* ChiD) and 2.0 mM DP2/DP3 in 50 mM buffer, was incubated at 40^{o}C for varied times starting from 0-720 min. After indicated incubation periods, 10 µL of reaction mixture was withdrawn and mixed with 10 µL of 0.1 N NaOH to stop the reaction. The reaction solution (20 µL) was analyzed on TLC and sugar products were detected with aniline-diphenylamine reagent. Lane S: a standard mix of DP1–DP6, lanes 0-720: incubation times of 0, 1, 2, 3, 5, 15, 30, 45, 60, 120, 180 and 720 min. Dotted lines with arrow indicate the transglycosylation products.

A-D. Hydrolysis of DP2 by *Sp* ChiA-ChiD.

E-F. Hydrolysis of DP3 by *Sp* ChiA-ChiD.

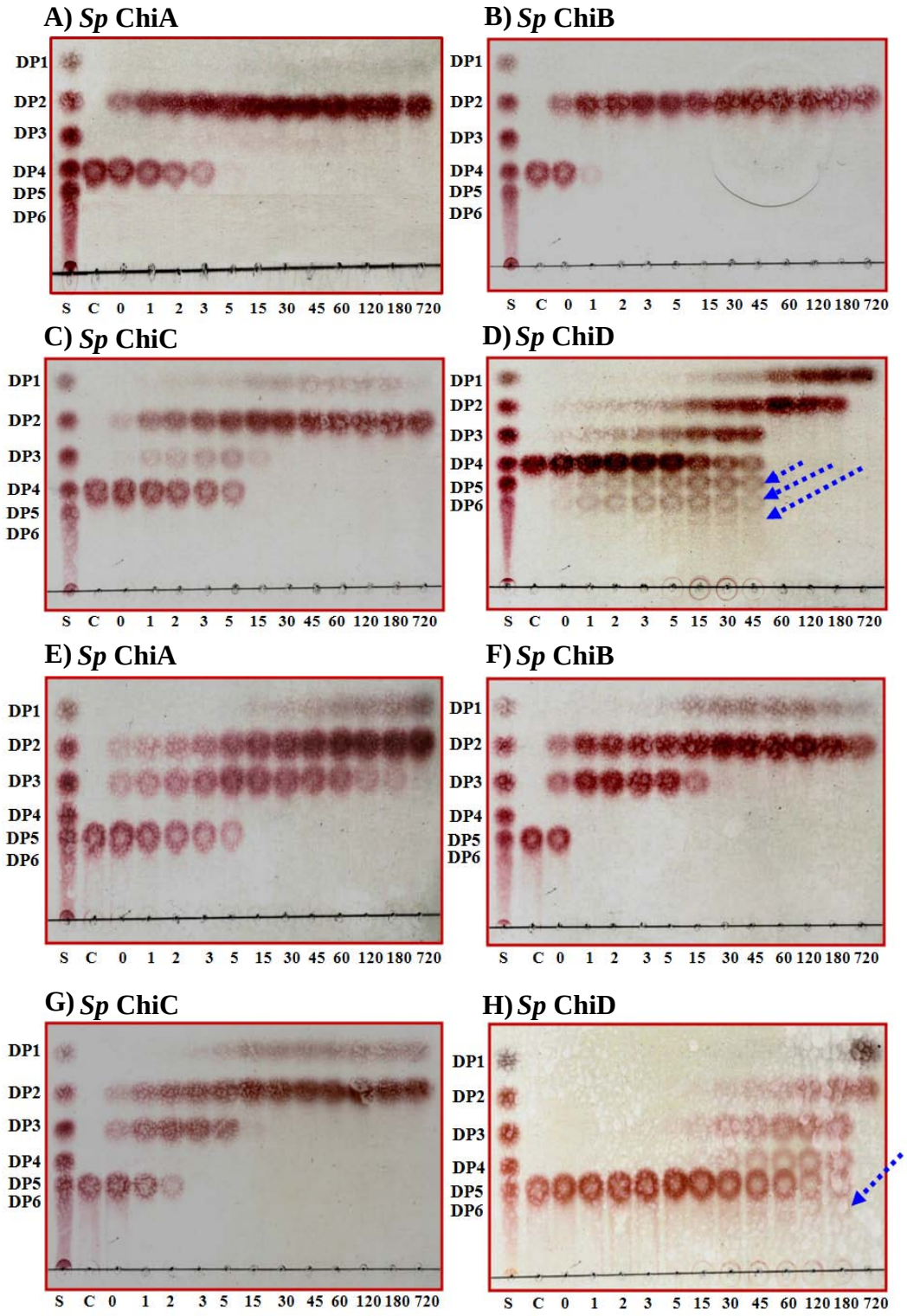

Fig. 3.12: Time course of DP4 and DP5 hydrolysis of *Sp* chitinases as analyzed by TLC

A reaction mixture, containing 5 µg *Sp* chitinases (*Sp* ChiA/*Sp* ChiB/*Sp* ChiC/*Sp* ChiD) and 2.0 mM DP4/DP5 in 50 mM buffer, was incubated at 40^{o}C for varied times starting from 0-720 min. After indicated incubation periods, 10 µL of reaction mixture was withdrawn and mixed with 10 µL of 0.1 N NaOH to stop the reaction. The reaction solution (20 µL) was analyzed on TLC and sugar products were detected with aniline-diphenylamine reagent. Lane S: a standard mix of DP1–DP6, lanes 0-720: incubation times of 0, 1, 2, 3, 5, 15, 30, 45, 60, 120, 180 and 720 min. Dotted lines with arrow indicate the transglycosylation products.

A-D. Hydrolysis of DP4 by *Sp* ChiA-ChiD

E-F. Hydrolysis of DP5 by *Sp* ChiA-ChiD

Sp ChiB, *Sp* ChiC and complete hydrolysis was achieved within 5, 0, 2 min, respectively, while *Sp* ChiD required up to 180 min with a slow rate of hydrolysis.

The hydrolysis of DP6 by *Sp* ChiA-ChiC resulted in DP2 as major product, while *Sp* ChiD released DP1 (Fig. 3.13). *Sp* ChiA, *Sp* ChiB and *Sp* ChiC initially yielded DP3 and DP4 as intermediate products which were further hydrolyzed to DP2 and DP1. On the other hand, *Sp* ChiD also released DP2-DP5 products as intermediate products till 180 min. Substrate degradation rate was higher for *Sp* ChiA, *Sp* ChiB and *Sp* ChiC and complete hydrolysis was observed within 5, 0 and 3 min, respectively, while *Sp* ChiD had lower degradation rate and complete utilization of the substrate was achieved by 180 min.

With DP1-DP6 CHOS substrates, *Sp* ChiA- ChiC resulted in formation of DP1 and DP2 as end products with DP2 as major product, while *Sp* ChiD released DP1 and DP2 as end products with DP1 as a major product. The liberated DP1 product observed from *Sp* ChiA-ChiC could be from the DP3 intermediate product or used substrate in case of DP3. *Sp* ChiA-ChiC have higher substrate hydrolysis rate for DP5 and DP6, lower for DP3 and DP4 substrates and not able to hydrolyse DP2, while *Sp* ChiD had higher substrate hydrolysis rate for DP3 and DP4 and less hydrolysis rate for DP2, DP5 and DP6. *Sp* ChiD produced CHOS that were 1 unit shorter than the starting substrate, such as DP5 from DP6. This result indicated that *Sp* ChiD could liberate a DP1 from the CHOS substrates. In contrast, reactions with *Sp* ChiA, *Sp* ChiB and *Sp* ChiC did not lead to intermediates 1 unit shorter than the starting substrate, and released 2 units shorter than the starting substrate indicating a distinct mode of cleavage.

3.2.4.6.2 HPLC analysis of reaction products

3.2.4.6.2.1 Colloidal chitin hydrolysis by *Sp* chitinases

The hydrolytic activity of *Sp* chitinases was studied using colloidal chitin as substrate at various incubation times. The HPLC profiles showed that all the four *Sp* chitinases released DP1-DP4 with DP2 as predominant product in initial reaction time. At the end of the reaction, the DP2 remained as a major end product from *Sp* ChiA-ChiC, while DP1 was the major end product of *Sp* ChiD (Fig. 3.14 and 3.15). During the reaction time course, DP3 and DP4 intermediate products of *Sp* ChiA-ChiD were further hydrolyzed into DP1 and DP2. The formation of DP3 was high for *Sp* ChiA-ChiD till 60 min, afterwards the degradation started slowly and very low amount was left after 720 min. Similar result was also observed

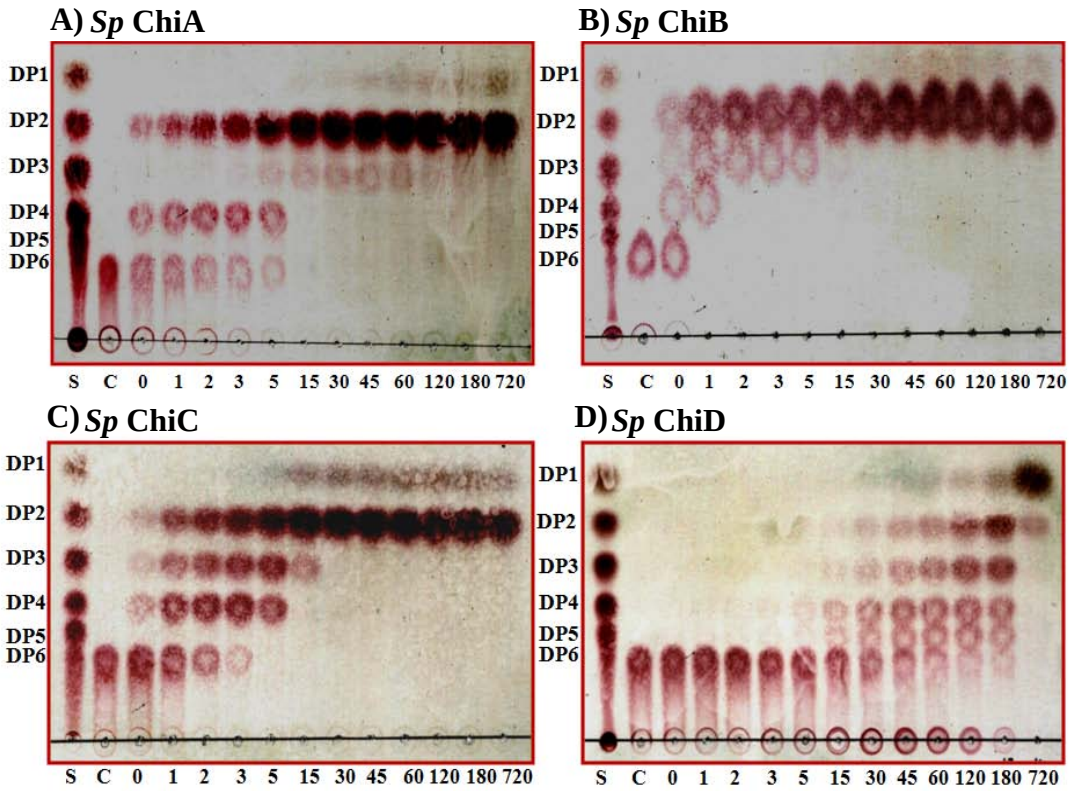

Fig. 3.13: Time course of DP6 hydrolysis of *Sp* chitinases as analyzed by TLC

A reaction mixture, containing 5 µg *Sp* chitinases (*Sp* ChiA/*Sp* ChiB/*Sp* ChiC/*Sp* ChiD) and 2.0 mM DP6 in 50 mM buffer, was incubated at 40^{o}C for varied times starting from 0-720 min. After indicated incubation periods, 10 µL of reaction mixture was withdrawn and mixed with 10 µL of 0.1 N NaOH to stop the reaction. The reaction solution (20 µL) was analyzed on TLC and sugar products were detected with aniline-diphenylamine reagent. Lane S: a standard mix of DP1–DP6, lanes 0-720: incubation times of 0, 1, 2, 3, 5, 15, 30, 45, 60, 120, 180 and 720 min.

A-D. Hydrolysis of DP6 by *Sp* ChiA-ChiD.

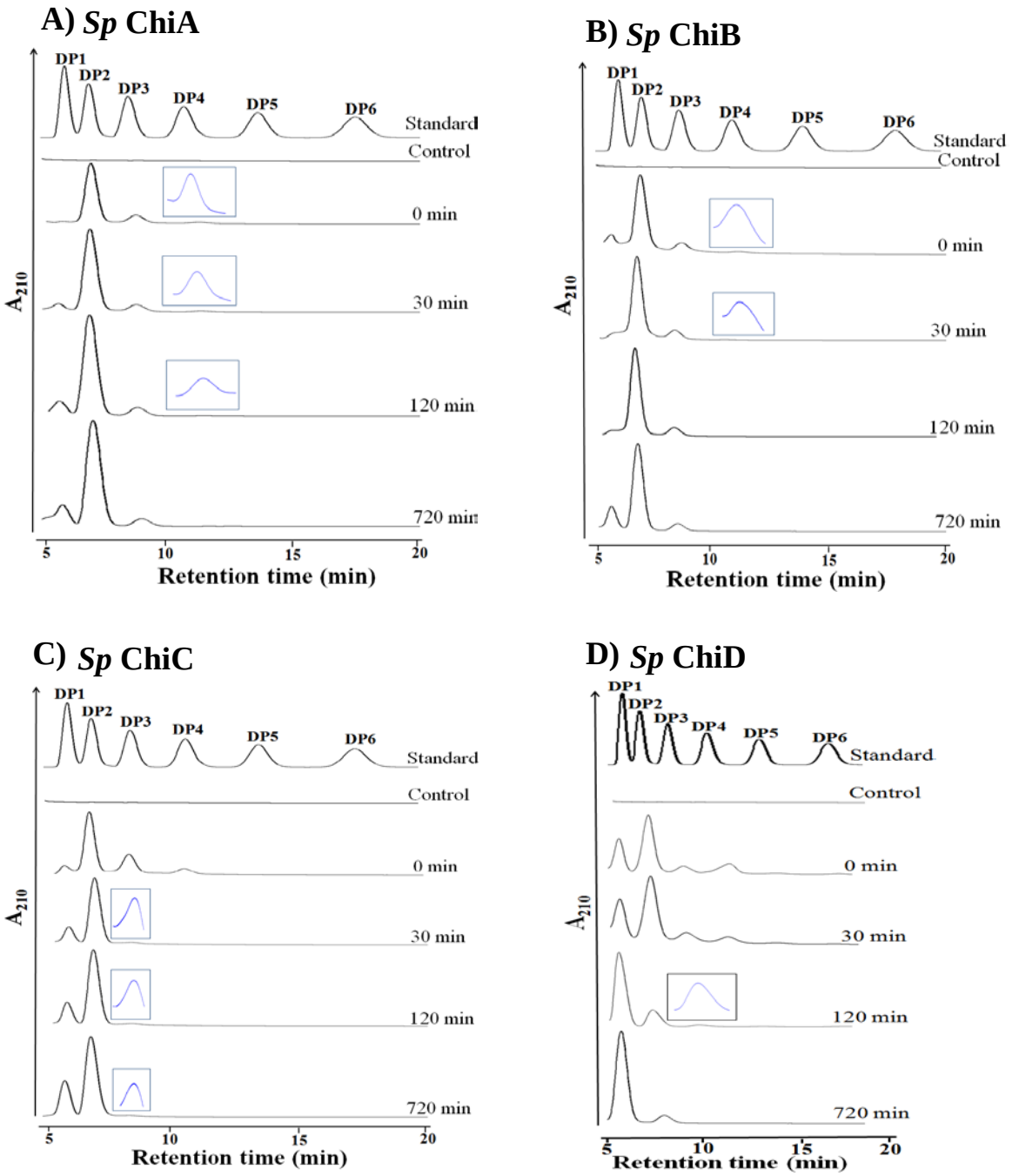

Fig. 3.14: Time course hydrolysis of colloidal chitin by *Sp* chitinases

The reaction mixture (1 mL) containing colloidal chitin (*Sp* ChiA-ChiC: 4 mg/mL and *Sp* ChiD: 25 mg/mL) in 50 mM buffer was incubated with *Sp* chitinases (*Sp* ChiA-ChiC: 0.3 µM and *Sp* ChiD: 3 µM) for different time periods starting from 0-720 min at 40°C. Each time point, 75 µL of reaction mixtures were withdrawn and equal amount of 75% acetonitrile was added to stop the reaction. The reaction mixtures (150 µL each) were centrifuged, and the supernatants were concentrated under reduced pressure without heating till complete evaporation of the solvent and finally dissolved in 20 µL of 35 % acetonitrile. The reaction solution (20 µL) was analyzed by isocratic HPLC using Shodex Asahipack NH2P-50 4E column and eluted CHOS were monitored by recording absorption at 210 nm.

The top most profile shows a standard mixture of CHOS ranging from DP-DP6. The other profiles indicate the reaction proceeding (incubation times indicated). Insets show the magnified low peak area products at specific retention time.

A-D. HPLC product profile of *Sp* ChiA-ChiD.

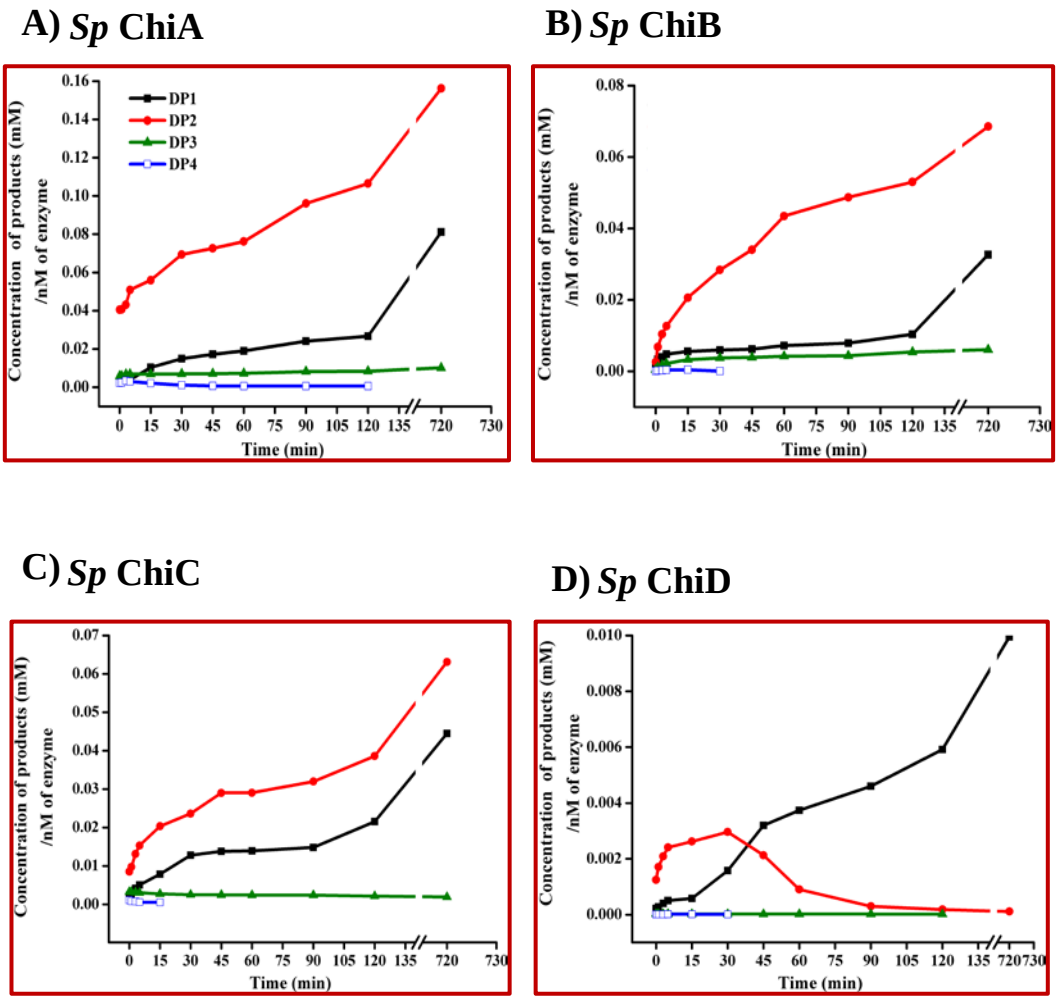

Fig. 3.15: Overview of concentrations of CHOS products generated during reaction time course of colloidal chitin hydrolysis with *Sp* chitinases

The reaction mixture (1 mL) containing colloidal chitin (*Sp* ChiA-ChiC: 4 mg/mL and *Sp* ChiD: 25 mg/mL) in 50 mM buffer was incubated with *Sp* chitinases (*Sp* ChiA-ChiC: 0.3 µM and *Sp* ChiD: 3 µM) for different time periods starting from 0-720 min at 40°C. Each time point, 75 µL of reaction mixtures were withdrawn and equal amount of 75% acetonitrile was added to stop the reaction. The reaction mixtures (150 µL each) were centrifuged, and the supernatants were concentrated under reduced pressure without heating till complete evaporation of the solvent and finally dissolved in 20 µL of 35 % acetonitrile. The reaction solution (20 µL) was analyzed by isocratic HPLC using Shodex Asahipack NH2P-50 4E column and eluted oligosaccharides were monitored by recording absorption at 210 nm. Products were quantified from respective peak areas of products by using standard calibration curves of CHOS ranging from DP1-DP6.

A-D. Time-course of colloidal chitin degradation by *Sp* ChiA-ChiD.

with DP3 in case of *Sp* ChiD but the degradation was more rapid than the other three enzymes and complete degradation was observed after 120 min. *Sp* ChiA, *Sp* ChiB, *Sp* ChiC and *Sp* ChiD degraded intermediate DP4 substrate after 120, 30, 15 and 30 min, respectively.

3.2.4.6.2.2 DP3-DP6 hydrolysis/TG catalyzed by *Sp* ChiD

3.2.4.6.2.2.1 DP3 as substrate

The hydrolysis of DP3 substrate yielded DP1-DP6 products among which DP1-DP2 and DP4-DP6 were hydrolysis and TG products, respectively (Fig. 3.16A&C). Formation of DP4 and DP5 started from 0 min, while DP6 started from 3 min. The concentrations of these TG products steadily increased till 15 min, and decreased later. Complete hydrolysis of DP4 and DP5 was observed after 45 min, while DP6 was hydrolyzed completely after 30 min. DP2 was released as a major product from DP3 substrate up to 120 min. At 0 min of reaction time, the yields of DP1, DP4 and DP5 compared to the DP2 were 62.4%, 10.6%, and 1.9%, respectively. At 15 min of reaction time, the maximum yields of DP4, DP5 and DP6, synthesized relatively to the major hydrolytic product, DP2, were 14.2%, 4.2% and 1.2%, respectively. By 720 min, DP1 and DP2 products only were present in the reaction among which DP1 formation was 4.11- fold higher than that of DP2.

3.2.4.6.2.2.2 DP4 as substrate

Sp ChiD released DP1-DP9 products from DP4 substrate among which DP1-DP3 and DP5-DP9 were hydrolysis and TG products, respectively (Fig. 3.16B&D). Formation of DP5-DP8 products started from 0 min and present till 120 min, while formation of DP9 started from 1 min and present till 90 min along with DP1-DP8 products. Hydrolysis of DP4 mainly resulted in formation of DP2 right through the start of the reaction till 120 min. At 0 min of reaction time, the yields of DP1, DP3, DP5 and DP6 compared to the DP2 were 54.6%, 54.8%, 6.2% and 6.5%, respectively. From DP4 substrate, DP5 and DP6 were the quantifiable TG products and these products reached maximum concentration at 45 min and 30 min, respectively. At 45 min of reaction time, the maximum yield of DP5 was synthesized (16.1%), relative to the major hydrolytic product DP2, while, DP6 was 10.6% at 30 min. By 720 min, only DP1 and DP2 were present in the reaction among which the DP1 product formation was 6.6-fold higher than that of DP2.

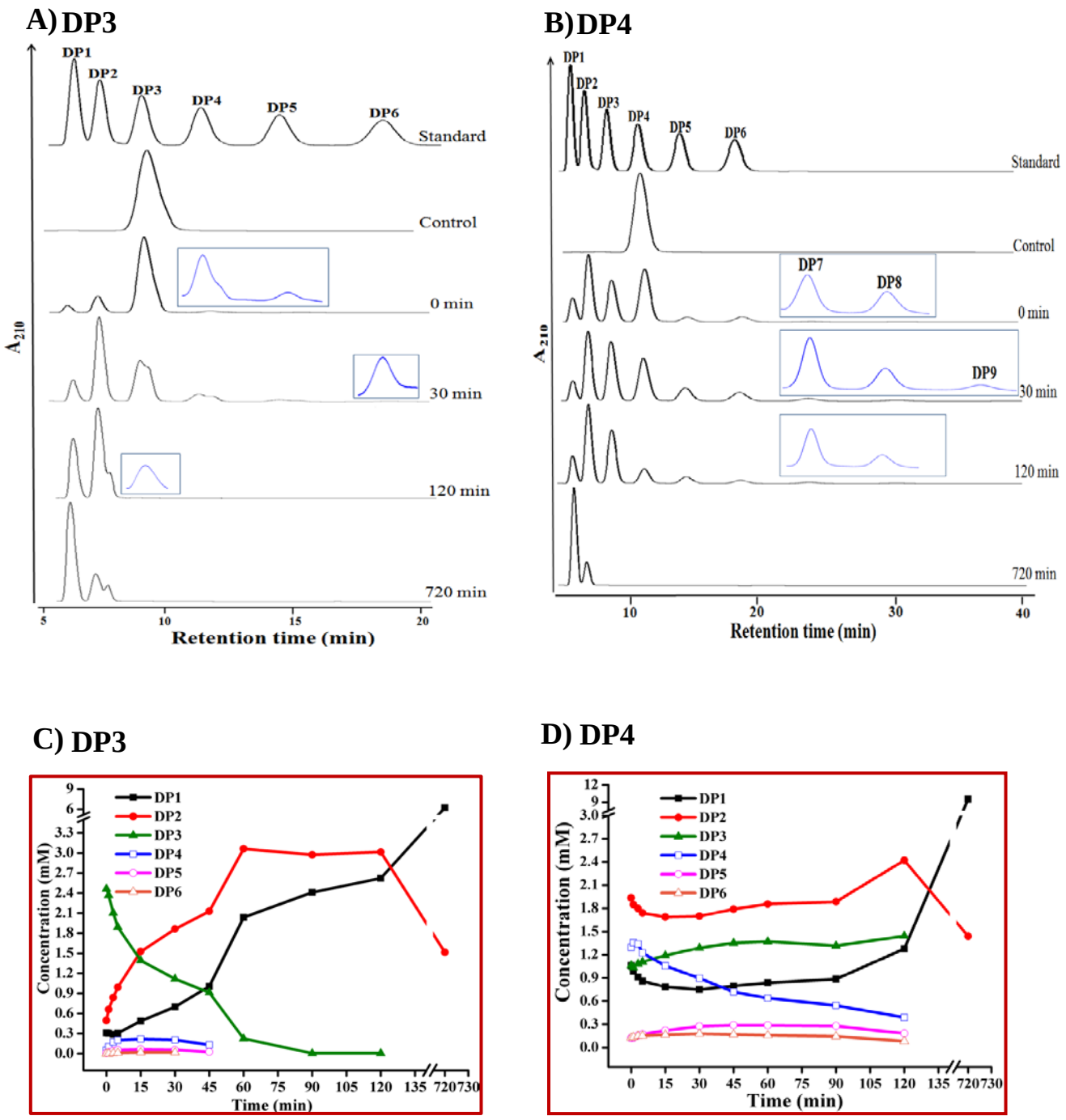

Fig. 3.16: Time course of DP3/DP4 hydrolysis and TG catalyzed by *Sp* ChiD

The reaction mixture containing 3.5 mM DP3/DP4 in 50 mM sodium acetate buffer pH 6 was incubated with 560 nM *Sp* ChiD for different time periods starting from 0-720 min at 40°C. Each time point, 75 µL of reaction mixtures were withdrawn and equal amount of 75% acetonitrile was added to stop the reaction. The reaction solution (20 µL) was analyzed by isocratic HPLC using Shodex Asahipack NH2P-50 4E column and eluted chitooligosaccharides were monitored by recording absorption at 210 nm.

A and B. HPLC profile of DP3 and DP4. The top most profile shows a standard mixture of CHOS ranging from DP1-DP6. The other profiles show how the reaction proceeded (incubation times indicated) of DP3 and DP4. Insets show the magnified view of the low peak area products.

C and D. Overview of concentrations of CHOS products generated during reaction time course of DP3 and DP4. Products were quantified from respective peak areas of products by using standard calibration curves of CHOS ranging from DP1-DP6.

3.2.4.6.2.2.3 DP5 as substrate

Sp ChiD released DP1-DP10 products from DP5 substrate among which DP1-DP4 and DP6-DP9 were hydrolysis and TG products, respectively (Fig. 3.17A&C). Formation of DP6-DP9 products started from 0 min and present till 120 min, while the formation of DP10 started from 1 min and present till 90 min along with DP1-DP9 products. In contrast to the other oligomeric substrate, DP5 hydrolysis resulted in formation of DP3 as a major product starting from 0-45 min. The yields of DP1, DP2, DP4 and DP6, compared to the DP3 at 0 min, were 19.25%, 68.44%, 18.26% and 5.07%, respectively. The product, DP6 was the only quantifiable TG product from the standard curve obtained with authentic oligosaccharide solutions (DP1-DP6). The maximum yield of DP6 synthesized, relatively to the major hydrolytic product DP2, was 11.25% at 90 min. At the end of the reaction (720 min), only DP1and DP2 products were present in the reaction among which the DP1 formation was 2.7-folds higher than that of DP2 product.

3.2.4.6.2.2.4 DP6 as substrate

Sp ChiD formed DP1-DP10 products from DP6 substrate among which DP1-DP5 and DP7-DP10 products were hydrolysis and TG products, respectively (Fig. 3.17B&D). Formation of TG products (DP7-DP10) started from 0 min onwards and present till 90 min, after wards the TG products got degraded. Hydrolysis of DP6 mainly yielded DP2 product starting from 0-120 min. At 0 min of reaction time, the yields of DP1, DP3, DP4 and DP5, compared to the DP2, were 56.0%, 58.0%, 36.8% and 17.8%, respectively. At the end of the reaction (720 min), DP1-DP5 products were present in the reaction among which the DP1 formation was 9.0, 232.16, 475.6 and 973.8-folds higher than that of DP2, DP3, DP4, and DP5, respectively.

3.2.4.6.3 Determination of products identity from DP3-DP6 substrates by MALDI-TOF-MS

Mass-based identities of *Sp* ChiD products, especially to know the TG products that were higher than the DP6, was analyzed with MALDI-TOF-MS. Reaction products from DP3, DP4, DP5 and DP6 substrates showed products ranging from DP2-DP7, DP2-DP10, DP2-DP12 and DP2-DP13 respectively (Fig. 3.18). Majority of the oligosaccharide species formed as Na adducts of the oligosaccharide Na salt.

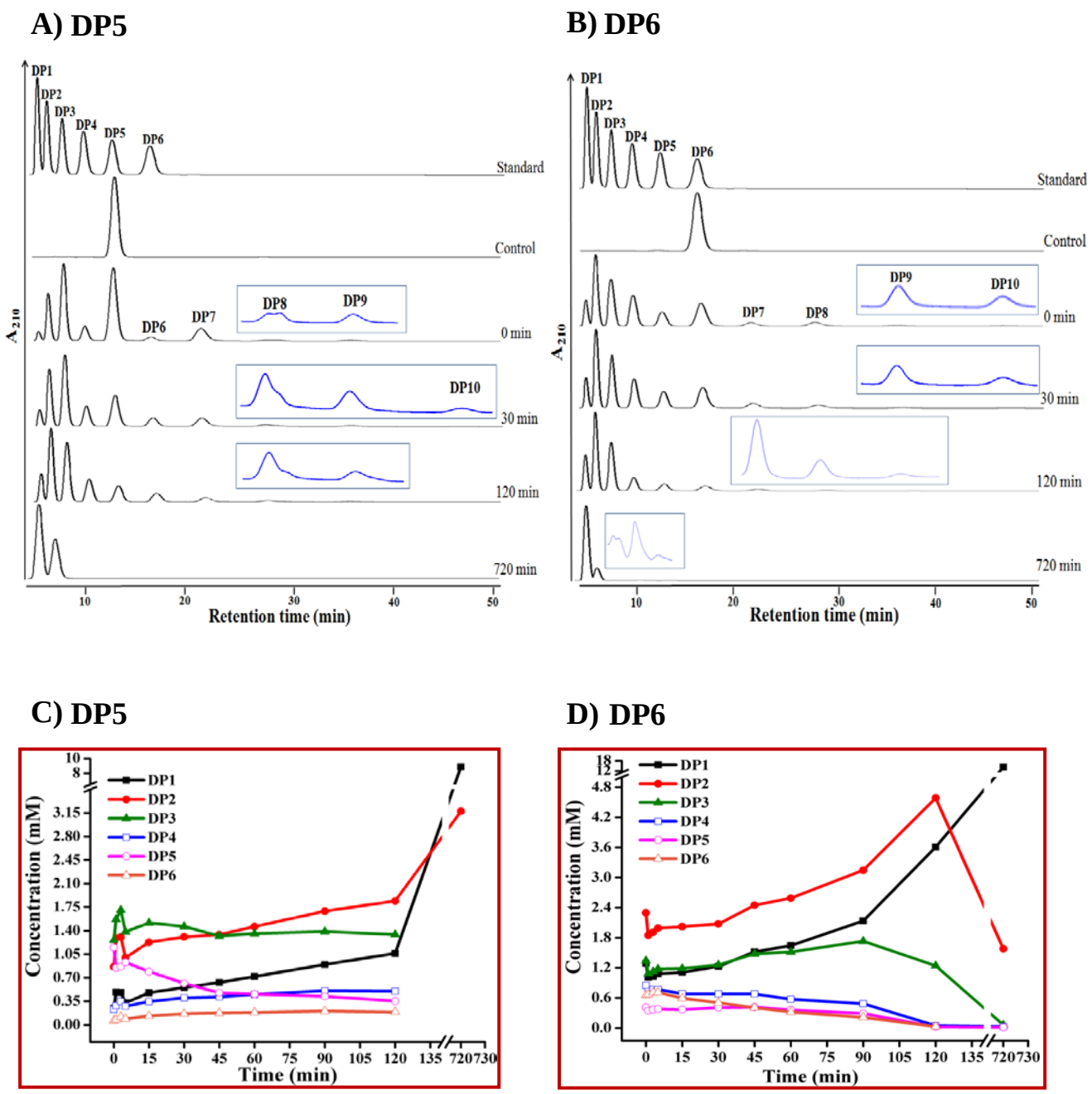

Fig. 3.17: Time course of DP5/DP6 hydrolysis and TG catalyzed by *Sp* ChiD

The reaction mixture containing 3.5 mM DP5/DP6 in 50 mM sodium acetate buffer, pH 6 was incubated with 560 nM *Sp* ChiD for different time periods starting from 0-720 min at 40°C. Each time point, 75 µL of reaction mixtures were withdrawn and equal amount of 75% acetonitrile was added to stop the reaction. The reaction solution (20 µL) was analyzed by isocratic HPLC using Shodex Asahipack NH2P-50 4E column and eluted chitooligosaccharides were monitored by recording absorption at 210 nm.

A and B. HPLC profile of DP5 and DP6. The top most profile shows a standard mixture of CHOS ranging from DP1-DP6. The other profiles show how the reaction proceeded (incubation times are indicated) of DP5 and DP6. Insets shows magnified view of the low peak area products.

C and D. Overview of concentrations of CHOS products generated during reaction time course of DP5 and DP6. Products were quantified from respective peak areas of HPLC of products by using standard calibration curves of CHOS ranging from DP1-DP6.

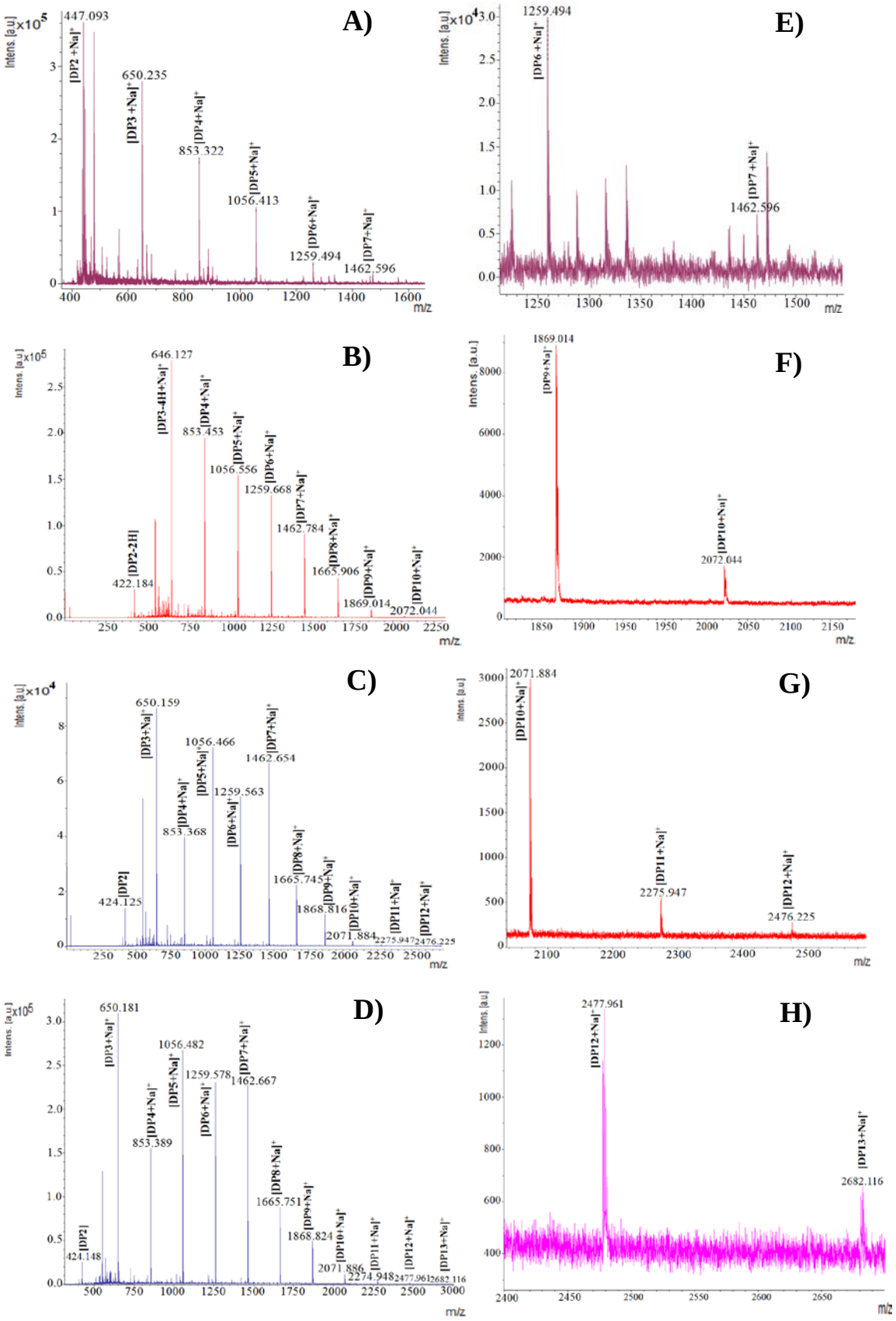

Fig. 3.18: MALDI-TOF-MS analysis of products from DP3-DP6 hydrolysis and TG catalyzed by *Sp* ChiD

After HPLC analysis of reaction products from DP3-DP6 substrate (15th min sample for DP3, DP5 and 30th min sample for DP4, DP6), 40 µL of reaction sample was concentrated under reduced pressure without heating till complete evaporation of solvent and finally dissolved in 4 µL of MilliQ H_2O. The reaction mixture (2 µL) was mixed with an equal volume of 2,5-dihydroxy benzoic acid (2,5-DHB) and the resultant solution was employed for mass measurements using a Ultraflex MALDI-TOF/TOF instrument. Peaks in all MALDI-TOF-MS spectra are labelled according to their observed atomic mass and the DP of the oligosaccharide. Most of the oligosaccharide species were observed as Na adducts of the oligosaccharide Na-salt.

A, B, C, D. MALDI-TOF-MS spectrum of the enzymatic products from DP3-DP6 substrate.

E, F, G, H. Magnification for low peak area products from DP3-DP6 substrate.

3.2.4.7.4 Effect of enzyme and substrate (DP6) concentrations on hydrolysis/TG activities of *Sp* ChiD.

Dose response studies of enzyme and substrate on *Sp* ChiD hydrolysis and TG efficiency were done using DP6 substrate.

Ten-fold lower concentration of enzyme resulted in formation of similar kind of products (DP1-DP10) as compared with normal conditions (560 nM) and substrate degradation rate was slow. Formation of DP4 was high, among the other products, up to 720 min as against predominant DP2 under normal conditions (Fig. 3.19A&E). At 0 min of reaction time, the yields of DP1, DP2, DP3 and DP5 compared to the DP4 were 37.7%, 75.4%, 49.3% and 49.7%, respectively. Along with DP1-DP5 products, TG products (DP7-DP9) were present even after 720 min. At 720 min, the yield of DP1, DP3, DP4 and DP5 compared to major hydrolytic product DP2 was 65.3%, 71.4%, 72.8% and 52.8%, respectively.

Ten-fold higher concentration of enzyme increased hydrolytic activity very significantly and decreased TG activity, resulted in formation of DP1-DP5 and DP7 products, respectively (Fig. 3.19B&F). Among the hydrolytic products (DP1-DP5), 99.1% of the products were DP1-DP3 and only 0.90 % of the products were DP4 and DP5. DP7 was the only TG product formed at 30 min of the reaction. In initial time periods, with high concentration of enzyme, DP2 formed predominantly up to 45 min (as observed in normal conditions), after that DP1 formation steeply increased. At 0 min of reaction, the yields of DP1, DP3, DP4 and DP5 compared to the DP2 were 78.9%, 16.6%, 0.7% and 0.4%, respectively. Substrate utilization rate was very high as expected and complete hydrolysis was observed within 60 min. By 720 min, all the products were hydrolysed to the final product DP1.

Ten-fold decrease in substrate concentration resulted in formation of maximum hydrolytic products (DP1-DP5) except the formation of DP7 as a TG product at 90 min and yielded DP2 as a major product at initial time periods (Fig. 3.19C&G). At 0 min of reaction, the yields of DP1, DP3, DP4 and DP5, compared to the DP2, were 52.3%, 50.2%, 90.7% and 39.6%, respectively. By 720 min, only DP1 and DP2 were present among which DP1 was 2.9-folds higher than that of DP2.

We could not go for ten-fold higher concentration of substrate because of poor solubility but 3-fold decrease of the substrate was tested. Three-fold decrease of the substrate concentration resulted in decrease in TG products formation in comparison with normal

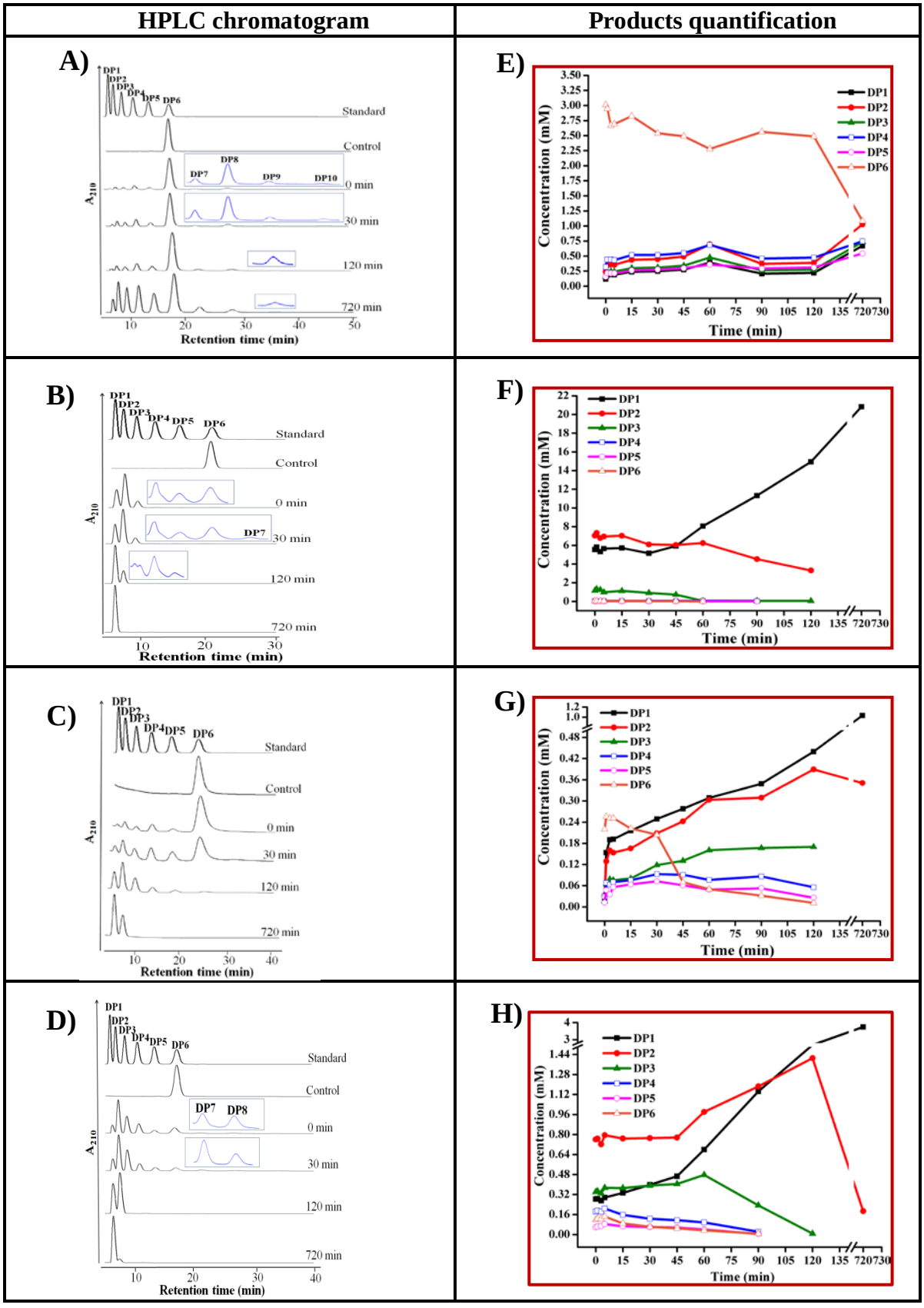

Fig. 3.19: Dose responsive effects of substrate (DP6) and enzyme on hydrolysis/TG catalyzed by *Sp* ChiD

The reaction mixture containing different concentrations of substrate (0.35 and 1.75 mM) and enzyme (56 and 5600 nM) in 50 mM sodium acetate buffer, pH 6 was incubated for different time periods starting from 0-720 min at 40°C. Each time point, 75 µL of reaction mixtures were withdrawn and equal amount of 75% acetonitrile was added to stop the reaction. The reaction solution (20 µL) was analyzed by isocratic HPLC using Shodex Asahipack NH2P-50 4E column and eluted oligosaccharides were monitored by recording absorption at 210 nm.

A, B, C, D. HPLC chromatograms from different concentrations of enzyme **(**56, 5600 nM) and substrate (0.35, 1.75 mM). The top most profile shows a standard mixture of CHOS ranging from DP1-DP6. The other profiles shows how the reaction proceeded (incubation times are indicated). Insets show the magnified view of the low peak area products.

E, F, G, H. Overview of concentrations of CHOS products generated during reaction time course from different concentrations of enzyme **(**56, 5600 nM) and substrate (0.35, 1.75 mM). Products were quantified from respective peak areas of products by using standard calibration curves of CHOS ranging from DP1-DP6.

conditions. Only DP7 and DP8 products were formed as TG products along with DP1-DP5 products, among which DP2 was the major product (Fig. 3.19D&H). At 0 min of reaction time, the yields of DP1, DP3, DP4 and DP5 compared to the DP2 were 37.2%, 44.7%, 24.1% and 7.7%, respectively. By 720 min, only DP1 and DP2 products were present among which DP1 was 19.9-folds higher than that of DP2.

3.2.4.7 Sequence analysis and modelling of *Sp* chitinases

The sequence alignment of catalytic domains of *Sp* ChiA-*Sp* ChiD and Hevamine were generated according to the previously generated structural alignment of *S. marcescens* ChiA, ChiB and hevamine (van Aalten *et al*., 2000). Sequence analysis also showed that the catalytic module of *Sp* ChiC like hevamine lacks an α + β-fold insertion between β-sheets 7 and 8 of the TIM-barrel fold while it's present in other *Sp* chitinases (Fig. 3.20). The catalytic sequence motifs (SXGG and DXDXE) were conserved among the all *Sp* chitinases.

For modelling the *Sp* ChiA, *Sp* ChiB and *Sp* ChiD, the sequences submitted to BLASTP in NCBI for searching the templates for sequences using parameters like protein BLAST against protein data bank (PDB). *Sp* ChiA, *Sp* ChiB and *Sp* ChiD displayed high sequence identity to the sequences of ChiA (94%, ACX42071), ChiB (94%, ACX42072) of *S. marcescens* and chitinase II from *Klebsiella pneumoniae* (78%, ACZ01996), respectively. Then the PDB files, PDM ID: 2WLY, 1E15 and 3QOK of ChiA, ChiB from *S. marcescens* and chitinase II from *K. pneumoniae* were downloaded. Then the hetero atoms from the template PDB was removed and saved the alignment in .ali extension, which is essential for the protein modeling tool called Modeller 9v8. We have generated about 40 models for each protein and then Ramachandran plots also generated for checking the protein structure quality using PROCHECK. Surface exposed aromatic amino acids in *Sp* ChiA (W33, W69, W167, Y170, F232, W245, W275, F396 and Y418) (Fig. 3.21A), *Sp* ChiB (W97, Y98, F190, F191, W220, Y240, W252, W403, Y481 and W479) (Fig. 3.21B) and *Sp* ChiD (Y29, Y89, W120, Y149, W158, W166, W210, Y219, F260, Y232, W247 and W296) (Fig. 3.21C) were also identified in the models. The superimposition of thefinal models Cα atoms on the template structure gave a root mean square deviation (RMSD) of 0.255 Å, 0.222 Å and 0.202 Å for *Sp* ChiA, *Sp* ChiB and *Sp* ChiD, respectively. However, closer inspections of these structures reveal that the conformations of the several regions were differing from the respective template structures. In *Sp* ChiA; α11, α17, α18, β6, loop between β9 and β10 (Fig. 3.22A), *Sp* ChiB;

```
Sp ChiC          ---------MSTNNIINAQAADDAAIMPDMTNKKIMMGFWHNWAAGASDGYQQGQFANMN 51
Heva             ------------------------------------GGIAIYWGQNGNE----GTLTQTC 20
Sp ChiB          ----------------------MSERKAVIGYYFIPTNQINNYTESDTSVVPFPVSNIT 37
Sp ChiD          ----------MVLTRKLLPLLVAVQLGMAGAGMAHAASYLSVGYFNGGGDVTAGPGGDIN 50
Sp ChiA          PLLEKNKPYKQDSGKVVGSYFVEWGVYGRNFTVDKLPAQNLTHLLYGFIPICGGDGINDS 60

Sp ChiC          LTDIPAEYNVVAVAFMKGEGIPTFKPYNLSD-----------AEFRRQVG-----VLNS 94
Heva             STRKYSYVNIAFLXFGNGQTPQINXNPAAGG-----------CTIVSNGX-----SCQI 63
Sp ChiB          PAKAKQLTHINFSFLDINSNLECAWDPATND-----------AKARDVVSRLTALKAHN 85
Sp ChiD          KLDVTQITHLNYSFGLIYNDEKQETNPALKDPSRLHQ--IYLSPKVMADLQLLPVLRKQN 108
Sp ChiA          LKEIEGSFQALQRSCQGREDFKVSIHDPFAALQKGQKGVTAWDDPYKGNFGQLMALKQAR 120

Sp ChiC          QGRAVLISLGG-ADAHIELKTGD-----------EDKLANEIIRLVETYG-FDGLDIDLE 141
Heva             QGIKVMLSLGGGIGSYTLASQAD-----------AKNVADYLWNNFXDAV-LDGIDFDIE 111
Sp ChiB          PNLRIMFSIGGWYYSNDLGVSHANYVNAVKTPAARTKFAQSCVRIMKDYG-FDGVDIDWE 144
Sp ChiD          PELKVLLSVGGWGARGFSGAAATAES--------RAVFIRSVQQVIKQYH-LDGIDLDWE 159
Sp ChiA          PDLKILPSIGGWTLSDPFFFMGDKAK--------RDRFVGSVKEFLQTWKFFDGVDIDWE 172
                        SXGG                                          DXXDXDXE

Sp ChiC          QAAIGAANNKTVLPVALKKVKSHYAAEGKN-----------FIVSMAPEFPYLRTNGTYL 190
Heva             HG-------STLYWDDLARYLSAYSXQGKK-----------VYLTAAPQCPFPDRXGTAX 153
Sp ChiB          YPQSSEVDGFVAALQEIRTLLNQQTLADGRQALP-----YQLTIAGAGGAFFLSRYYSKL 199
Sp ChiD          YPVNGAWGLVESQPADRANFTLLLAELHKALDKG-----KLLTIAVGANVKSPQE-WVDV 213
Sp ChiA          FPGGQGANPKLGSAQDGATYVQLMKELRAMLDQLSAETGRKYELTSAISAGKDKIDKVDY 232

Sp ChiC          DYITALEGYYDFIAPQYYN--------------QGGDGIWVDEANGGKGAWITQNNDAMK 236
Heva             -------GLFDYVWVQFYN--------------NPPCQYSSGNINNIINSWN-------- 184
Sp ChiB          PQIVASLDYINLMTYDLAGPWEKITNHQAGLFGDSAGPTFYNALREANLGWSWEELTRAF 259
Sp ChiD          KGIAPYLDYINLMTYDMAYG----TQYFNSNLYDSKQWPTVAAADRYSANFVVDNYLAAG 269
Sp ChiA          NTAQNSMDHIFLMSYDFYG----AFDLKNLGHQTALKAPSWKPDTAYTTVNGVNALLTQG 288

Sp ChiC          EDFLYYLT---------ESLVTGTRGYSKIPAAKFVIGLPTNN----------------- 270
Heva             ------------------------RWTTSINAGKIFLGLPAAP----------------- 203
Sp ChiB          PSPFSLTV---------DAAVQQHLMLEGVPSNKIVMGVPFYGRAFKGVSSSNGGQYSSH 310
Sp ChiD          LKPAQLNLGIGFYGRVPKRATEPGIDWDKADAAKNPVTQPYFTARETAVFKAMGLDLTKD 329
Sp ChiA          VKPGKIVVG----------TAMYGRGWTGVNGYQNNIPFTGTATGPVKGTWENG------ 332

Sp ChiC          ------------------------------------------------------------D 271
Heva             ------------------------------------------------------------E 204
Sp ChiB          STPGEDPFPGTDYWLVGCEECVRDKDPRIASYRQLEQMLLGNYGYQRLWNDKTKTPYLYH 370
Sp ChiD          SYFKYN--------------------DIVSKLLNDPQRRFTAHWDSDAQVPYLTMKSAE 368
Sp ChiA          ----------------------------IVDYRQIANEFMSGEWQYSYDATAEAPYVFK 363

Sp ChiC          AAATGYVVDKMAVYNAFARLDAKGLSIKGLMTWSVNWDNGRSKAGVAYNWEFKTRYAALI 331
Heva             AAGSGYVPPDVLXR---ILPEIKKSXYGGVMLWSXFYDDKNGYSSSILDSV--------- 252
Sp ChiB          AANGLFVTYDDVESFKYKAKYIKQQQLGGVMFWHLGQDNRNGDLLASLDRYFNAT----- 425
Sp ChiD          GKPLFAISYENPRSVALKADYIKSKGLGGAMFWEYGADDNNRLAHQLAESLGINGGKQ-- 426
Sp ChiA          PSTGDLITFDDARSVQAKGKYVLDKQLGGLFSWEIDADNGD-ILNNMNSSLGNSAGTQ-- 420

Sp ChiC          Q 332
Heva             -
Sp ChiB          -
Sp ChiD          -
Sp ChiA          -
```

Fig. 3.20: Sequence alignments for *Sp* chitinases

Catalytic domains of *Sp* ChiA-*Sp* ChiD and Heva (hevamine from *Hevea brasiliensis*) were aligned using clustalw2 (www.ebi.ac.uk/Tools/msa/clustalw2/). The *Sp* ChiC and *Sp* ChiD sequences are aligned with *Sp* ChiA, *Sp* ChiB and hevamine according to the previously generated structural alignment of ChiA, ChiB from *S. marcescens* and hevamine (van Aalten *et al.*, 2000). The stretches of residues constituting the α+β domain present in *Sp* ChiA, *Sp* ChiB and *Sp* ChiD but lacking in *Sp* ChiC and hevamine, are shaded grey. Small insertions in the hevamine sequence have been replaced by the letter 'X'. Diagnostic sequence motifs containing residues that are crucial for catalysis (SXGG and DXXDXDXE) are shaded yellow and shown below the alignment.

A) *Sp* ChiA

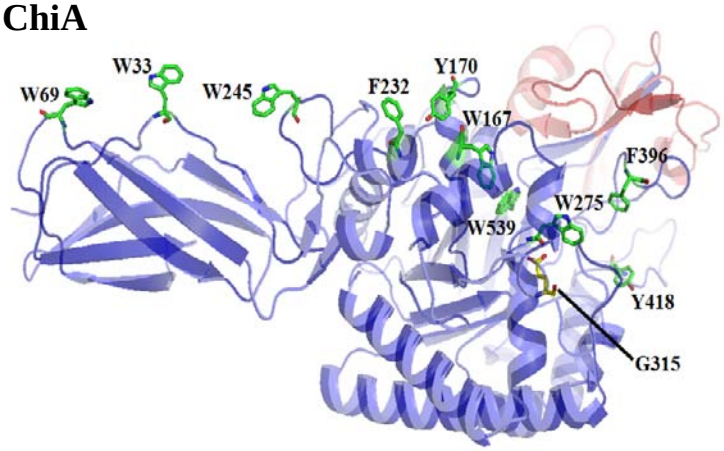

B) *Sp* ChiB

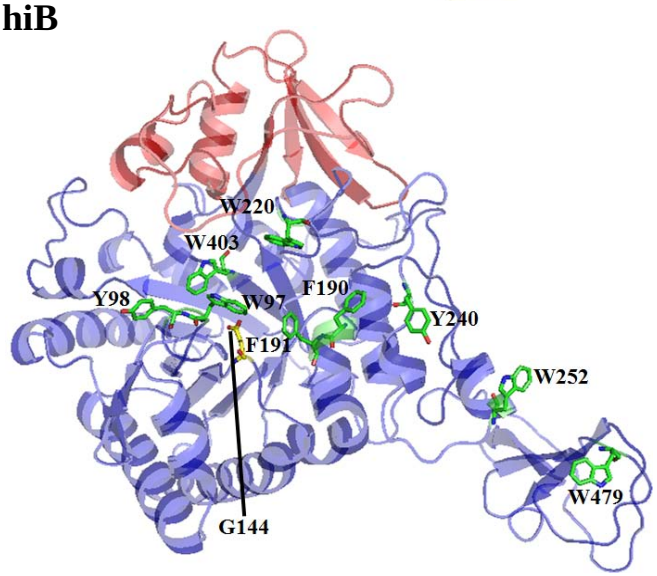

C) *Sp* ChiD

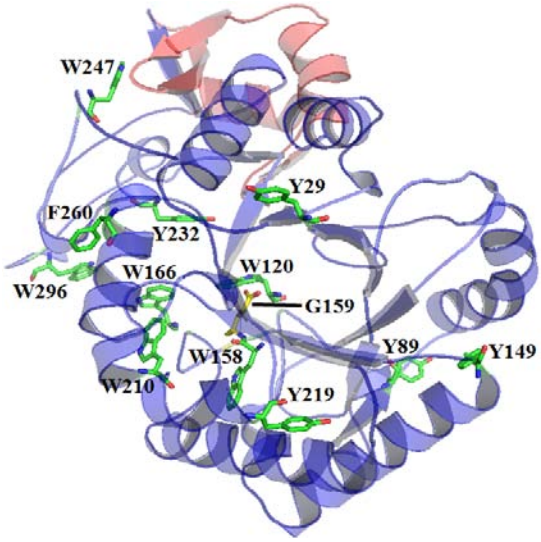

Fig. 3.21: The 3D models of *Sp* ChiA, *Sp* ChiB and *Sp* ChiD

The models of *Sp* ChiA, *Sp* ChiB and *Sp* ChiD were generated by Modeller9v8 (http://www.salilab.org/modeller/) using *S. marcescens* ChiA (PDB ID: 2WLY), ChiB (PDB ID: 1E15) and chitinase II (PDB ID: 3QOK) from *Klebsiella pneumoniae*, respectively as structural templates. The core domain is shown in blue-colored cartoon representation. The region representing the α + β domain that constitutes one of the "walls" of the substrate-binding cleft is colored red. Solvent-exposed aromatic amino acids in substrate-binding cleft are shown in stick representation with carbon, oxygen and nitrogen atoms colored light green, red and dark blue, respectively. The catalytic glutamate is shown in stick representation with carbon, oxygen and nitrogen atoms colored yellow, red and dark blue, respectively. The figures were prepared using PyMOL (http://www.pymol.org/).

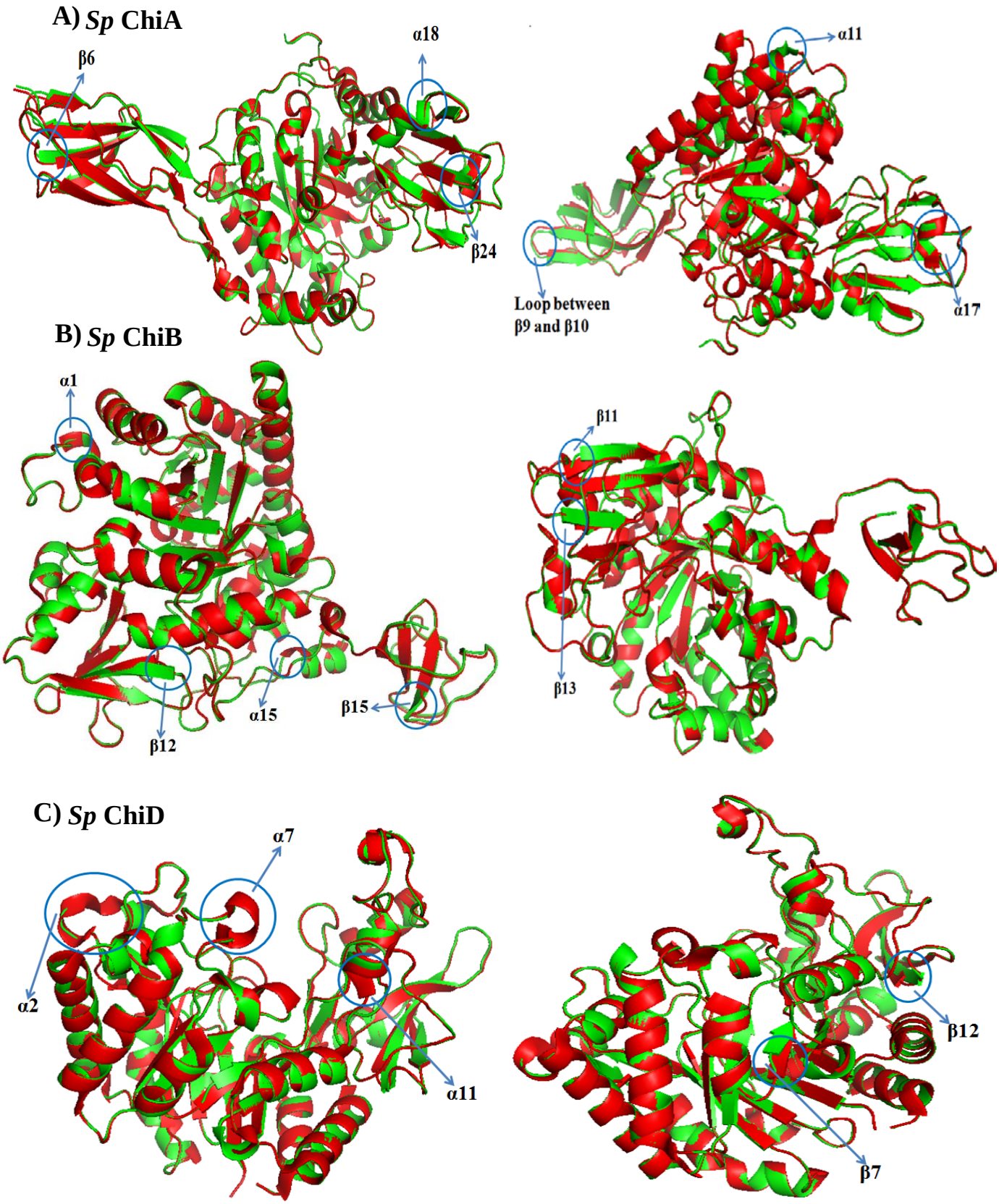

Fig. 3.22: Stereo view of the superimposed structures of *Sp* ChiA, *Sp* ChiB and *Sp* ChiD

Sp ChiA, *Sp* ChiB and *Sp* ChiD structures (green) were superimposed with that of templates (red) of ChiA, ChiB from *S. marcescens* and chitinase II from *Klebsiella pneumoniae*, respectively. Differential regions between the structures were labelled in circle.

A. *Sp* ChiA

B. *Sp* ChiB

C. *Sp* ChiD

α1, α15, β11, β13 and β15 (Fig. 3.22B), *Sp* ChiD; α2, α7, α11, β7 and β12 (Fig. 3.22C) were observed as a differential regions.

3.3 Cloning and characterization of *S. proteamaculans* 568 chitin binding proteins (*Sp* CBPs)

3.3.1 Amplification and cloning of CBPs from *S. proteamaculans* 568

Three *Sp* CBPs were amplified using gene specific primers with gDNA of *S. proteamaculans* 568 as template. All the *Sp* CBPs were predicted to contain N-terminal leader peptides directing sec-dependent secretion. So the gene was cloned without the signal peptide-encoding position (*Sp cbp21*: 66 bp, *Sp cbp28*: bp and *Sp cbp50*: 63 bp). Signal peptide was predicted using the SignalP server (http://www.cbs.dtu.dk/services/SignalP/). The amplicons, 0.51 kb of *Sp cbp21* ,0.762 kb of *Sp cbp28* and 1.350 kb of *Sp cbp50* were cloned in the *Nco* I and *Xho* I sites of pET 22b (+) and *Eco* RI and *Xho* I sites of pET- 28a (+), respectively (Fig. 3.23A-C). The clones were confirmed by double digestion (Fig. 3.23D-F) and the insert sequence was confirmed by automated DNA sequencing (Europhins, India).

3.3.2 Expression and purification of *Sp* CBPs

All the three *Sp* CBPs genes were over expressed with a C-terminal His-tag in *E. coli*. The expressed CBPs were separated either from periplasmic fraction (*Sp* CBP21 and *Sp* CBP28) or from whole cell lysate (*Sp* CBP50) and obtained as soluble proteins. The *Sp* CBPs were purified using Ni-NTA agarose chromatography. SDS-PAGE analysis (Fig. 3.24) of the purified *Sp* CBPs revealed a molecular weight 18.6, 28.0 and 50.0 which correspond to *Sp* CBP21, *Sp* CBP28 and *Sp* CBP50, respectively.

3.3.3 Binding studies of *Sp* CBPs

3.3.3.1 Insoluble substrates

The binding preferences of *Sp* CBPs were assessed by incubating the protein with different insoluble polymeric substrates of chitin [α-chitin, β-chitin and colloidal chitin and cellulose (Avicel)]. The amount of *Sp* CBPs bound to the substrate was analyzed by determining the protein concentrations in the supernatants of the reaction mixtures after 24 h of incubation. The results showed that *Sp* CBP28 was not able to bind to the tested substrates (results not shown), while both *Sp* CBP21 and *Sp* CBP50 bound equally well to β-chitin (86.2% and

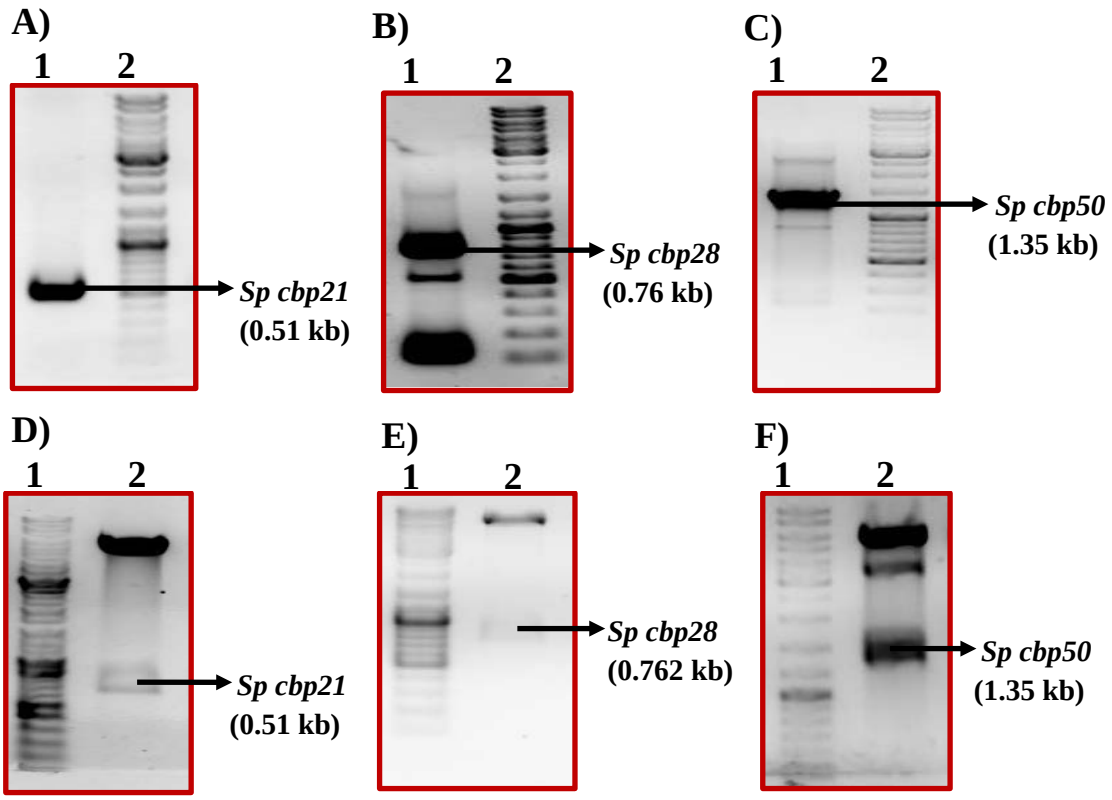

Fig. 3.23: Amplification and cloning of *S. proteamaculans* 568 chitin binding proteins (*Sp* cbps)

A-C. *Sp cbp21* (lane A1), *Sp cbp28* (lane B1), *Sp cbp50* (lane C1) were PCR-amplified with gene specific primers using gDNA as template and resolved on a 1% agarose gel. The molecular weight marker used was DNA ladder mix (100 bp – 10 kb; lanes A2, B1, C2, and D2).

D-F. The amplicons were ligated to *Nco* I and *Xho* I sites of pET- 22b (+) [*Sp cbp*21 and *Sp cbp*28], *Eco* RI and *Xho* I sites of pET- 28a (+) [*Sp cbp50*]. The presence of insert was confirmed by double digestion with respective restriction enzymes. Lane D2: *Sp cbp21* (0.51 kb), lane E2: *Sp cbp28* (0.762 kb), lane F2: *Sp cbp50* (1.352 kb). The molecular weight marker used was DNA ladder mix (100 bp – 10 kb; lanes D1, E2 and F1).

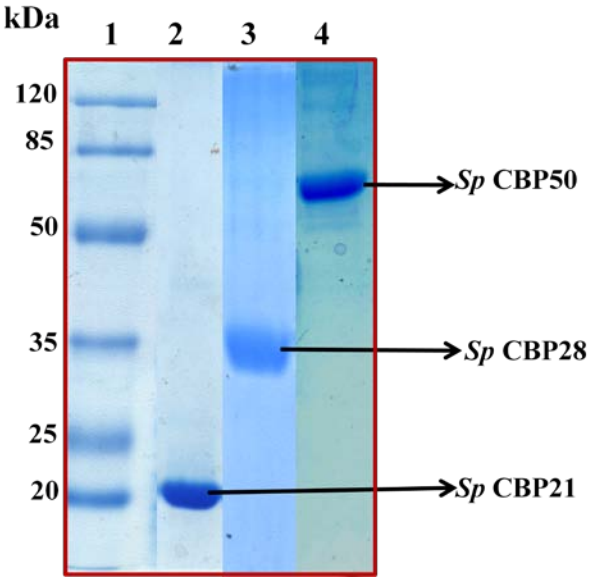

Fig. 3.24: Ni-NTA agarose purification of *Sp* CBPs

Recombinant *Sp* CBP21, *Sp* CBP28 and *Sp* CBP50 were purified using Ni-NTA agarose column chromatography. Elution buffer containing 250 mM imidazole was used to elute *Sp* CBPs from the column and loaded on 12% SDS-PAGE followed by staining with Coomassie brilliant blue G-250. The sizes of the standards are indicated in kDa. Lane 1: Protein standard, lane 2-4: Purified *Sp* CBP21, *Sp* CBP28 and *Sp* CBP50.

77.0%), followed by colloidal chitin (68.8% and 65.6%), α-chitin (30.9% and 25.6%) and Avicel (25.9% and 19.3%) (Fig. 3.25A&B).

3.3.3.1.1 Time - course binding of *Sp* CBP21 and *Sp* CBP50 to α- and β-chitin

In order to find the incubation time needed for the *Sp* CBPs to saturate with natural chitin variants, the time course of binding was monitored for both the *Sp* CBPs as a function of time**.** After separating the protein bound to chitin, the decrease in concentration of the unbound protein (remaining in the supernatant) was monitored at different time points up to 24 h. The binding of *Sp* CBP21 to β-chitin took place rapidly and reached equilibrium within 6 h, while *Sp* CBP50 reached equilibrium after 12 h (Fig. 3.25C). On the other hand *Sp* CBP21 and *Sp* CBP50 have established binding equilibrium to α-chitin after 24 h (Fig. 3.25D).

3.3.3.1.2 Equilibrium adsorption isotherms of *Sp* CBP21 and *Sp* CBP50 to α and β-chitin

Adsorption isotherms of *Sp* CBP21 and *Sp* CBP50 to α- and β-chitin were carried out with fixed concentration of substrate but varied concentrations of the CBPs. When the dissociation binding constants (K_d) of α and β-chitin were estimated from the non-linear regression function (Fig. 3.26 and Table 3.2), the K_d value of the *Sp* CBP21 to α-chitin (5.3 ± 1.04 µM) was much lower than the K_d value of *Sp* CBP50 to α-chitin (9.35 ± 1.68 µM), whereas the K_d value of *Sp* CBP21 to β-chitin (2.22 ± 0.43 µM) was slightly lower than the K_d value of *Sp* CBP50 to β-chitin (2.38 ± 0.5 µM).

3.3.3.2 Soluble substrates

Binding of recombinant *Sp* CBPs to soluble polysaccharides was studied using native PAGE, with and without soluble polysaccharides embedded in the gel. Electrophoretic mobility of *Sp* CBPs has not changed in presence of glycol chitin, CM cellulose and laminarin substrates in comparison with the absence of ligand (Fig. 3.27).

3.3.4 Scanning electron microscopy (SEM) of α-chitin treated with *Sp* CBP21 and *Sp* CBP50

Surface morphological changes of α-chitin treated with *Sp* CBP21 and *Sp* CBP50 were studied using SEM after 24 h of treatment with *Sp* CBP21 or *Sp* CBP50. SEM studies revealed significant changes in surface features of chitin treated with both *Sp* CBPs. The

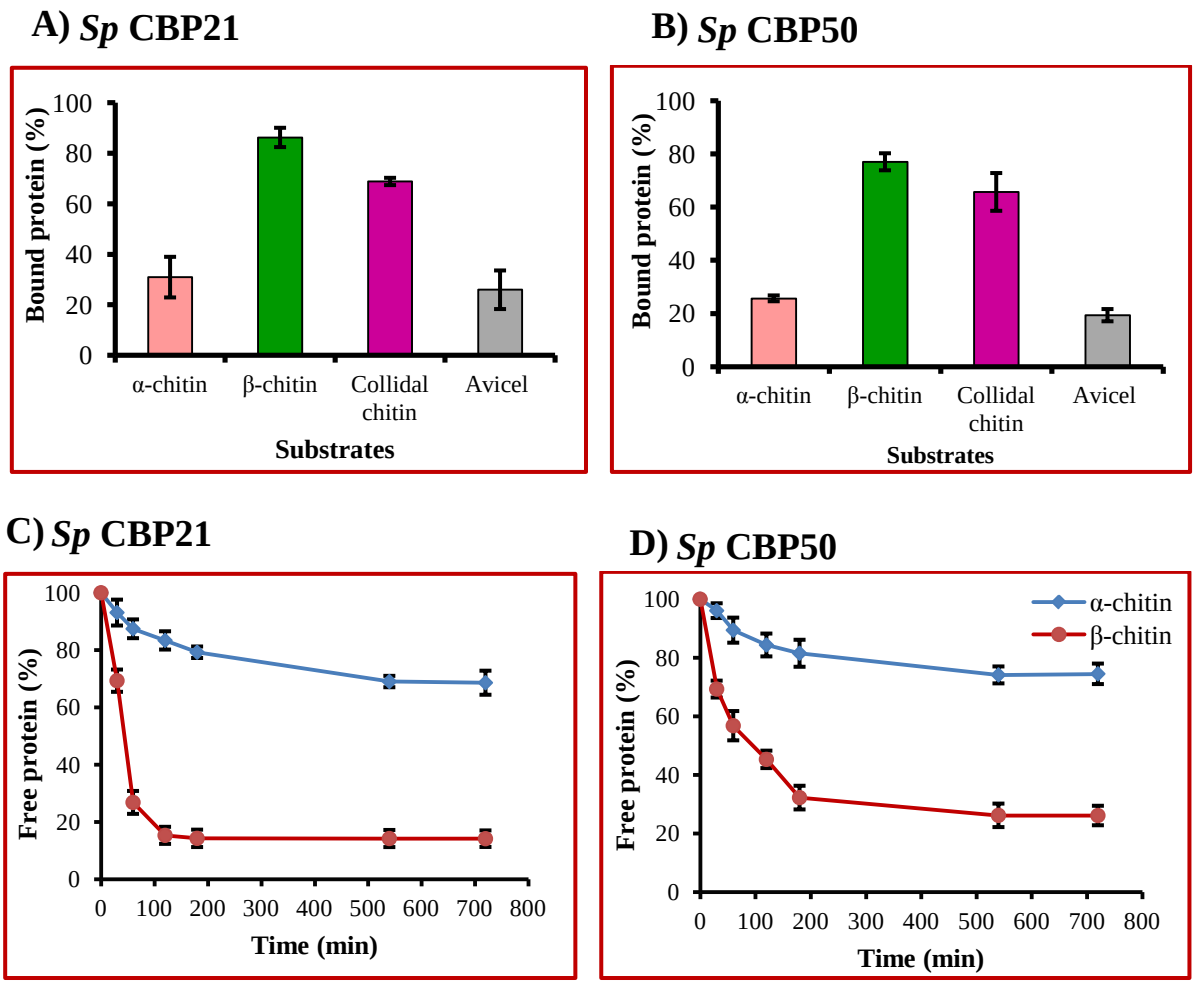

Fig. 3.25: Binding of *Sp* CBPs to insoluble polymeric substrates

The reaction mixture (1 mL) containing 100 µg of *Sp* CBP21/*Sp* CBP50 and 1 mg of one of the insoluble substrates (α-chitin, β-chitin, colloidal chitin and Avicel) was incubated in 50 mM sodium phosphate buffer pH 7.0 under constant shaking at 1300 rpm at 37°C for 24 h.

A & B. The amount of bound protein was calculated from the difference of protein concentration between the protein added and the supernatant obtained by centrifugation after binding incubation. Vertical bars represent standard deviation of triplicate experiments.

C & D. A decrease in free protein concentration after binding to α- and β-chitin was determined at different time points till 24 h. Vertical bars represent standard deviation of triplicate experiments.

A and C. *Sp* CBP21

B and D. *Sp* CBP50

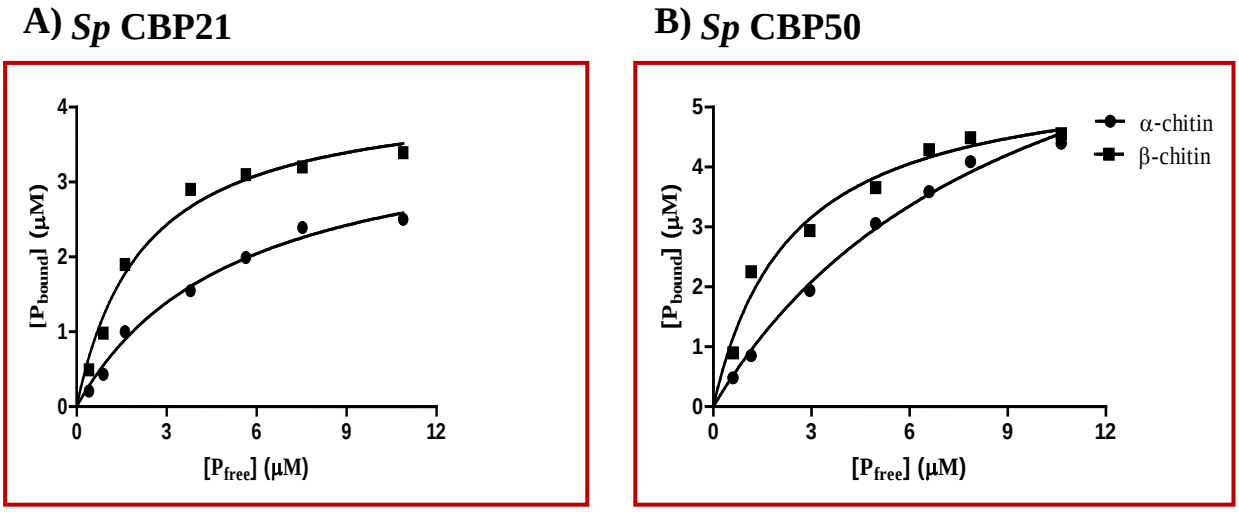

Fig. 3.26: Equilibrium adsorption isotherms of *Sp* CBP21 and *Sp* CBP50 to α- and β-chitin

The reaction assay (1 mL) contained 1.0 mg substrates and varied concentrations of *Sp* CBP21 and CBP50 starting from 0 to 7.0 µM was incubated (*Sp* CBP21 with α- and β-chitin, 12 h and 6 h respectively; *Sp* CBP50 with α- and β-chitin, 12 h) at 37°C. The reaction mixtures were centrifuged and concentration of bound protein (P_{bound}) and non-bound protein (P_{free}) was determined and plotted against each other. All data sets were fitted to the equation for one-site binding by non-linear regression. Each data point represents the average of values obtained in three independent binding experiments.

A. *Sp* CBP21

B. *Sp* CBP50

Protein	Substrate	K_d (μM)	B_{max} (μmoles of protein/g)
Sp CBP21	α-chitin	5.31 ± 1.03	4.23 ± 0.34
	β-chitin	2.22 ± 0.45	3.85 ± 0.26
Sp CBP50	α-chitin	9.34 ± 1.67	8.56 ± 0.87
	β-chitin	2.37 ± 0.50	5.66 ± 0.38

Table 3.2: Binding parameters of *Sp* CBP21 and *Sp* CBP50 to α- and β-chitin

GraphPad Prism software version 5.0 was used to calculate B_{max} and K_d.

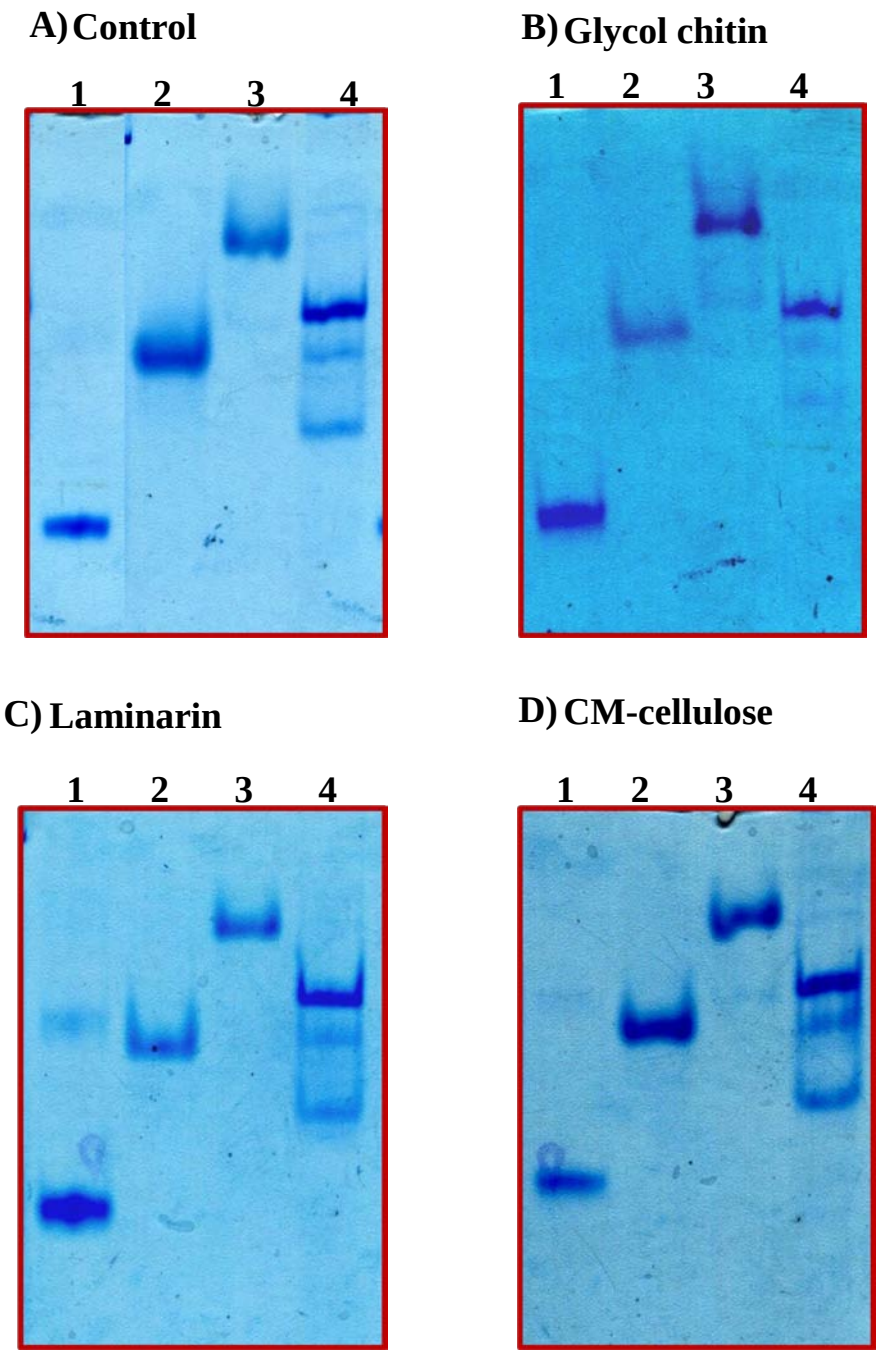

Fig. 3.27: Binding of *Sp* CBPs towards soluble polymeric substrates

Affinity non-denaturing gel electrophoresis was performed at 4°C by preparing 8% polyacrylamide gels. Ten micrograms of *Sp* CBPs and BSA were electrophoresed without (A) or with 0.1% (w/v) substrates incorporated with glycol chitin (B), laminarin (C) and CM-cellulose (D). Proteins were visualized by Coomassie blue G-250 staining after electrophoresis. Lane 1: BSA, lane 2-4: *Sp* CBP21, *Sp* CBP28 and *Sp* CBP50.

surface of untreated chitin appeared smoother than the treated *Sp* CBP21 and *Sp* CBP50 and displayed amorphous and more porous texture (Fig. 3.28).

3.3.5 Degradation of α- and β-chitin by *Sp* chitinases in the presence or absence of *Sp* CBP21 and *Sp* CBP50

In presence of *Sp* CBP21, *Sp* chitinases released increased amount of products formation from α-chitin when compared to the absence of *Sp* CBP21 (Fig. 3.29A). The increased product formation in the presence of *Sp* CBP21 was higher for *Sp* ChiD followed by *Sp* ChiC, *Sp* ChiB and *Sp* ChiA. In the presence of *Sp* CBP21, *Sp* chitinases also released increased amount of products from β-chitin when compared to the absence of *Sp* CBP21 (Fig. 3.29B). The increased product formation in the presence of *Sp* CBP21 was higher for *Sp* ChiB followed by *Sp* ChiD, *Sp* ChiC and *Sp* ChiA.

Sp CBP50 also increased the products formation when *Sp* CBP50 was added to the *Sp* chitinases in the reaction mixtures. In presence of *Sp* CBP50, *Sp* chitinases released increased amount of products from α-chitin when compared to the absence of *Sp* CBP50 (Fig. 3.29C). The increase in product formation with the presence of *Sp* CBP50 was higher for *Sp* ChiD followed by *Sp* ChiC, *Sp* ChiB and *Sp* ChiA. In presence of *Sp* CBP50 also increased the products formation of *Sp* chitinases in β-chitin when compared to the absence of *Sp* CBP50 (Fig. 3.29D). The increase in formation of products in the presence of *Sp* CBP50 was higher for *Sp* ChiB followed by *Sp* ChiD, *Sp* ChiC and *Sp* ChiA.

3.3.6 Sequence analysis of *Sp* CBPs and modeling of *Sp* CBP21

The sequence alignment of *Sp* CBPs was generated by aligning the sequences with CBP21 from *S. marcescens*, the only available three-dimensional structure of a family 33 CBP is that of CBP21 from *S. marcescens*, which binds exclusively to β-chitin (Suzuki *et al*., 1998, Vaaje-Kolstad *et al*., 2005a). The alignment showed conserved residues which are responsible for chitin binding. All the important residues are conserved in *Sp* CBP21 (Tyr-54, Glu-55, Glu-60, His-114, Asp-182, and Asn-185) and *Sp* CBP50 (Tyr-48, Glu-49, Glu-54, His-108, Asp-176, and Asn-179), while *Sp* CBP28 matches only one residue (Asp-176) (Fig. 3.30).

For modelling the *Sp* CBP21, the sequence displayed high sequence identity to the sequences of *S. marcescens* (93%, BAA31569). Then the PDB files, PDM ID: 2BEM of CBP21 from *S. marcescens* was downloaded. Then the hetero atoms from the template PDB and saved the

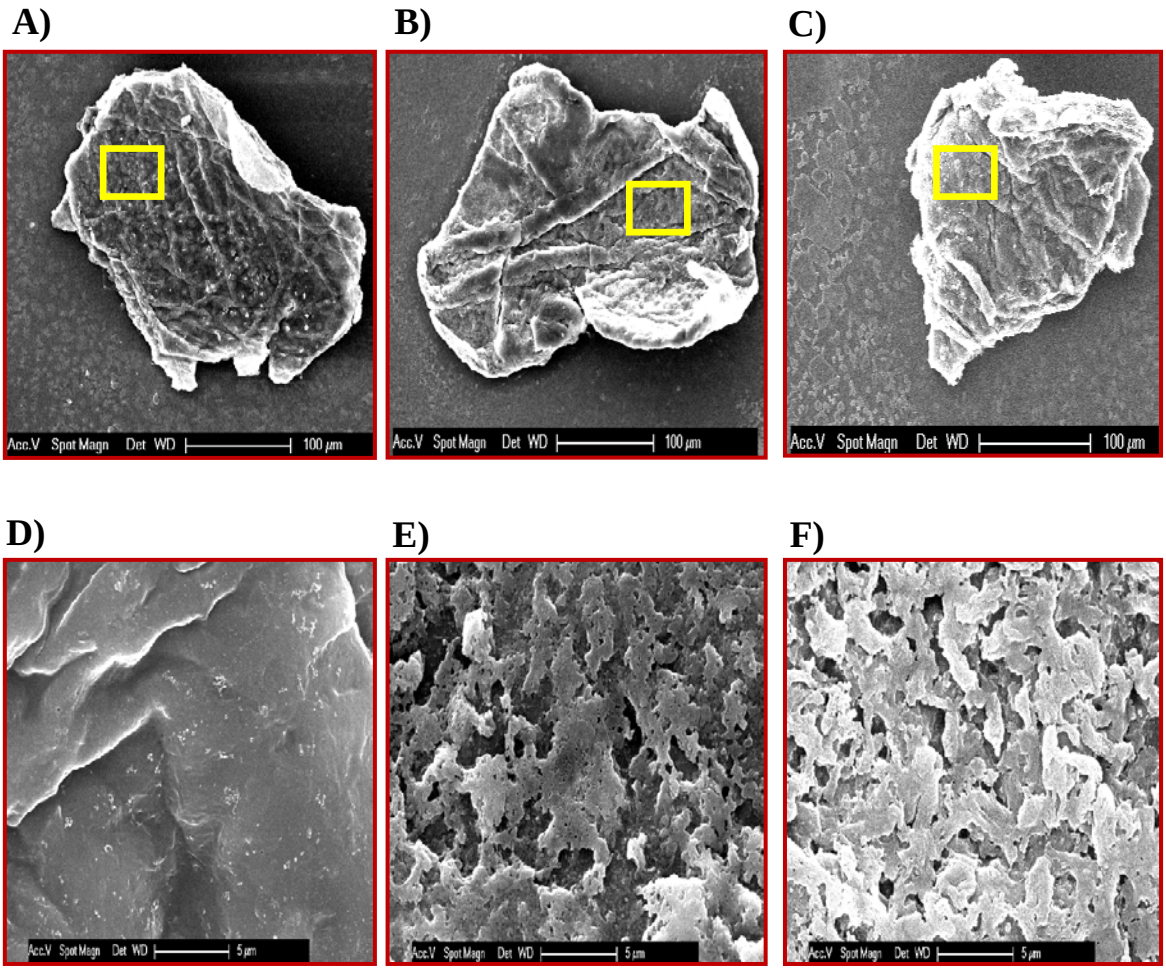

Fig. 3.28: Scanning electron micrographs of α-chitin treated with *Sp* CBP21 and *Sp* CBP50

With *Sp* CBP21 or *Sp* CBP50, 0.1 mg/mL was incubated with 0.1 mg/mL of α-chitin in 50 mM sodium phosphate buffer pH 7.0 for 24 h at 37°C. After incubation, the samples (10 µL drops) were applied onto cover slips, and dried at 37°C to fix the sample and scanning was performed.

A-C. Control (no CBPs were added), *Sp* CBP21 and *Sp* CBP50 treated particles with 250x magnification. Scale bars represent 100 μm.

D-F. The respective particles shown in the yellow framed drawn on the 250x magnified images were targeted for higher magnification (5000x magnification). Scale bars represent 5 μm.

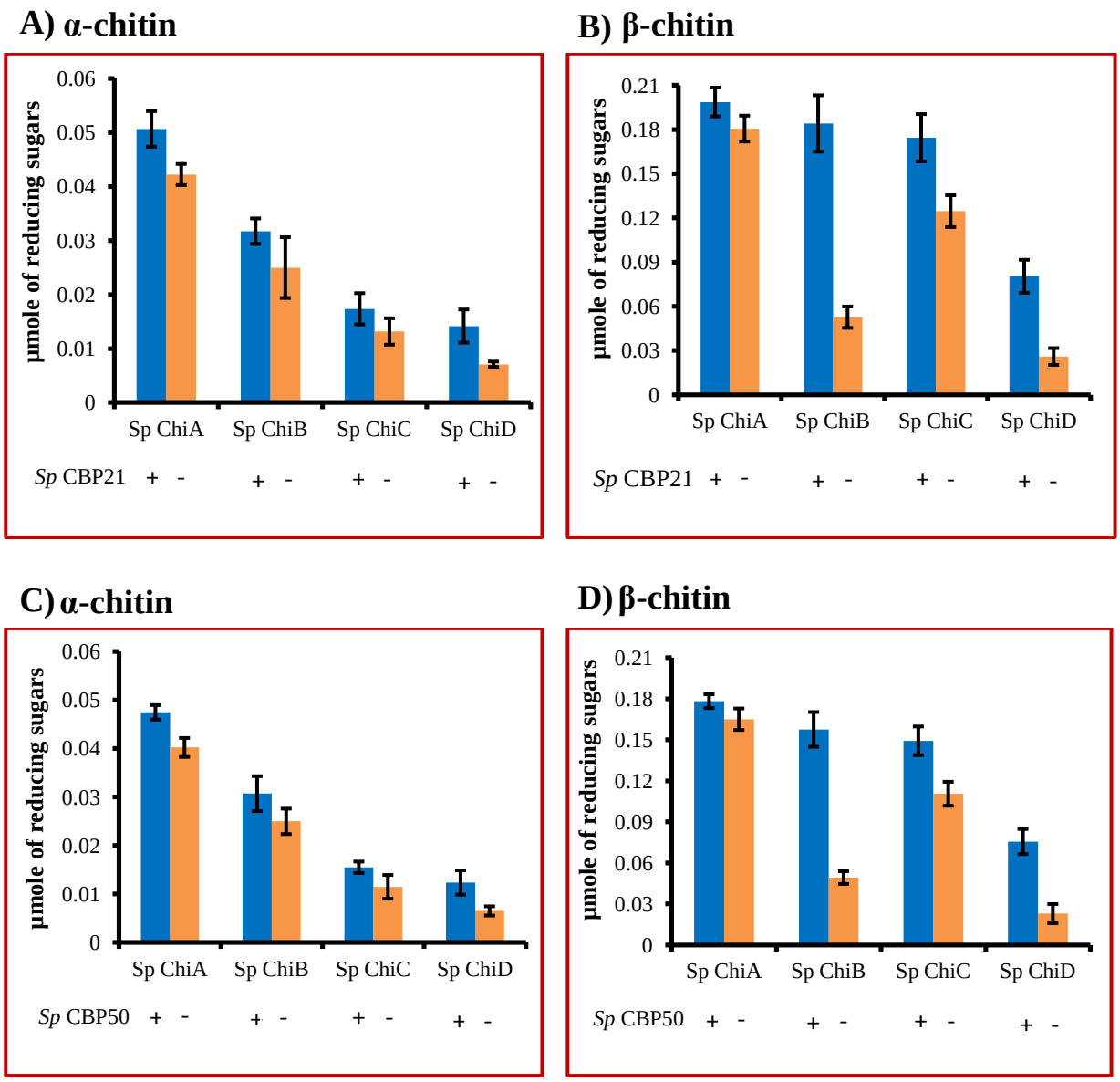

Fig. 3.29: Degradation of α- and β-chitin by *Sp* chitinases in the absence or presence of *Sp* CBP21 and *Sp* CBP50

Reaction mixture (200 µL) contained 1mg/mL of chitin substrates, 1 µM of *Sp* chitinase (*Sp* ChiA/*Sp* ChiB/ *Sp* ChiC/*Sp* ChiD) were incubated with *Sp* CBP21 (α-chitin: 5.3 µM and β-chitin: 2.2 µM) and *Sp* CBP50 (α-chitin: 9.4 µM and β-chitin: 2.3 µM) in 50 mM sodium phosphate buffer pH 7.0. After incubation at 37°C for 24 h, products formation was quantified by standard reducing end assay. Vertical bars represent standard deviation of triplicate experiments.

A and B. Degradation of α- and β-chitin by *Sp* chitinases in the presence or absence of *Sp* CBP21

C and D. Degradation of α- and β-chitin by *Sp* chitinases in the presence or absence of *Sp* CBP50

alignment in .ali extension, which is essential for the protein modelling tool called Modeller 9v8. We have generated about 40 models for each protein and then Ramachandran plots also generated for checking the protein structure quality using PROCHECK (Fig. 3.31A). The superimposition of thefinal model Cα atoms on the template structure gave a root mean square deviation (RMSD) of 0.182 Å. Closer inspections of these structures reveal that the conformations of the several regions (α5, β4, β5, β6, β7) were differing from the template structure (Fig. 3.31B).

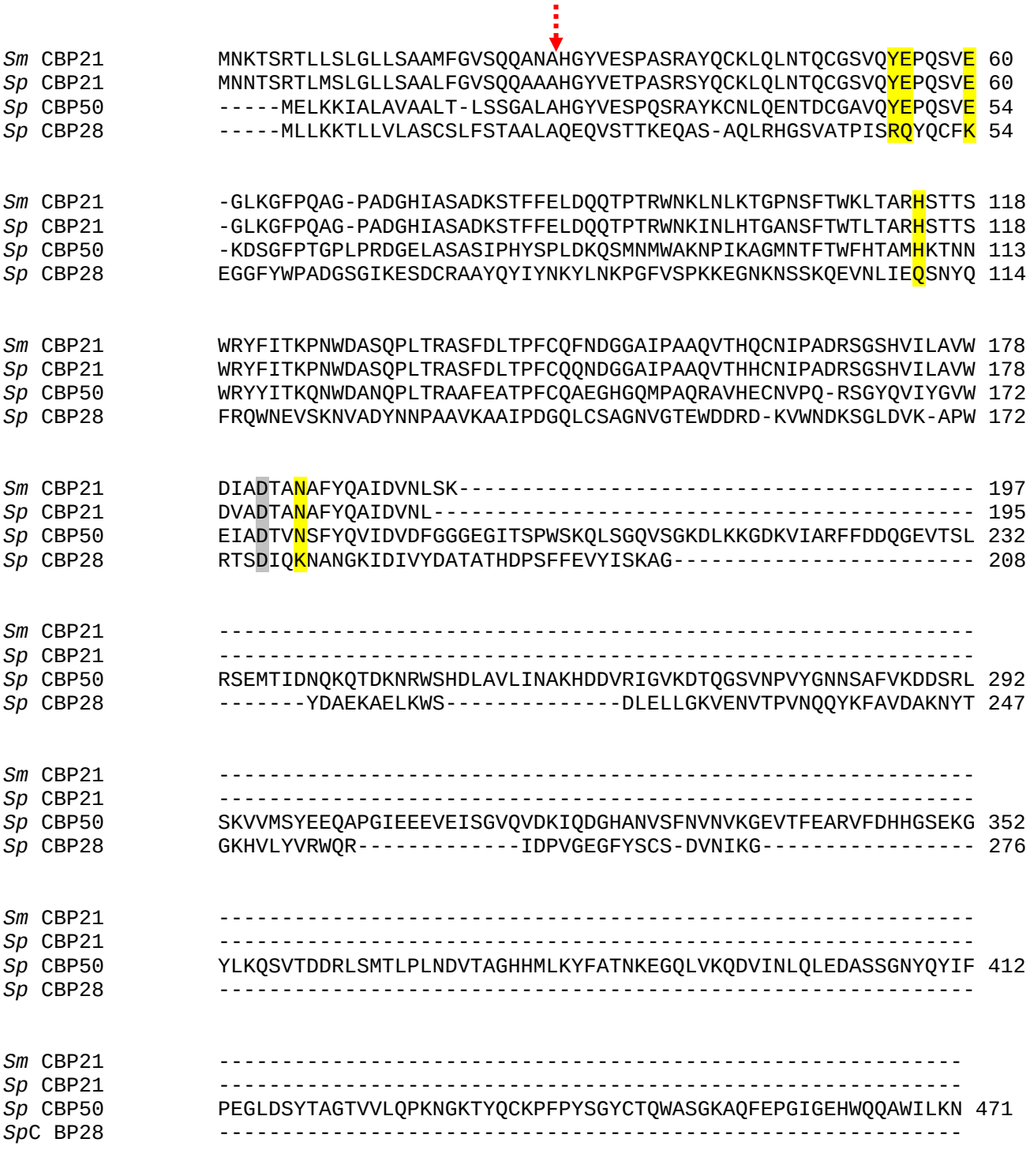

Fig. 3.30: Sequence alignment for *Sp* CBPs

Full-length sequences of *Sp* CBP21, *Sp* CBP28, *Sp* CBP50 and *Sm* CBP21 (CBP21 from *S. marcescens*) were aligned using clustalw2 (www.ebi.ac.uk/Tools/msa/clustalw2/). Residues that are thought to be located in the binding surface for chitin present in *Sp* CBP21, *Sp* CBP21, *Sp* CBP50 and not present in *Sp* CBP28 are shaded in yellow (as derived from the crystal structure of CBP21 of *S. marcescens*, as well as mutagenesis studies [Vaaje-Kolstad *et al.*, 2005 a & b]). Residue involved in the chitin-binding and functional properties of CBP21 of *S. marcescens* (Vaaje-Kolstad *et al.*, 2005a & b), but also conserved in *Sp* CBP28 are shaded grey. The arrows indicate the terminal amino acid of the N-terminal signal sequence for respective CBPs.

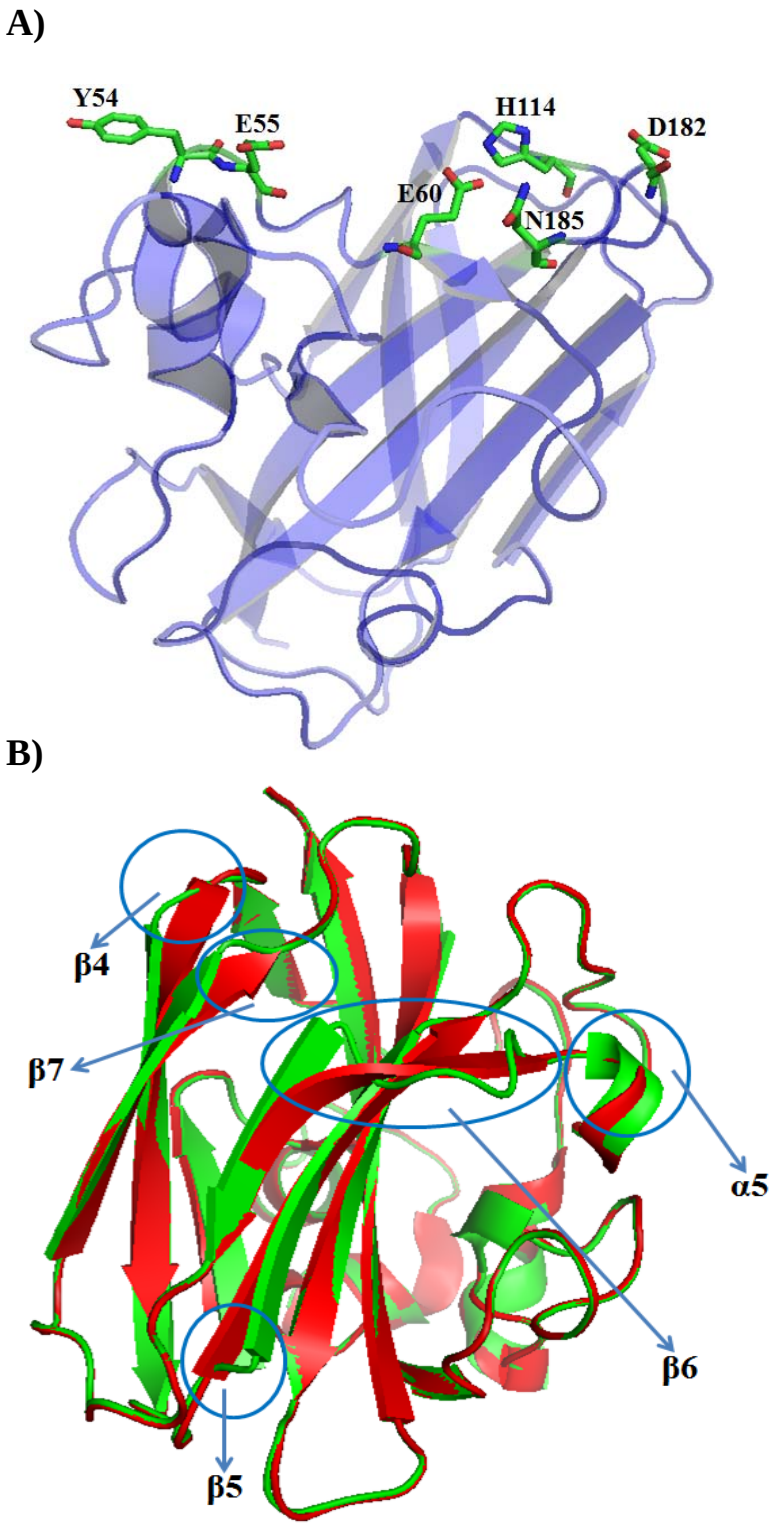

Fig. 3.31: The 3D model of *Sp* CBP21

A. The model *Sp* CBP21 was generated by Modeller9v8 (http://www.salilab.org/modeller/) using CBP21 (PDB ID: 2BEM) from *S. marcescens* as structure template. The structure model is shown in blue-colored cartoon representation. Residues that are important for chitin binding was shown in sticks representation with carbon, oxygen and nitrogen atoms colored light green, red and dark blue, respectively. The figure was prepared using PyMOL (http://www.pymol.org/).

B. Stereo view of the superimposed structure of *Sp* CBP21 with CBP21 from *S. marcescens*. Differential regions between the structures were labelled in circle.

DISCUSSION

4.1 Selection of *S. proteamaculans* 568 for chitinolysis

Chitin is an insoluble homopolymer of β-(1, 4)-linked *N*-acetylglucosamine (GlcNAc) and second most abundant polysaccharide after cellulose in nature. The decomposition of chitin, therefore, is important in terms of the carbon and nitrogen cycles in the biosphere. For the complete hydrolysis of chitin to GlcNAc, the concerted action of a combination of chitinase is essential. Chitinases randomly cleave glycosidic linkages of GlcNAc to produce soluble oligosaccharides, mainly chitobiose, which are further hydrolyzed to GlcNAc by β-*N*-acetylglucosaminidases. Chitinases play a central role in the chitin degradation process by bacteria, although the process is exceedingly complex. Several bacterial chitinase genes have been cloned from both terrestrial and marine environments, and their biochemical properties, catalytic mechanisms, and tertiary structures have been elucidated. *S. proteamaculans* 568 belongs to family *Enterobacteriaceae*, was isolated as a root endophyte from a tree species *Populus trichocarpa* (Taghavi *et al*., 2009) and promotes growth and health of the poplar trees. The organism is rod shaped, Gram-negative, facultative anaerobe and its full genome sequence available since 2007. Genomic sequence reveals that *S. proteamaculans* contains at least 4 chitinases, 1 chitobiase and 3 CBPs.

We have amplified and sequenced the 16S rDNA gene of *S. proteamaculans* 568 to confirm the taxonomic status of the strain. The BLAST search of the 16S rDNA sequence showed 100% homology to *S. proteamaculans* 568. Phylogenetic tree was constructed along with closely related 16S rDNA sequences of *Serratia* species (Fig. 3.1). Similar kind of confirmation for *Serratia* sp. KCK was done using 16S rDNA and also phylogenetic tree was constructed (Kim *et al*., 2007).

Since chitinases diffuse through agar, assays to identify chitinolytic bacteria or genomic clones encoding chitin-degrading enzymes was performed by monitoring the degradation of polymeric chitin incorporated into an agar medium. Though these assays have a limited sensitivity, they represent a simple and inexpensive method to identify chitinolytic microorganisms (Howard *et al*., 2003). The larger and clearer zone of chitin hydrolysis around the colony was attributed to the chitinolytic ability of the organism. *S. proteamaculans* 568, tested for the chitinolytic ability on chitinase detection agar plate, was strongly positive for chitin hydrolysis as there was a clear halo around the colony (Fig. 3.2). Kishore *et al*. (2005) screened 393 bacterial isolates from peanut plant and selected 95 potential chitinolytic bacteria for biological control of peanut diseases. Cody

(1989) used a similar method for detection of chitinolytic bacteria and selected 17 out of 52 strains representing species of *Bacillus*. Liu *et al*. (2002) also screened 70 strains of *B. thuringiensis* and 38 strains had chitinase activity both on inducing plate and inducing broth. The halo zone of chitin-clearance around *S. proteamaculans* 568 thus confirmed the chitinolytic potential of the strain.

4.2 Cloning and characterization of chitinases from *S. proteamaculans* 568

4.2.1 Search for homologs of *Sp* chitinases at NCBI using BLAST

The *Sp* ChiA, *Sp* ChiB, *Sp* ChiC and *Sp* ChiD were named according to the amino acid homology of the sequences to the reported *S. marcescens* ChiA-ChiC. *Sp* ChiA, *Sp* ChiB and *Sp* ChiC showed high sequence identity to ChiA (94%), ChiB (94%) and ChiC (87%) of *S. marcescens*, respectively. As there are no reports on the presence of a fourth chitinase in *S. marcescens*, we have designated the fourth chitinase of *S. proteamaculans* as a *Sp* ChiD. All four *Sp* chitinases cloned, over expressed in *E. coli*, and purified using Ni-NTA agarose column chromatography (Fig. 3.3 and 3.4).

4.2.1.1. *Sp* ChiA

The amino acid sequence of *Sp* ChiA was BLASTed at NCBI database to search for protein homologs. The results displayed 94% sequence identity to the sequence of ChiA from *S. marcescens* (ACX42071), 90% to ChiA from *S. plymuthica* (AAB49933), 75% to ChiA from *Aeromonas hydrophila* subsp. *hydrophila* ATCC 7966 (ABK39408), 52% to ChiA from *V. fischeri* MJ11 (ACH65744), 36% to ChiA from *V. parahaemolyticus* 16 (EED27456). The SignalP 3.0 (http://www.cbs.dtu.dk/services/SignalP/) program predicted the presence of a putative signal peptide, typical of Gram-negative and Gram-positive bacteria, with a cleavage site located between amino acid residues Ala-23 and Ala-24. The sequences were tested for functional domains or motifs using SMART (a Simple Modular Architecture Research Tool) data base. *Sp* ChiA contains an N-terminal polycystic kidney disease domain (PKD) (Asp-61 through Thr-133), and a family 18 catalytic domain (Lys-158 through Gly -544).

4.2.1.2 *Sp* ChiB

The BLAST search for *Sp* ChiB homologs displayed 94% identity to ChiB of *S. marcescens* (ACX42072), 36% to ChiA1 from *B. circulans* (AAA81528) and ChiCW from *B. cereus*

(AF416570), 28% to ChiA from *V. harveyi* 1DA3 (EEZ89790), and ChiB from *Clostridium* sp. 7_2_43FAA (EEH99347). *Sp* ChiB contains an N-terminal family 18 catalytic domain (Asn-16 through Asp-408) and C-terminal chitin binding domain (ChBD) (Val-453 through Val-495), which belongs to carbohydrate binding module family 5 (CBM5).

4.2.1.3 *Sp* ChiC

Sp ChiC showed 87% identity to ChiC of *S. marcescens* (ABI79318), 67% to chitinase from *P. fluorescens* Pf-5 (AAY91366), 54% to ChiC1 from *V. harveyi* HY01 (EDL70608), 50% to chitinase from *Lactococcus. lactis* subsp. *lactis* CV56 (ADZ64556), 29% to chitinase from *Hahella chejuensis* KCTC 2396 (ABC27762) and 27% to ChiD from *Paenibacillus* sp. HGF7 (EGL15866). *Sp* ChiC contains family 18 catalytic domain (Lys-25 through Glu-322), C-terminal fibronectin type 3 domain (Fn3) (Pro-342 through Ser-416) and a C-terminal chitin binding domain (Pro-437 through Thr-483) which belongs to CBM12 family.

4.2.1.4 *Sp* ChiD

Sp ChiD had 78% homology with chitinase II from *Klebsiella pneumonia* (ACZ01996), 40% to chitinase from *B. subtilis* (ACU33923), 35% to ChiC from *B. cereus* m1293 (AAB70917), 33% to ChiA from *Stenotrophomonas maltophilia* (EEK46733) and Chi80 from *B. ehimensis* (BAC76694) and 26% to ChiB from *S. marcescens* (ACX42072), with an N-terminal signal peptidase site (between Ala-19 and Gly-20), and a family 18 catalytic domain (Ser-29 through Asp-406).

4.2.2 Catalytic activity

Sp chitinases have different domain structures and the peptide sequences of these four enzymes share very low similarity (>25%) by sequence comparison among the *Sp* chitinases although these enzymes belong to family-18 chitinases. We, therefore, investigated the kinetics of *Sp* chitinases.

Michaelis-Menten kinetic parameters were determined using different concentration of colloidal chitin as a substrate. Since substrate inhibition was apparent at higher substrate concentration for this type of chitinases (Brurberg *et al*., 1996; Synstad *et al*., 2004). Kinetic analysis revealed that V_{max}, k_{cat} and k_{cat}/K_m decreased from *Sp* ChiA to ChiD, while K_m increased from *Sp* ChiA-ChiD except that the *Sp* ChiC affinity towards substrate was slightly lower than the *Sp* ChiB. The overall catalytic efficiency (k_{cat}/K_m) of *Sp* ChiA was 37.6, 23.3,

0.7-folds higher than *Sp* ChiB, *Sp* ChiC and *Sp* ChiD, respectively (Fig 3.5 and Table 3.1). The *Sp* ChiA had highest activity against colloidal chitin among the four *Sp* chitinases, while *Sp* ChiD was least effective in colloidal chitin hydrolysis. *Sp* ChiA kinetic values were higher than the ChiA from *Serratia* sp. KCK values (V_{max} , 0.302 µmol h^{-1}; K_m 12.62 mg ml^{-1}; k_{ca} 0.019 h^{-1}; k_{cat}/K_m 0.0015 h^{-1}mg/ml) (Kim *et al*., 2007) and both the cases colloidal chitin was used as a substrate and only difference is the later enzyme kinetics were studied using Lineweaver-Burk calculation and the *Sp* chitinases kinetics were studied using Michaelis-Menten kinetics. The kinetic values of *Sp* ChiD were far away from the values of *Sp* ChiA-ChiC, probably because the *Sp* ChiD doesn't have auxiliary domain, while other *Sp* chitinases possess additional domains along with catalytic domains. Similar effect on catalytic activity of chitinases was observed in *Bacillus cereus* 28-9 chitinolytic system (Huang and Chen, 2005), where the bacterium produces two chitinases, ChiCH and ChiCW. ChiCW contains Fn3 and ChBD along with catalytic domains, and only catalytic domain was present in ChiCH. ChiCW had higher catalytic efficiency over ChiCH.

The difference in the kinetic parameters among *Sp* chitinases also could be due to difference in the sequences of catalytic domains in conjunction with different auxiliary domains presence (*Sp* ChiA-ChiC) or absence (*Sp* ChiD). It is conceivable that the primary role of these auxiliary domains (CBMs, PKD and Fn3) is to potentiate catalytic activity by disrupting the substrate, rather than simply to promote enzyme-substrate binding. Watanabe *et al*. (1994) have shown that deletion of the two Fn3 domains of ChiA1 from *Bacillus circulans* did not affect chitin-binding, but strongly reduced chitin hydrolysing activity.

4.2.3 Effect of pH on the activity of *Sp* chitinases

All the four *Sp* chitinases were optimally active in mildly acidic to neutral pH (5.0-7.0) (Fig 3.6). *Sp* ChiA was active over a broad range of pH (5.0-11.0) with an optimum at neutral pH, similar (but not identical) to ChiA from *S. marcescens* 2170 (Suzuki *et al*., 2002), *Serratia* sp.KCK (Kim *et al*., 2007) and *S. proteamaculans* 18A1 (Mehmood *et al*., 2009), *B. licheniformis* (Songsiriritthigul *et al*., 2010) which showed optimum activity at pH 6.0, 8.0 5.5 and 6.0, respectively. Similar to ChiB of *S. marcescens* 2170 (Suzuki *et al*., 2002), the *Sp* ChiB was optimally active at pH 6.0. In contrast to ChiC of *S. marcescens* 2170 (Suzuki *et al*., 2002) (optimum pH 5.0), the *Sp* ChiC had maximum activity at pH 6.0. The *Sp* ChiD was optimally active at pH 6.0 similar to *Sp* ChiB and *Sp* ChiC.

4.2.4 Effect of temperature on the activity of *Sp* chitinases

All the four *Sp* chitinases displayed optimum activity at 40^{o}C (Fig. 3.7). Similar to *Serratia* sp.KCK (Kim *et al*., 2007). *Sp* ChiA had optimal temperature of 40°C, while optimum temperatures for ChiA of *S. marcescens* 2170 (Suzuki *et al*., 2002) and *S. proteamaculans* 18A1 (Mehmood *et al*., 2009) were higher (60^{o}C and 55^{o}C, respectively) than *Sp* ChiA. The *S. marcescens* 2170 ChiB and ChiC showed maximum activity at 60^{o}C and 65^{o}C, respectively (Suzuki *et al*., 2002).

4.2.5 Activity on polymeric carbohydrate substrates

The role of the four *Sp* chitinases in chitin hydrolysis was assessed through their hydrolyzing activity against different chitinous substrates. *Sp* ChiA, *Sp* ChiB and *Sp* ChiC were adaptable for the hydrolysis of insoluble β-chitin, and *Sp* ChiD was useful for the hydrolysis of soluble chitin and chitosan. Suzuki *et al*. (2002) described the hydrolyzing activities of ChiA, ChiB, and ChiC1 from *S. marcescens* 2170 against various chitinous substrates. ChiA was adopted to hydrolyze insoluble chitin, and ChiC1 was used for the hydrolysis of soluble chitin. ChiB activity closer to that of ChiC1 than to ChiA against insoluble chitin, and closer to ChiA than to ChiC1 against soluble chitin. Judging from these experimental data, it seems likely that chitinolytic bacteria produce multiple chitinases with different substrate specificities against a variety of chitinous substrates. In contrast to *S. marcescens* 2170 ChiB, *Sp* ChiB activity was closer to *Sp* ChiA against insoluble and soluble substrates except with α-chitin, which showed only 50.2 % of activity of *Sp* ChiA (Fig. 3.8). ChiA from *S. marcesens* and *Alteromonas* sp. strain O-7 maximum activity on crystalline α-chitin among the other chitinases produced by these two bacteria. The PKD domain was found in N-terminal region of both the chitinases that were effective in hydrolysis of crystalline α-chitin (Orikoshi *et al*., 2005a). In contrast to the *Sp* ChiA, Mehmood *et al*. (2009) reported that ChiA from *S. proteamaculans* 18A1 showed highest activity on glycol chitin followed by the colloidal chitin, unprocessed β-chitin and the unprocessed α-chitin. Similar to ChiA from *Serratia* sp. KCK (Kim *et al*., 2007) *Sp* ChiA, activity on chitin and chitin-derivatived substrates was broader than those of most other organisms (Lan *et al*., 2006, Xia *et al*., 2001).

4.2.6 Substrate binding properties of *Sp* chitinases

4.2.6.1 Insoluble substrates

To test whether the highest activity of *Sp* chitinases, in hydrolysis of insoluble and soluble substrates, was related to the substrate binding, the binding activity of four *Sp* chitinases was compared to different substrates (Fig. 3.9). In judgement with the activity analysis, to the α-chitin *Sp* ChiA had binding maximum among the four *Sp* chitinases. In comparison with the hydrolytic activities, *Sp* ChiA and *Sp* ChiB had less binding to β-chitin when compared to *Sp* ChiC. *Sp* ChiB and *Sp* ChiC bound almost equal to colloidal chitin and had highest binding in comparison with the *Sp* ChiA. *Sp* ChiB-ChiD showed no activity, but still bound to able to bind to Avicel. *Sp* ChiD, which showed very less activity on polymeric substrates possess only catalytic GH18 domain and no auxiliary binding domains, showed more than 65% binding to the tested polymeric substrates. ChiCH from *Bacillus cereus* 28-9 which is deficient of auxiliary domains and contains only catalytic GH18 domain displayed only 30% binding to colloidal chitin and Avicel (Huang and Chen, 2005). The importance of the auxiliary domains, most importantly ChBD (chitin-binding domain) in binding to insoluble substrates was known. The ChBD truncated mutants of *B. circulans* ChiA1 had approximately 34% relative binding ability toward the regenerated chitin (Watanabe *et al*., 1990 and 1994). $ChBD_{ChiA1}$ is required for ChiA1 to bind specifically to the insoluble chitin. Similar results were reported in *Bacillus* sp. strain J813 chitinase (Sampei *et al*., 2004). Tantimavanich *et al*. (1998) reported that Chi62 and Chi50 chitinases from *B. licheniformis* TP-1 could not bind to the crystalline chitin because they lack the C-terminal ChBD. In contrast, Chuang *et al*. (2008) showed that deletion of the 145 C-terminal amino acid residues of BlChi1, which removes the entire putative ChBD of BlChi1, did not alter the binding abilities and specificities of BlChi4 and BlChi4G419 toward various substrates. Deletion of the C-terminal 304 amino acid residues of *Aeromonas caviae* ChiA (Lin *et al*., 2001), which presumably removes the entire chitin-binding region of ChiA from *A. caviae*, resulted almost similar binding specificity to chitin and colloidal chitin substrates as compared to the full length protein.

4.2.6.2 Soluble substrates

Binding of four *Sp* chitinases to soluble polysaccharides was investigated by native PAGE with and without polysaccharides. Electrophoretic mobility of the *Sp* chitinases was only affected by the presence of glycol chitin (Fig. 3.10). In contrast to ChiCH from *Bacillus*

cereus 28-9 (Huang and Chen, 2005), *Sp* ChiD showed affinity towards soluble chitin substrate as the enzyme showed maxium activity over soluble chitin/chitosan substrate.

These results demonstrated that difference in the hydrolyzing activity observed among four *Sp* chitinases was not solely due to the difference in the binding activities or auxiliary binding domains, and are rather due to the interactions from several aromatic residues located at the the catalytic domain of chitinases such as Trp, Tyr and Phe essential for complete substrate binding (Uchiyama *et al*., 2001).

4.2.7 Activities on oligomeric and polymeric chitinase substrates

4.2.7.1 TLC analysis of products

To determine the final and intermediate products of the chitinase reaction, the products obtained from various CHOS (DP1-DP6) were analyzed by silica gel TLC. TLC analysis of the hydrolytic activity of four *Sp* chitinases on CHOS clearly revealed that when the *Sp* ChiA-ChiC were incubated with DP2, no detectable products were observed, while *Sp* ChiD hydrolyzed DP2 to DP1, suggesting that DP2 was not the substrate for *Sp* ChiA-ChiC. DP1 formed from DP2 due to chitobiase activity of *Sp* ChiD (Fig. 3.11-3.13). From DP3-DP6 substrates, DP2 formed as a major end product along with minor fraction of DP1 product from *Sp* ChiA-ChiC enzyme as observed in ChiA-ChiC from *S. marcescens* 2170 (Suzuki *et al*., 2002), while *Sp* ChiD formed DP1 as major end product at the end of the reaction. DP3 and DP4 were poor substrates for *Sp* ChiA-ChiC, whereas *Sp* ChiD showed maximum hydrolysis of these substrates. With a qualitative method of detection like TLC, we also observed that at equivalent time point of reaction, i.e. at 60 min, *Sp* ChiA-ChiC enzymes showed a more complete degradation with longer chain substrates with the rate of degradation following the tendency DP6 >DP5>DP4 >DP3, while *Sp* ChiD followed the tendency DP3 > DP4 > DP5 ≅ DP6 ≅DP2. The pattern of hydrolysis products and the tendency of *Sp* ChiD hydrolysis towards the CHOS were similar to the chitobiase for e.g. *Vh*Nag2 from *Vibrio harveyi* 650 (Suginta *et al*., 2010). The only difference with *Vh*Nag2 is the hydrolysis rate was slow in case of *Sp* ChiD. Previous reports on the 3D-structures of hevamine chitinase and *S. marcescens* chitinase A clearly suggested that the catalytic pocket of the enzymes comprised an array of at least six binding subsites (Terwisscha van Scheltinga *et al*., 1994, Papanikolau *et al*., 2001). If this would also be the case for *Sp* ChiA-ChiC, the binding affinity of the enzymes with DP3 and DP4 should not be strong because a full

occupancy of binding would be satisfied by six sugar moieties. We need to investigate further to confirm such an assumption.

In addition, intermediate oligomeric products were also detected in the reaction of *Sp* chitinases on CHOS. *Sp* ChiA-ChiC, released DP3 and DP4 reaction intermediates from DP5 and DP6 substrates. *Sp* ChiC formed DP3 as intermediate from DP4 substrates where as *Sp* ChiA and *Sp* ChiB released directly DP2 end product without forming any intermediate product. When DP3 was produced as a reaction intermediate, it was relatively stable because its low affinity prevented rapid hydrolysis. Apparently, all monomers found as end products arose from these intermediate DP3. *Sp* ChiD could liberate a 1 unit shorter than the starting substrate i.e. from DP6 substrate it produces DP5, DP4, DP3, DP2 and also formed higher length CHOS products from the DP3- DP5 substrates (because of resolution constraint in TLC, we could not see the products higher than the DP6 from DP6 substrate) indicating TG activity of the enzyme. TG is a common phenomenon in few of the glycoside hydrolases in the case of high substrate concentrations (Taira, *et al*., 2009). TLC results indicating the endo type of activity of all four *Sp* chitinases, in which the enzymes will act randomly on internal sites of the glycosidic bonds (Table 4.1A).

4.2.7.2 HPLC analysis of products

4.2.7.2.1 With polymeric substrates

Reaction time course of hydrolysis of colloidal chitin was analyzed by HPLC (Fig. 314-3.15). Hydrolysis of colloidal chitin with *Sp* ChiA- ChiD initially yielded DP2 and small amounts of DP1, DP3 and DP4. DP4 products from *S. marcescens* ChiA and ChiB have not been detected previously (Suzuki *et al*., 2002 and Horn *et al*., 2006b). However, differences were observed in generation of minor products. Production of DP1, DP3 and DP4 were relatively high with *Sp* ChiC followed by *Sp* ChiA, *Sp* ChiB and *Sp* ChiD. As the hydrolysis proceeded, a portion of the initially produced DP3 and DP4 were also hydrolysed along with chitin, resulting formation of major end product DP2 with *Sp* ChiA-ChiC and DP1 with *Sp* ChiD. *Sp* ChiA yielded high concentration of DP2 among the *Sp* ChiA-ChiC at the end of 720 min. The consecutive sugars in cellulose or chitin are rotated by 180°, with the consequence that only every second sugar will have a productive configuration when the polymer is threaded through the active site of an enzyme (Zakariassen *et al*., 2009). So this could be the reason for *Sp* ChiA-ChiD, releasing DP2 as major end product. Formation of monomers from CHOS or polymeric substrates by chitinase like *Sp* ChiD is an unusual

property. Most of the bacterial chitinases or chitinases from other source release DP2 as major end product.

4.2.7.2.2 With oligomeric (DP3-DP6) substrates

For a better resolution of reaction products, especially the TG products, and quantification of products, we have analysed the reaction products from oligomeric substrates with time course using isocratic HPLC. In agreement with the TLC results, from DP3-DP6, *Sp* ChiD released one-residue shortened oligomers also along with one-residue elongated oligomers. DP2 was formed as a major hydrolysis product at initial reaction time points as the reaction progresses the formation of DP1 increased, at the end of recording (720 min) DP1 formation was high indicating the chitobiase property of *Sp* ChiD. The TG reaction occurred as early as 0 min after initiation, yielded picomole quantities of the elongated oligomers. From HPLC experiments, the TG products of DP4-DP6, DP5-DP9, DP6-DP10 and DP7-DP10 were identified from DP3, DP4, DP5 and DP6 substrates, respectively (Fig. 3.16-3.17).

4.2.7.3. Product analysis by MALDI-TOF-TOF

Further we have analyzed the reaction products using more sensitive MALDI-TOF-TOF from the respective substrates by taking only one time point reaction sample after HPLC analysis (Table. 4.1B). Few higher length TG products like DP7, DP10, DP11-12 and DP11-DP13 formed from DP3, DP4, DP5 and DP6 substrates, respectively (Fig.3.18). Based on HPLC analysis of TG products, Aguilera *et al*. (2003) reported, chitotriosidase from human macrophages synthesized the TG products up to DP6-DP9 from 5 mM DP5. Chitinase A from *Vibrio carchariae* synthesized; DP4-DP6 from DP3, DP5-DP8 from DP4, DP6-DP8 from DP5 from 1mM of respective substraters (Suginta *et* al., 2005). Using MALDI-TOF-TOF analysis Taira *et al*. (2009) showed that plant class V chitinase (CrChi-A) from a cycad (*Cycas revoluta*) yielded up to DP9 from DP6 (1 mM) substrate. Ohnuma *et al*. (2011a & b) reported TG production from a class V chitinase from *Nicotiana tabacum* (NtChiV) and *Arabidopsis thaliana* (AtChiC). NtChiV produced TG product DP7-DP8 from DP6 and DP6 from DP4, from 5 mM of substrate, while AtChiC produced DP7-DP8 from 4.6 mM DP6 substrate.

From HPLC and MALDI-TOF-TOF data it was that the higher length TG products formed were directly proportional to the size of substrates provided to the enzyme. Based on the observation of HPLC products profile, the TG products which are generated from the

A)

S.No	Enzyme	Products from chitooligosaccharides and polymer substrates						Mode of action
		Chitooligosaccharides					Polymer (Colloidal chitin)	
		DP2	DP3	DP4	DP5	DP6		
1.	*Sp* ChiA	-	DP1-DP2 (DP2)	(DP2)	DP1-DP3 (DP2)	DP1-DP4 (DP2)	DP1-DP4 (DP2)	Endo
2	*Sp* ChiB	-	DP1-DP2 (DP2)	(DP2)	DP1-DP3 (DP2)	DP1-DP4 (DP2)	DP1-DP4 (DP2)	Endo
5.	*Sp* ChiC	-	DP1-DP2 (DP2)	DP1-DP3 (DP2)	DP1-DP3 (DP2)	DP1-DP4 (DP2)	DP1-DP4 (DP2)	Endo
4.	*Sp* ChiD	DP1	DP1-DP7 (DP1)	DP1-DP10 (DP1)	DP1-DP12 (DP1)	DP1-DP13 (DP1)	DP1-DP4 (DP2)	Endo, TG activity on COS substrates.

B)

S.No	Substrate	Products detected in HPLC	Products detected in MALDI-TOF/TOF
1.	DP3	DP1-DP6	DP2-DP7
2.	DP4	DP1-DP9	DP2-DP10
3.	DP5	DP1-DP10	DP2-DP12
4.	DP6	DP1-DP10	DP2-DP13

Table. 4.1: A. Summary of products from oligosaccharide & polymer substrates catalysed by *Sp* chitinases. Brackets represent the major end products.
B. Summary of products detected from DP3-DP6 substrates catalysed by *Sp* ChiD.

Sp ChiD were not stable. As the reaction progresses the quantity of products either increased or decreased slightly. This phenomenon was observed in all the products including used substrates (data not shown). Since *Sp* ChiD is able to remove single N-acetylglucosamine moiety from CHOS substrates, the higher chain length products formed from respective substrates were presumably arose from the condensation of oligomers from the two reaction intermediates. The reaction intermediates could be two hydrolysis products or hydrolysis products condensed with used substrates itself.

4.2.7.4. Dose responsive effects of enzyme and substrate concentration on hydrolysis/TG activities of *Sp* ChiD

Dose responsive effects of enzyme and substrate on *Sp* ChiD (hydrolysis/TG) were studied by altering the enzyme and substrate concentration in different ratios (Fig. 3.19). Ten-fold lower concentration of enzyme formed similar kind of products (DP1-DP10) as observed in standardized conditions but the substrate degradation was slow. In early time points (till 30 min), the formation of DP8 was high (based on peak area) DP_{n+2} (n= 4, 5, 6) products formation is high as compared to other TG products. The *Sp* ChiD synthesized DP_{n+2} product by combining major hydrolytic product (DP2) with substrate (DP6) used. Similar kinds of results were also observed in standardized conditions with DP4-DP6 substrates (data not shown). Ten-fold higher concentration of enzyme reduced the number of TG product to one only. This could be because of high level of hydrolytic activity suppressing the TG activity. Ten-fold lower concentration of substrate resulted in formation of only one TG product. This could be due to the concentration of product or intermediate products are not sufficient for the enzyme to condense or synthesize the number of TG products. Three-fold lower concentration decreased TG products and formed only DP7 and DP8 products. Decrease in substrate concentration did not affect the product profile and relative proportion of products as well. Based on the above results, we propose that *Sp* ChiD TG efficacy (number of TG products and concentrations) depends mainly on the ratios of enzyme/substrate concentrations. TG formation was inversely proportional to enzyme and directly proportional to the substrate concentration. Taken together, these results may be applicable for other transglycosylating chitinases particularly when used for the synthesis of CHOS.

The TG reaction catalyzed by GHs takes place through two steps: an acceptor molecule binds to the catalytic cleft, and then the glycosidic linkage is newly generated (Nakatani and Monte, 2002, Leemhuis *et al*., 2003, Johansson *et al*., 2004). Thus, the amino acid residues

responsible for acceptor binding seem to be important for TG activity. TG appears to be a common phenomenon in GHs and can in principle be controlled by favoring binding and correct positioning of a sugar to the intermediate. Recently Zakariassen *et al*. (2011) explained the enzymatic features that determine TG activity by investigation through site-directed mutagenesis on two family 18 chitinases, ChiA and ChiB from *S. marcescens*, with inherently little TG activity. Mutation of the middle Asp in the diagnostic DxDxE motif, which interacts with the catalytic Glu during the catalytic cycle, yielded the strongly TG mutants ChiA-D313N and ChiB-D142N, respectively. Correlations between a lower K_m and increased TG have been observed for β-mannanase Man5A from blue mussel *Mytilus edulis* (Larsson *et al*., 2006), endo-β-N-acetylglucosaminidase from *Mucor hiemalis* (Umekawa *et al*., 2008) and chitinase A from *Vibrio carchariae* (Suginta *et al*., 2005).

Hypertransglycosylating chitinases such as *Sp* ChiD mayfind applications for synthetic purposes. Because of an increased demand for bioactive carbohydrate oligomers, it is pertinent to have access to several technologies yielding oligomeric products of desired isomerism in high yields. An example is inhibition of the human acidic mammalian chitinase (AMCase), a family 18 Chitinase that is a therapeutic target in asthma amelioration. CHOS with specific number and sequences of acetylated and deacetylated units have been shown to inhibit family 18 chitinases due preferences of acetylated sugar moieties in individual subsite yielding nonproductive binding (Cederkvist *et al*., 2008). Relatively short CHOS are easily produced by enzymatic hydrolysis of chitosan (Cederkvist *et al*., 2008). A partially, deacetylated soluble form of chitin, and can by TG technology be used to produce longer oligosaccharides of particular length and sequence of acetylated and deacetylated units. Partially deacetylated CHOS are hydrolyzed slower than fully acetylated, which is most beneficial when using TGases. Moreover, TG technology is complementary to glycosynthase technology, which requires the use of mutated glycosyl hydrolases that are no longer hydrolytically active (Perugino *et al*., 2004 and Shaikh *et al*., 2008).

4.2.8 Sequence analysis and homology modelling of *Sp* ChiA, *Sp* ChiB and *Sp* ChiD

Sequence alignment of *Sp* ChiA-ChiC showed 86-95% identity with ChiA-ChiC from *S. marcescens*. Sequence analysis also showed that the catalytic module of *Sp* ChiC, like hevamine, lacks an α + β-fold insertion between β-sheets 7 and 8 of the TIM-barrel fold (Fig. 3.20), while it was present in *Sp* ChiA, *Sp* ChiB and *Sp* ChiD. The insertion domain (α + β-fold), which was responsible for deepening the substrate-binding groove in many

family 18 chitinases (Suzuki *et al*., 1999). A deep substrate-binding groove is considered to be characteristic of enzymes that act in an exo-fashion and/or that tend to stick tightly to the substrate whilst degrading it in a processive manner (Horn *et al*., 2006b). Enzymes lacking the α+ β-fold insertion have a shallow catalytic cleft, as illustrated by the crystal structure of the plant family 18 sub-group B chitinase hevamine (Terwisscha van Scheltinga *et al*., 1994). Such shallow catalytic clefts are typically seen amongst endo-acting, non processive carbohydrate-degrading enzymes. Detailed studies using chitosan as substrate have shown that ChiC1 from *S. marcescens* is indeed a non-processive enzyme (Horn *et al*., 2006, Terwisscha van Scheltinga *et al*., 1994). Based on the results from ChiA and ChiB of *S. marcecsens* (Horn *et al*., 2006b), because of presence of α + β-fold in *Sp* ChiA, *Sp* ChiB and *Sp* ChiD, which extends the substrate binding cleft deep, we conclude that these enzymes act in a processive manner (Fig. 3.21). *Sp* ChiA, *Sp* ChiB and *Sp* ChiD models were generated using the structural templates of *Serratia marcescens* ChiA, ChiB and chitinase II from *Klebsiella pneumonia*, while there is no structural template available for *Sp* ChiC to generate model.

Enzymes acting on crystalline polysaccharides face several challenges. They need to associate with the insoluble substrate, disrupt the polymer packing and, importantly, guide a single polymer chain into the catalytic center. Processive cellulases or chitinases have been shown to have long and deep active site clefts, or even tunnels (Rouvinen *et al*., 1990). Single polymer chains are threaded through these clefts or tunnels, while disaccharides are being cleaved off at the catalytic center. This mechanism is considered to improve catalytic efficiency because the enzyme remains closely associated with the detached single polymer chain in between hydrolytic steps. Furthermore, the detached chain is prevented from re-associating with the crystalline material, which would make it less accessible. Thus reducing the number of times the enzyme has to carry out the energetically unfavorable process of gaining access to a single chain. Processive enzymes often have long and deep substrate-binding clefts as illustrated by the first structures of processive cellulases (Rouvinen *et al*., 1990, Divne *et al*., 1994). The substrate-binding sites in processive chitinases and cellulases are lined with aromatic residues, in particular tryptophan residues. These residues are thought to facilitate processivity by functioning as a flexible and hydrophobic sheath along which the polymer chain can slide during the processive mode of action (Divne *et al*., 1998, Varrot *et al*., 2003).

Discussion

The crystal structures of ChiA (Perrakis *et al*., 1994) and ChiB (van Aalten et al., 2000) from *S. marcescens* revealed deep substrate-binding clefts, in part due to the presence of a 70-90-residue insertion in the catalytic domain ('α + β domain' [Perrakis *et al*., 1994]), which is characteristic for these chitinases but which is absent in other chitinases (such as in hevamine and ChiC [van Scheltinga *et al*., 1994]). Both ChiA and ChiB contain an additional substrate-binding domain which extends the substrate binding cleft on the side where the nonreducing end of the substrate binds in ChiA (Perrakis *et al*., 1994) and on the side where the reducing end of the substrate binds in ChiB (van Aalten *et al*., 2000). In ChiA the deep substrate-binding cleft seems rather accessible, whereas the substrate-binding cleft of ChiB is more 'tunnel-like' (van Aalten *et al*., 2001, Davies *et al*., 1995). On the basis of structural characteristics (Perrakis *et al*., 1994, van Aalten *et al*., 2000) and enzymological work (Uchiyama *et al*., 2001, Suzuki *et al*., 2002, Brurberg *et al*., 1996) was suggested that ChiA and ChiB are exochitinases which degrade chitin chains from opposite ends, ChiA from the reducing end and ChiB from the non reducing end. The structure of ChiC from *S. marcescens* is not known, but its amino acid sequence shows that it consists of a catalytic domain and two putative chitin-binding domains, which are located C-terminally in the sequence (Suzuki *et al*., 1999). The catalytic domain of ChiC lacks the α + β domain which makes up a wall in the substrate binding grooves of ChiA and ChiB. This suggests that ChiC has a much more open substrate-binding groove, as observed in the crystal structure of the endochitinase hevamine (van Scheltinga *et al*., 1994).

All four *Sp* chitinases contain all residues known to be important for catalysis in family 18 chitinases (for e.g serine in the diagnostic SXGG sequence motif). The role of this serine in the catalytic mechanism of family 18 GHs is to help in the stabilization of a temporary surplus of negative charge that develops on thefirst aspartate of the catalytic sequence motif DXDXE during catalysis (van Aalten *et al*., 2001, Synstad *et al*., 2004). For ChiB from *S. marcescens*, it was shown that this charge stabilization is in fact achieved by serine in the SXGG motif. Surface exposed aromatic amino acids were conserved in *Sp* ChiA, *Sp* ChiB when compared to ChiA, ChiB of *S. marcescens* except L481 present in *Sp* ChiB in place of Y481 in ChiB of *S. marcescens*. Katouno *et al*. (2004) showed that mutation of Y481 in ChiB from *S. marcescens*, which is located most distally to the catalytic cleft among the aromatic residues, decreased the activity as well, although the effect was slightly weaker than those of the other aromatic amino acid mutations. Superimposed structures of *Sp* ChiA,

Sp ChiB and *Sp* ChiD with respective templates were differing mostly in the α/β-barrel domain (Fig. 3.22), which is the catalytic domain of chitinase.

4.3 Cloning and characterization of CBPs from *S. proteamaculans*

4.3.1 Search for homologs of *Sp* CBPs at NCBI using BLAST

A genome wide sequence analysis of the *S. proteamaculans* 568 revealed that it contains three family 33 CBPs. The *Sp* CBP21 was named according to the homology of reported *S. marcescens* CBP21. *Sp* CBP21 showed high sequence identity to CBP21 (93%). There are no reports on the presence of two more additional CBPs in *S. marcescens*, we have designated these two additional CBPs as *Sp* CBP28 and *Sp* CBP50 according to the molecular weight of the protein (molecular weight without the signal peptide). All three CBPs were cloned and over expressed in *E. coli* and purified using Ni-NTA agarose column (Fig. 3.23& 3.24).

4.3.1.1 *Sp* CBP21

The amino acid sequence of *Sp* CBP21 was BLASTed at NCBI database to search for homologs. The result displayed 93% to CBP21 from *S. marcescens* (BAA31569), 57% to CBP from *B. cereus* G9241 (EAL13960) and CBP from *B. thuringiensis* serovar *tochigiensis* BGSC 4Y1, 44% to Cbp21 from from *B. anthracis* str. CDC 684 (ACP12567), 41% to CHB2 from *Streptomyces reticuli* (EEM22267), 30% to CbpD from *Stenotrophomonas* sp. SKA14 (EED38588) and 27% to CbpD from *P. aeruginosa* (AF196565). *Sp* CBP21 contains a signal peptidase site located between amino acids residues Ala-27 and His-28 and ChBD present from His-28 through Asn-194.

4.3.1.2 *Sp* CBP28

Sp CBP28 showed 36% homology to CBP1 from *Pseudoalteromonas piscicida* (BAB79619) and CBP from *V. cholerae* NCTC 8457 (EAZ71564), 33% to CBP from *B. thuringiensis* BMB171 (ADH07314) and CBP from *B. cereus* ATCC 1457 (AAP09751), 31% to CBP from *Streptomyces* sp. e14 (EFF90245). *Sp* CBP28 contains a signal peptidase site located between amino acids residues Ala-22 and Gln-23 and ChBD present from His-39 through Asn-273.

4.3.1.3 *Sp* CBP50

The BLAST search for *Sp* CBP50 homologs displayed 62% to N-acetylglucosamine-binding protein A from *Enterobacter cloacae* subsp. *cloacae* ATCC 13047 (ADF60226), 57% to CBP21 from *S. marcescens* (BAA31569), 46% to CBP from *Shewanella* sp. HN-41 (ABK37291), 45% to CBP from *Aeromonas hydrophila* subsp. *hydrophila* ATCC 7966 (ABK37291), 40% to CHB2 from *Streptomyces reticuli* (CAA74695) and 24% to CbpD from *Vibrio harveyi* HY01 (EDL70242). *Sp* CBP50 contains a signal peptidase site located between amino acids residues Ala-21 and His-22 and ChBD present from His-22 through Asp-188.

4.3.2 Binding of *Sp* CBPs to insoluble and soluble polymeric substrates

In addition to appearing as discrete domains in enzymes, ChBMs also exist independently. CBPs are found in families 14, 18, and 33, where families 14 and 18 constitute small anti-fungal proteins that share a structurally similar chitin-binding motif (Suetake *et al*., 2000). Family 33 CBPs are mainly found in bacteria and viruses. Bacterial family 33 CBPs are expressed and secreted during chitin degradation and have been hypothesized to invade the chitin matrix and dissolve individual polymers, making them more accessible to degradation by chitinases (Vaaje-Kolstad *et al*., 2005a). Binding studies of *Sp* CBPs to chitin variants and cellulose substrates revealed that *Sp* CBP28 not able to bind to any of the substrates tested. *Sp* CBP21 and *Sp* CBP50 were similar to the CBP21 from *S. marcescens* which showed maximum binding to β-chtin (Vaaje-Kolstad *et al*., 2005b) and followed the order of binding; β-chtin>α-chtin>colloidal chitin>Avicel (Fig.3 25). Binding of *Sp* CBPs towards the soluble substrates was also examined especially to investigate whether *Sp* CBP28 has binding to soluble substrates, no binding was observed even to soluble substrates as observed in case of CBP21 from *S. marcescens* (Vaaje-Kolstad *et al*., 2005b) (Fig. 3.27).

The difference in substrate preference was mainly attributed to the difference in the sequence of respected proteins. The only available three-dimensional structure of a family 33 CBP was CBP21 from *S. marcescens*, which binds exclusively to β-chitin (Suzuki *et al*., 1998). The combination of sequence and structural information with the results of site-directed mutagenesis studies showed that the surface of family 33 CBPs contains a patch of highly conserved, mostly polar residues (Tyr54, Glu55, Glu60, His114, Asp182, and Asn185) that are important for binding to chitin and for the positive effect on efficiency of chitinase (Vaaje-Kolstad *et al*., 2005b). *Ll*CBP33A which binds equally to α- and β-chitin has two

substitutions in the conserved surface patch, both the residues were known to be important for CBP21 functionality (Vaaje-Kolstad *et al*., 2005b); (a) Ser63 occurs at a position at which CBP21 has a tyrosine (Tyr54) and where several other family 33 CBPs have another aromatic residue, tryptophan (e.g. Trp57 in CHB1 from *St. olivaceoviridis*, which has been shown to be important for the ability of CHB1 to bind α-chitin [Zeltins and Schrempf, 1997]); (b) Asn64 occurs instead of a glutamate residue (Glu55 in CBP21). The closest homologue of *Ll*CBP33A from species other than *L. lactis* is ChbB from *B. amyloliquefaciens* (66% sequence identity), which binds both α- and β-chitin (Chu *et al*., 2001). ChbB differs from CBP21 in the same two positions as *Ll*CBP33A: Tyr54 is replaced by Asp62 and Glu55 is replaced by Asn63. CBP21 of *S.marcescens* catalyzes cleavage of glycosidic bonds in crystalline chitin (Vaaje-Kolstad *et al*. 2010), thus opening up the inaccessible polysaccharide material for hydrolysis by normal glycoside hydrolases. This enzymatic activity was discovered after detection of traces of previously unidentified chitooligosaccharides upon incubation of β-chitin nano whiskers with CBP21.

Sequence alignment of *Sp* CBP21, *Sp* CBP28 and *Sp* CBP50 with CBP21 from *S. marcescens* displayed 93%, 54% and 18% identity, respectively. The conserved surface-located polar residues was highly conserved in *Sp* CBP21 (Tyr-54, Glu-55, Glu-60, His-114, Asp-182, and Asn-185) and *Sp* CBP50 (Tyr-48, Glu-49, Glu-54, His-108, Asp-176, and Asn-179), while *Sp* CBP28 matches only one residues (Asp-176) (Fig. 3.30) out of six conserved polar residues. Because of sequence homology and presence of conserved polar surface residues in both *Sp* CBP21 and *Sp* CBP50, the proteins showed similar β-chitin binding preference as shown by CBP21 of *S. marcescens*, while least homology and absence of other polar residues could be the reasons for *Sp* CBP28 for not able to bind to substrates.

4.3.2.1 Time-course of binding of *Sp* CBPs to natural chitin variants

Binding of the *Sp* CBP21 and *Sp* CBP50 to natural chitin variants was investigated as a function of time. Fig. 3.25C&D, demonstrated that the binding process of *Sp* CBP21 and *Sp* CBP50 to β-chtin took place rapidly and reached equilibrium within 6 and 12 h, respectively, while CBP21 from *S. marcescens* established binding equilibrium after 16 h of incubation (Vaaje-Kolstad *et al*., 2005b). On the other hand *Sp* CBP21 and *Sp* CBP50 showed to α-chitin relatively slow binding and reached equilibrium by 12 h. CBP (*Ll*CBP33A) from *Lactococcus lactis* subsp. *lactis* (Vaaje-Kolstad *et al*., 2009) established binding equilibrium by approximately 12 h of incubation for both α-chtin and β-chtin.

4.3.2.2 Equilibrium adsorption isotherms of *Sp* CBP21 and *Sp* CBP50 to natural chitin variants

Second binding assay was meant for estimation of equilibrium binding constants (K_d) and binding capacities (B_{max}) were analysed for *Sp* CBP21 and *Sp* CBP50 (Fig. 3 26 and Table 3.2). In agreement with the binding assay, the lower K_d values of *Sp* CBP21 and *Sp* CBP50 have shown that both the proteins have high binding strength towards the β-chitin when compared to the α-chitin. *Sp* CBP21 and *Sp* CBP50, K_d values towards the β-chitin were relatively higher, while B_{max} values were lower when compared to the K_d and B_{max} values of reported CBPs from *S. marcescens* and *B. thuringiensis* serovar *konkukian* (Vaaje-Kolstad *et al*., 2005b, Mehmood *et al*., 2011).

4.3.3 Effect of *Sp* CBP21 and *Sp* CBP50 on chitin hydrolysis of *Sp* chitinases

Vaaje-Kolstad *et al*., (2005a) reported that the CBPs which bind to the insoluble crystalline substrate, leading to structural changes in the substrate and increased substrate accessibility of the chitinases. The CBP21 of *S. marcescens* strongly promoted hydrolysis of crystalline β-chitin by chitinases A and C, while it was essential for full degradation by chitinase B from *S. marcescens*. Vaaje-Kolstad *et al*. (2009) also showed that the *Ll*CBP33A increased the hydrolytic efficiency of *Ll*Chi18A to both α- and β-chitin. These results show the general importance of CBPs in chitin turnover. We have tested the *Sp* CBP21 and *Sp* CBP50 in the presence of four *Sp* chitinases in hydrolysis of natural chitin variants. The results show that all the four *Sp* chitinases efficiency on addition of *Sp* CBP21 and *Sp* CBP50 increased with both the substrates. *Sp* CBP21 and *Sp* CBP50 had showed almost similar synergism with *Sp* chitinases in degrading natural chitin variants. In presence of *Sp* CBP21; *Sp* ChiA, *Sp* ChiB, *Sp* ChiC and *Sp* ChiD product formation efficiency increased by ~0.2, 0.25, 0.32 and 1-fold, respectively (Fig. 3.29A) from α-chitin. In β-chitin, *Sp* ChiA, *Sp* ChiB, *Sp* ChiC and *Sp* ChiD product formation efficiency increased by ~0.1, 2.5, 1.1 and 2-fold, respectively from β-chitin (Fig. 3.29B). In presence of *Sp* CBP50; *Sp* ChiA, *Sp* ChiB, *Sp* ChiC and *Sp* ChiD increase in product formation efficiency increased by ~0.17, 0.32, 0.45 and 1-fold, respectively (Fig. 3.29C) from α-chitin, where as in β-chitin *Sp* ChiA, *Sp* ChiB, *Sp* ChiC and *Sp* ChiD product formation efficiency increased by ~0.08, 3.2, 1.25 and 2-fold, respectively from β-chitin (Fig. 3.29D). In the presence of *Sp* CBP21 and *Sp* CBP50; *Sp* ChiA- ChiD showed only minor effects on α-chitin hydrolysis and the product formation was almost equal except for *Sp* ChiD where the efficiency increased ~ 1- fold. The *Sp* chitinases as such had

less activity on α-chitin and similarly *Sp* CBP21 and *Sp* CBP50 also showed only minor binding preference.

The addition of *Sp* CBP21 and *Sp* CBP50 have only minor effects on *Sp* ChiA and *Sp* ChiC in hydrolysis of β-chitin while *Sp* ChiB and *Sp* ChiD efficiency increased significantly high. These results are comparable with the reported ChiB from *S. marcescens* which depends heavily on CBP21 in β-chitin degradation (Vaaje-Kolstad *et al*., 2005a), interestingly in both the organisms *cbp21* gene is located 1.5 kb downstream to the *chiB* and was reported that *S. marcescens* CBP21 protein is produced along with ChiB and the other two chitinases, ChiA and ChiC (Suzuki *et al*., 1998, Watanabe *et al*., 1997, Suzuki *et al*., 2001). Recently Vaaje-Kolstad *et al*. (2010) reported that CBP21 from *S. marcescens* was an enzyme that acts on the surface of crystalline chitin, where it introduces chain breaks and generates oxidized chain ends, thus promoting further degradation by chitinases. So it was suggest naming of CBP21was a "chitin oxidohydrolase". Overall, in both the chitin substrates (α- and β-chitin) among the other *Sp* chitinases *Sp* ChiD obtained major benefit from *Sp* CBP21 and *Sp* CBP50. CBP-mediated enhancement of substrate availability increased the *Sp* ChiD efficiency as the enzyme is weak in hydrolyzing insoluble substrates when compared to other *Sp* chitinases.

4.3.4 Sequence analysis of *Sp* CBPs and homology modelling for *Sp* CBP21

Alignment of all three *Sp* CBPs to CBP21 from *S. marcescens* showed that the presence of highly conserved polar residues important in binding (Tyr, Glu, Glu, His, Asp, and Asn) in *Sp* CBP21 and *Sp* CBP50, the residues are use full to enhance. Chitinase efficiency as observed in CBP21 from *S. marcescens* (Vaaje-Kolstad *et al*., 2005a, b) (Fig. 3.30). In CBP28 only one polar residue (Asp) was conserved. Mostly the β- sheets were differing in *Sp* CBP21 when superimposed with the template structure (Fig. 3.31B). Because of less sequence homology with CBP21 from *S. marcescens*, we are not able to generate models for *Sp* CBP28 and *Sp* CBP50.

4.4 Upstream sequence analysis of *Sp* chitinolytic genes

We have also analysed the upstream sequences of *Sp* chitinolytic genes, because all these genes are involved in a single catabolic pathway (chitin hydrolysis). Genome sequence of *S. proteamaculans* 568 revealed that the *Sp* chitinolytic genes were scattered throughout the genome except *Sp cbp21* and *Sp chiB* were placed in 1.5 kb distance. The gene *Sp cbp21* is

located 1.5 kb downstream to the *Sp chiB*, but the two genes are not in the same operon. Similar type of arrangement of *cbp21* and *chiB* was also observed in *S. marcescens* (Suzuki *et al*., 1998 and 2001). A conserved 8 bp [C(C/T/A) C(C/T) (T/G) G (C/A) (C/G)] region was observed in the upstream intergenic sequences of all *Sp* chitinolytic genes (Table 4.2) indicate that these chitinolytic genes might be coordinately controlled by the same regulatory protein(s). Similar kind of 8 bp (5´-ACAACATG-3´) conserved region was observed in *Alteromonas* sp. Strain O-7 (Orikoshi *et al*., 2005b).

Gene name	Length	Strand	Start site	Sites		
chiD	229	+	31	GCCCTTTTCT	CCCCGGCC	CAAATCTCGA
chiC	179	+	79	AAAGGTTTCA	CCCCGGCC	TCGTTAAAAA
chiB	297	-	40	ACCGATATCC	CACCGGCC	GTGATTGGCA
cbp50	255	-	74	TCCGCAATAA	CTCTGGCC	GATTAAAATG
chiA	379	-	287	GCCCATAATA	CCCCTGAC	GTAAAATACC
cbp28	320	+	226	CTCATTTATC	CACTTGCC	GTTACGCCCA
cbp21	406	-	392	AAGTCA	CTCCTGAC	TGAAGTTGTA

Table 4.2: Upstream sequence analysis of *Sp* chitinolytic genes

Upstream intergenic regions of genes encoding for chitinases and chitin binding proteins were retrieved from the genome data base of *S. proteamaculans* 568 and analysed using MEME 4.3.0 motif discovery tool. Consensus sequences in the upstream of *Sp* chitinolytic genes were displayed over the table.

SUMMARY & CONCLUSION

Back ground and objective

Chitin, an unbranched homopolymer of 1,4-β-linked N-acetyl-D-glucosamine (GlcNAc), is the secondmost abundant and renewable polysaccharide (after cellulose) on Earth. Fungal cell walls, insect exoskeletons, and shells of crustaceans are the main sources of chitin. Chitinases are chitin-degrading enzymes, and hydrolyze the β-(1, 4) linkages of chitin. Chitinases have potential applications in agriculture, medicine and environmental fields. *S. proteamaculans* 568 is one of the complex chitinolytic strains with several genes coding for chitinolytic machinery. Complete genome sequence of *S. proteamaculans* revealed 4 chitinases and 3 chitin binding proteins (CBPs) and one chitobiase which is capable of converting the *N*-acetylglucosamine dimers produced by the chitinases to monomers. The properties of 4 chitinases (*Sp* ChiA, *Sp* ChiB, *Sp* ChiC and *Sp* ChiD) and 3 CBPs (*Sp* CBP21, *Sp* CBP28 and *Sp* CBP50) were investigated in this study.

5.1 Cloning and characterization of *S. proteamaculans* 568 chitinases

The identity of *S. proteamaculans* 568 was confirmed by 16S rDNA analysis. *S. proteamaculans* 568 was screened for its chitinolytic ability on chitin containing agar plate. After 5 days of culturing a zone of clearance was observed around the colony that confirmed the chitinolytic potential of the organism.

Four chitinases (*Sp* ChiA, *Sp* ChiB, *Sp* ChiC and *Sp* ChiD) were amplified without signal peptide, cloned in pET 22b or pET 28a expressed in *E. coli* and purified using Ni-NTA agarose column chromatography. Purified enzymes were characterized in terms of kinetics, optimum pH and temperature, substrate preference, binding preferences towards the insoluble and soluble substrates, products analysis from CHOS and colloidal chitin using TLC, HPLC and MALDI-TOF-TOF.

Kinetic analysis revealed that *Sp* ChiA had highest catalytic efficiency among the other chitinases, while *Sp* ChiB and *Sp* ChiC displayed the values nearer to the *Sp* ChiA. *Sp* ChiD had the lowest catalytic efficiency and kinetic values were much inferior to other *Sp* chitinases. *Sp* chitinases displayed optimum activity between pH 5.0-7.0. Compared to the other *Sp* chitinases *Sp* ChiA was active over a broad range of pH. All four *Sp* chitinases were optimally active at 40^{o}C. *Sp* ChiA-ChiC showed maximum activity on β-chitin, while *Sp* ChiD had maximum activity on soluble chitosan with 99% DDA. Among the *Sp* chitinases, *Sp* ChiA had highest hydrolytic activity on α-chitin, which is abundant form of

chitin on earth. All four *Sp* chitinases exhibited binding maximum toward the β-, and/or colloidal chitin. *Sp* chitinases showed binding and or towards only soluble chitin (glycol chitin) from among the tested soluble polysaccharides.

All *Sp* chitinases released DP2 product from polymeric and CHOS substrates because of endo mode of action. From the oligomeric substrates, *Sp* ChiA, *Sp* ChiB and *Sp* ChiC released dimer (DP2) as major end product, while *Sp* ChiD formed monomer (DP1) due to chitobiase activity. *Sp* ChiD synthesized higher length oligosaccharide products from CHOS substrates due to transglycosylation (TG) activity. HPLC and MALDI-TOF-MS revealed that *Sp* ChiD released DP7-DP13, DP6-DP12, DP5-DP10 and DP4-DP7 from DP6, DP5, DP4 and DP3 substrates, respectively. The TG activity of *Sp* ChiD was dependant on the enzyme concentration, size and concentration of the substrate. Formation of TG products was directly proportional to the size and concentration of the substrate and indirectly proportional to the enzyme concentration. All *Sp* chitinases released DP1-DP4 products from polymeric substrates. DP2 was predominatly produced by *Sp* ChiA-ChiC, while DP1 was predominant for *Sp* ChiD. Because of the presence of α + β insertion domain in *Sp* ChiA, *Sp* ChiB and *Sp* ChiD, these enzymes were categorised as a processive enzymes, where as in *Sp* ChiC there was no such α + β insertion present. Hence *Sp* ChiC appears to be a non processive enzyme. *Sp* ChiA, *Sp* ChiB and *Sp* ChiD models were also generated using templates of ChiA, ChiB of *S. marcescens* and chitinase II of *Klebsiella pneumoniae*, respectively.

5.2 Cloning and characterization of *S. proteamaculans* 568 chitin binding proteins (CBPs)

All three CBPs (*Sp* CBP21, *Sp* CBP28 and *Sp* CBP50) were cloned in pET 22b or pET 28a, over expressed in *E.coli* and purified using Ni-NTA agarose column and characterized. Characterization of CBPs includes the binding towards the soluble and insoluble polymeric substrates, scanning electron microscopic study of chitin treated with CBPs and synergistic effect of CBPs with chitinases in chitin degradation. *Sp* CBP21 and *Sp* CBP50 were able to bind chitin variants preferentially to β-chitin while *Sp* CBP28 was not able to bind to any of the test substrates. None of the CBPs were able to bind soluble polysaccharide substrates. *Sp* CBP21 attained binding equilibrium by 6 h and 12 h to α- and β-chitin, respectively, while *Sp* CBP50 reached binding equilibrium by 12 h to both α- and β-chitin, respectively. *Sp* CBP21 and *Sp* CBP50 had low K_d to β-chitin indicating that these two CBPs had higher

affinity to β-chitin compared to α-chitin. *Sp* CBP21 and *Sp* CBP50 showed synergism with *Sp* chitinases and increased the activity of enzymes. *Sp* CBP21 and *Sp* CBP50 showed almost similar tendency in synergism with *Sp* chitinases and the effect was significantly higher with β-chitin. Among the *Sp* chitinases, *Sp* ChiD released maximum amount of products in presence of *Sp* CBP21 and *Sp* CBP50 from α-,β- chitin, while *Sp* ChiB, released highest amount of products in the presence of *Sp* CBP21 and *Sp* CBP50 in β-chitin substrate. Finally *Sp* CBP21 model was prepared using CBP21 of *S. marcescens*.

Major findings in the present work

- Four chitinases (*Sp* ChiA, *Sp* ChiB, *Sp* ChiC and *Sp* ChiD) and three CBPs (*Sp* CBP21, *Sp* CBP28 and *Sp* CBP50) were cloned, heterologously expressed and purified.
- *Sp* ChiA, *Sp* ChiB and *Sp* ChiC showed maximum activity on β-chitin where as *Sp* ChiD had highest activity on soluble chitin/chitosan substrate.
- *Sp* ChiA, *Sp* ChiB and *Sp* ChiC released DP2 as major end product from oligomeric and ploymeric substrates, while *Sp* ChiD released DP1as the major end product.
- *Sp* ChiA, *Sp* ChiB and *Sp* ChiC require a minimum of DP3 substrate to perform enzymatic activity, where as DP2 was sufficient for *Sp* ChiD (chitobiase activity).
- *Sp* ChiD showed TG activity on CHOS substrates ranging from DP3 to DP6.
    - ❖ Formation of higher chain length oligomers was directly proportional to the size of the substrate provided.
    - ❖ High enzyme concentration increased the hydrolysis activity and significantly reduced the TG activity.
- All four *Sp* chitinases are endo enzymes, based on sequence analysis *Sp* ChiA, *Sp* ChiB, *Sp* ChiD were determined as processive enzymes, while *Sp* ChiC was a non-processive enzyme
- *Sp* CBP21 and *Sp* CBP50 bind to the β-chitin more preferentially, while *Sp* CBP 28 did not bind to the chitinous substrates used.
- *Sp* CBP21 and *Sp* CBP50 showed synergistic effect with chitinases in hydrolysis of chitin.
- *Sp* chitinolytic genes have conserved 8 bp region in their upstream sequences.

REFERENCES

References

Aam, B. B., Heggset, E. B., Norberg, A. L., Sørlie, M., Vårum, K. M., and Eijsink, V. G. H. 2010. Production of chitooligosaccharides and their potential applications in medicine. *Mar. Drugs*. **8**: 1482-1517.

Adachi, W., Sakihama, Y., Shimizu, S., Sunami, T., Fukazawa, T., Suzuki, M., Yatsunami, R.,Nakamura, S., and Takenaka, A. 2004. Crystal structure of family GH-8 chitosanase with subclass II specificity from *Bacillus* sp. K17. *J. Mol. Biol*. **343**: 785-795.

Aguilera, B., Ghauharali-van der Vlugt, K., Helmond, M. T. J., Out, J. M. M., Donker-Koopman, W. E., Groener, J. E. M., Boot, R. G., Renkema, G. H., van derMarel, G. A., van Boom, J. H., Overkleeft, H. S., and Aerts, J.M. F.G. 2003. Transglycosidase activity of chitotriosidase: Improved enzymatic assay for the human macrophage chitinase. *J. Biol. Chem.* **278**: 40911-40916.

Aksu, Z.M. 2005. Application of biosorption for the removal of organic pollutants: a review. *Process. Biochem*. **40**: 997-1026.

Arai, N., Shiomi, K., Yamaguchi, Y., Masuma, R., Iwai, Y., Turberg, A., Kolbl, H., and Omura, S. 2000. Argadin, a new chitinase inhibitor produced by *Clonostachys* sp. FO. 7314. *Chem. Pharm. Bull (Tokyo)*. **48**: 1442-1446.

Aronson N.N.Jr., Halloran, B.A., Alexeyev, M.F., Zhou, X.E., Wang, Y., Meehan, E.J., and Chen, L. 2006. Mutation of a conserved tryptophan in the chitin-binding cleft of *Serratia marcescens* chitinase A enhances transglycosylation. *Biosci. Biotechnol. Biochem*. **70**: 243-251.

Aronson, N.N.Jr., Halloran, B.A., Alexyev, M.F., Amable, L., Madura, J.D., Pasupulati, L., Worth, C., and Patrick van Roey, P. 2003. Family 18 chitinase-oligosaccharide substrate interaction: subsite preference and anomer selectivity of *Serratia marcescens* chitinase A. *Biochem. J*. **376**: 87-95.

Atkins, E.D.T. 1985. Conformation in polysaccharides and complex carbohydrates. *J. Biosci*. **8**: 375-387.

Bahrke, S., Einarsson, J.M., Gislason, J., Haebel, S., Letzel, M.C., Peter-Katalinic, J., and Peter, M.G. 2002. Sequence analysis of chitooligosaccharides by matrix-assisted laser desorption ionization postsource decay mass spectrometry. *Biomacromolecules* **3**: 696-704.

References

Bhattacharya, D., Nagpure, A., and Gupta, R.K. 2007. Bacterial chitinases: properties and potential. *Crit. Rev. Biotechnol*. **27**: 21-28.

Bhushan, B., and Hoondal, G.S. 1998. Isolation, purification and properties of a thermostable chitinase from an alkalophilic *Bacillus* sp.BG-11. *Biotechnol. Lett*. **20**: 157-159.

Boer, H.,Munck, N., Natunen, J.,Wohlfahrt, G., Söderlund, H., Renkonen, O., and Koivula, A. 2004. Differential recognition of animal type beta 4-galactosylated and alpha 3-fucosylated chito-oligosaccharides by two family 18 chitinases from *Trichoderma harzianum*. *Glycobiol*. **14**: 1303-1313.

Bokma, E., Rozeboom, H. J., Sibbald, M., Dijkstra, B. W., and Beintema, J. J. 2002. Expression and characterization of active site mutants of hevamine, a chitinase from the rubber tree *Hevea brasiliensis*. *Eur. J. Biochem*. **269**: 893-901.

Brameld, K.A., and Goddard, W.A. 1998. Substrate distortion to a boat conformation at subsite -1 is critical in the mechanism of family 18 chitinases. *J. Am. Chem. Soc*. **120**: 3571-3580.

Brurberg, M.B., Nes, I.F., and Eijsink, V.G., 1996. Comparative studies of chitinases A and B from *Serratia marcescens*. *Microbiology*. **142:** 1581-1589.

Cantarel, B.L.,Coutinho, P.M., Rancurel, C., Bernard, T., Lombard, V., and Henrissat, B. 2009. The Carbohydrate-Active enZYmes database (CAZy): An expert resource for Glycogenomics. *Nucleic Acids Res*. **37**: 233-238.

Cederkvist, F., Zamfir, A.D., Bahrke, S., Eijsink, V.G.H., Sørlie, M.; Peter-Katalinic, J., and Peter, M.G. 2006. Identification of a high-affinity-binding oligosaccharide by (+) nanoelectrospray quadrupole time-of-flight tandem mass spectrometry of a noncovalent enzyme-ligand complex. *Angewandte Chemie-Int. Ed*. **45**: 2429-2434.

Cederkvist, H.F., Parmer, M.P., Vårum, K.M., Eijsink, G.H.V., and Sørlie, M. 2008. Inhibition of a family 18 chitinase by chitooligosaccharides. *Carbohydr. Polym*. **74:** 41-49.

Chang, M. C., Lai, P. L., and Wu, M. L. 2004. Biochemical characterization and site-directed mutational analysis of the double chitin-binding domain from chitinase 92 of *Aeromonas hydrophila* JP101. *FEMS Microbiol. Lett*. **235**: 61-66.

References

Cheng, C.Y.,Chang, C.H., Wu, Y.J., and Li, Y.K. 2006. Exploration of glycosyl hydrolase family 75, a chitosanase from *Aspergillus fumigatus*. *J. Biol. Chem*. **281**: 3137-3144.

Choi, B.K., Kim, K.Y., Yoo, Y.J., Oh, S.J., Choi, J.H., and Kim, C.Y.2001. In vitro antimicrobial activity of a chitooligosaccharide mixture against *Actinobacillus actinomycetemcomitans* and *Streptococcus mutans*. *Int. J. Antimicrob. Agents.* **18**: 553-557.

Chou, Y.T., Yao, S., Czerwinski, R., Fleming,M., Krykbaev, R., Xuan, D., Zhou, H., Brooks, J., Fitz, L., Strand, J., Presman, E., Lin, L., Aulabaugh, A., and Huang, X. 2006. Kinetic characterization of recombinant human acidic mammalian chitinase. *Biochemistry*. **45**: 4444-4454.

Chu, H.H., Hoang, V., Hofemeister, J., and Schrempf, H. 2001. A *Bacillus amyloliquefaciens* ChbB protein binds beta- and alpha-chitin and has homologues in related strains. *Microbiology*. **147**: 1793-1803.

Chuang, H.H., Lin, H.Y., and Lin, F.P. 2008. Biochemical characteristics of C-terminal region of recombinant chitinase from *Bacillus licheniformis*-implication of necessity for enzyme properties. *FEBS J*. **275:** 2240-225.

Cody, R.M., 1989. Distribution of chitinase and chitobiase in *Bacillus*. *Curr. Microbiol*. **19:** 201-205.

Dahiya, N., Tewari, R., and Hoondal, G.S. 2006. Biotechnological aspects of chitinolytic enzymes: a review. *Appl. Microbiol. Biotechnol*. **71**: 773-782.

Davies, G., and Henrissat, B. 1995. Structures and mechanisms of glycosyl hydrolases. *Structure*, **3**: 853-859.

Day, R.B., Okada, M., Ito, Y., Tsukada, K., Zaghouani, H., Shibuya, N., and Stacey, G. 2001. Binding site for chitin oligosaccharides in the soybean plasma membrane. *Plant Physiol*. **126**: 1162-1173.

De Jong, A.J., Heidstra, R., Spaink, H.P., Hartog, M.V., Meijer, E.A., Hendriks, T., Schiavo, F.L., Terzi, M., Bisseling, T., Van Kammen, A., and De Vries, S.C. 1993. Rhizobium lipooligosaccharides rescue a carrot somatic embryo mutant. *Plant Cell*. **5**: 615-620.

References

Delic, I., Robbins, P., and Westpheling, J. 1992. Direct repeat sequences are implicated in the regulation of two *Streptomyces* chitinase promoters that are subject to carbon catabolite control. *Proc. Natl. Acad. Sci. U.*S.A. **89**:1885-1889.

Dev, A., Mohan, J.C., Sreeja, V., Tamura, H., Patzke, G.R., Hussain, F., Weyeneth, S., Nair, S.V., and Jayakumar, R. 2010. Novel carboxymethyl chitin nanoparticles for cancer drug delivery applications. *Carbohydr. Polym.* **79**: 1073-1079.

Divne, C., Ståhlberg, J., Reinikainen, T., Ruohonen, L., Pettersson, G., Knowles, J. K., Teeri, T. T., and Jones, T. A. 1994. The three-dimensional crystal structure of the catalytic core of cellobiohydrolase I from *Trichoderma reesei*. *Science*. **265:** 524-528.

Divne, C., Ståhlberg, J., Teeri, T.T., and Jones, T.A. 1998. High-resolution crystal structures reveal how a cellulose chain is bound in the 50 Å long tunnel of cellobiohydrolase I from *Trichoderma reesei*. *J. Mol. Biol*. **275:** 309-325.

Eijsink, V.G.H., Vaaje-Kolstad, G., Vårum, K.M, and Horn, S.J. 2008. Towards new enzymes for biofuels: lessons from chitinase research. *Trends Biotechnol*. **26**: 228-235.

Eneyskaya, E.V., Golubev, A. M., Kachurin, A.M., Savel'ev,A.N., and Neustroev, K.N. 1997. Transglycosylation activity of alpha-D-galactosidase from *Trichoderma reesei* - An investigation of the active site. *Carbohydr. Res*. **305**: 83-91.

Evvyernie, D., Yamazaki, S., Morimoto, K., Karita, S., Kimura, T., Sakka, K., and Ohmiya, K. 2000. Identification and characterization of *Clostridium paraputrificum* M-21, a chitinolytic, mesophilic and hydrogen-producing bacterium. *J. Biosci. Bioeng*. **89**: 596-601.

Felix, G., Baureithel, K., and Boller, T. 1998. Desensitization of the perception system for chitin fragments in tomato cells. *Plant Physiol*. **117**: 643-650.

Folders, J., Tommassen, J., van Loon, L.C., and Bitter, W. 2000. Identification of a chitin-binding protein secreted by *Pseudomonas aeruginosa*. *J. Bacteriol*. **182**: 1257-1263.

Fujita, K., Sato, R., Toma, K., Kitahara, K., Suganuma, T.,Yamamoto, K., and Takegawa, K. 2007. Identification of the catalytic acid -base residue of *Arthrobacter* endo-beta-N-acetylglucosaminidase by chemical rescue of an inactive mutant. *J. Biochem*. **142**: 301-306.

Fukamizo, T., Honda, Y., Goto, S., Boucher, I., and Brzezinski, R. 1995. Reaction mechanism of chitosanase from *Streptomyces* sp. N174. *Biochem. J*. **311**: 377-383.

References

Fukamizo, T., Sasaki, C., Schelp, E., Bortone, K., and Robertus, J.D. 2001. Kinetic properties of chitinase-1 from the fungal pathogen *Coccidioides immitis*. *Biochemistry*. 2001. **40**: 2448-2454.

Haebel, S., Bahrke, S., and Peter, M.G. 2007. Quantitative sequencing of complex mixtures of heterochitooligosaccharides by vMALDI-linear ion trap mass spectrometry. *Anal. Chem.* 2007, **79**: 5557-5566.

Henrissat, B., and Davies, G. 1997. Structural and sequence-based classification of glycoside hydrolases. *Curr. Opin. Struct. Biol*. **7:** 637-644.

Hoell, I.A., Dalhus, B., Heggset, E.B., Aspmo, S.I., and Eijsink, V.G.H. 2006. Crystal structure and enzymatic properties of a bacterial family 19 chitinase reveal differences from plant enzymes. *FEBS J*. **273**: 4889-4900.

Horn, S.J., Sikorski, P., Cederkvist, J.B., Vaaje-Kolstad, G., Sørlie, M., Synstad, B., Vriend, G., Vårum, K.M., and Eijsink, V.G.H. 2006a. Costs and benefits of processivity in enzymatic degradation of recalcitrant polysaccharides. *Proc. Natl. Acad. Sci. U.SA*. **103**: 18089-18094.

Horn, S.J., Sørbotten, A., Synstad, B., Sikorski, P., Sørlie, M., Vårum, K.M., and Eijsink, V.G. 2006b. Endo/exo mechanism and processivity of family 18 chitinases produced by *Serratia marcescens*. *FEBS J*. **273**: 491-503.

Howard, M.B., Ekborg, N. A., Weiner, R.M., and Hutcheson, S.W. 2003. Detection and characterization of chitinases and other chitin-modifying enzymes. *J. Ind. Microbiol. Biotechnol*. **30:** 627-635.

Huang, C.J., and Chen, C.Y., 2005. High-level expression and characterization of two chitinases, ChiCH and ChiCW, of *Bacillus cereus* 28-9 in *Escherichia coli*. *Biochem. Biophys. Res. Commu.* **327:** 8-17.

Imato, T., and Yagishita, K. 1971. A simple activity measurement of lysozyme. *Agr. Boil. Chem.* **35**:1154-1156.

Iseli, B., Armand, S., Boller, T., Neuhaus, J.M., and Henrissat, B. 1996. Plant chitinases use two different hydrolytic mechanisms. *FEBS Lett*. **382**: 186-188.

References

Ishihara, M., Obara, K.,Nakamura, S., Fujita, M., Masuoka, K., Kanatani, Y., Takase, B., Hattori, H., Morimoto, Y., Ishihara, M., Maehara, T., and Kikuchi, M. 2006. Chitosan hydrogel as a drug delivery carrier to control angiogenesis. *J. Artif. Organs*. **9**: 8-16.

Ito, Y., Kaku, H., and Shibuya, N. 1997. Identification of a high-affinity binding protein for N-acetylchitooligosaccharide elicitor in the plasma membrane of suspension-cultured rice cells by affinity labeling. *Plant J*. **12**: 347-356.

Izumida, H., Imamura, N., and Sano, H. 1996. A novel chitinase inhibitor from a marine bacterium, *Pseudomonas* sp. *J. Antibiot (Tokyo)*. **49**: 76-80.

Je, J.Y., and Kim, S.K. 2006. Antioxidant activity of novel chitin derivative. *Bioorg. Med. Chem. Lett*. **16**: 1884-1887.

Johansson, P., Brumer III, H., Baumann, M.J., Kallas, A.M., Henriksson, H., Denman, S.E., Teeri, T.T., and Jones T.A. 2004. Crystal structures of a poplar xyloglucan endotransglycosylase reveal details of transglycosylation acceptor binding. *Plant Cell*. **16:** 874-886.

Kageyama, C., Kato, K., Iyozumi, H., Inagaki, H., Yamaguchi, A., Furuse, K., and Baba, K. 2006. Photon emissions from rice cells elicited by N-acetylchitooligosaccharide are generated through phospholipid signaling in close association with the production of reactive oxygen species. *Plant Physiol. Biochem*. **44**: 901-909.

Kamiyama, K., Onishi, H., and Machida, Y.1999. Biodisposition characteristics of N-succinyl-chitosan and glycol- chitosan in normal and tumor-bearing mice. *Biol. Pharm. Bull*. **22**: 179-186.

Katouno, F., Taguchi, M., Sakurai, K., Uchiyama, T., Nikaidou, N., Nonaka, T., Sugiyama, J., and Watanabe, T. 2004. Importance of exposed aromatic residues in chitinase B from *Serratia marcescens* 2170 for crystalline chitin hydrolysis. *J. Biochem*. **136:** 163-168.

Kawai, R., Igarashi, K., Kitaoka, M., Ishii, T., and Samejima, M. 2004. Kinetics of substrate transglycosylation by glycoside hydrolase family 3 glucan -β-glucosidase from the white-rot fungus *Phanerochaete chrysosporium*. *Carbohyd. Res*. **339:** 2851-2857.

References

Kim, H.S., Timmis, K.N., and Golyshin, N.P. 2007. Characterization of a chitinolytic enzyme from *Serratia* sp. KCK isolated from kimchi juice. *Appl. Microbiol. Biotechnol*. 2007. **75:** 1275-1283.

Kim, J., Yun, S., and Ounaies, Z. 2006. Discovery of cellulose as a smart material. *Macromolecules*. **39**: 4204-4206.

Kishore, G.K., Pande, S., and Podile, A.R. 2005. Biological control of late leaf disease of peanut (*Arachis hypogaea*) with chitinolytic bacteria. *Phytopathology*. **95:** 1157-1165.

Kolbe, S., Fischer, S., Becirevic, A., Hinz, P., and Schrempf, H. 1998. The *Streptomyces reticuli* alpha-chitin-binding protein CHB2 and its gene. *Microbiology*. **144**: 1291-1297.

Kumar, S., Dudley, J., Nei, M., and Tamura, K. 2008. MEGA: a biologistcentric software for evolutionary analysis of DNA and protein sequences. *Brief Bioinform*. **9:** 299-306.

Kurita, K., Ishii, S., Tomita, K., Nishimura, S., and Shimoda, K. 1994. Reactivity characteristics of squid β-chitin as compared with those of shrimp chitin: High potentials of squid chitin as a starting material for facile chemical modifications. *J. Polym. Sci. Part A: Polym. Chem*. **32**: 1027-1032.

Laemmli, U. 1970. Cleavage of structural proteins during the assembly of the head of bacteriophage T4. *Nature*. **227**: 680-685.

Lan, X., Zhang, X., Hu, J., and Shimosaka, M. 2006. Cloning, expression and characterization of a chitinase from the chitinolytic bacterium *Aeromonas hydrophila* strain SUWA-9. *Biosci. Biotechnol. Biochem*. **70:** 2437-2442.

Larsson, A. M., Anderson, L., Xu, B., Munoz, I. G., Usón, I.,Janson, J.C., St albrand, H., and St ahlberg, J. 2006. Three-dimensional crystal structure and enzymatic characterization of β-mannanase Man5A from blue mussel *Mytilus edulis*. *J. Mol. Biol*. **357:** 1500-1510.

Le Dévédec, F., Bazinet, L., Furtos, A., Venne, K., Brunet, S., and Mateescu, M.A. 2008. Separation of chitosan oligomers by immobilized metal affinity chromatography. *J. Chromatogr. A*, **1194**: 165-171.

Leemhuis, H., Rozeboom, H.J., Wilbrink, M., Euverink, G.J.W., Dijkstra, B.W., and Dijkhuizen, L. 2003. Conversion of cyclodextrin glycosyltransferase into a starch hydrolase

by directed evolution: The role of alanine 230 in acceptor subsite +1. *Biochemistry*. **42:** 7518-7526.

Li, D.C., 2006. Review of fungal chitinase. *Mycopathol*. **161**: 345-360.

Lin, F.P., Juang, W.Y., Chang, K.H., and Chen, H.C. 2001. G561 site-directed deletion mutant chitinase from *Aeromonas caviae* is active without its 304 C-terminal amino acid residues. *Arch. Microbiol*. **175:** 220-225.

Liu, M, Cai, Q.X., Liu, B.H., Yan, J.P., and Yuan, Z.M., 2002. Chitinolytic activities in *Bacillus thuringiensis* and their synergistic effects on larvicidal activity. *J. Appl. Microbiol*. **93:** 374-379.

Lopatin, S.A., Derbeneva, M.S., Kulikov, S.N., Varlamov, V.P., and Shpigun, O.A. 2009. Fractionation of chitosan by ultrafiltration. *J. Anal. Chem*. **64**: 648-651.

Lü, Y., Yang, H., Hu, H., Wang, Y., Rao, Z., and Jin, C. 2009. Mutation of Trp137 to glutamate completely removes transglycosyl activity associated with the *Aspergillus fumigatus* AfChiB1. *Glycoconj. J*. **26**: 525-534.

Ly, H. D., and Withers, S. G. 1999. Mutagenesis of glycosidases. *Annu. Rev. Biochem*. **68**: 487-522.

Mehmood, M.A., Xiao, X., Hafeez, F.Y., Gai, Y., and Wang, F. 2009. Purification and characterization of a chitinase from *Serratia proteamaculans*. *World. J. Microbiol. Biotechnol*. **25:** 1955-1961.

Mehmood, M.A., Xiao, X., Hafeez, F.Y., Gai, Y., and Wang, F. 2011. Molecular characterization of the modular chitin binding protein Cbp50 from *Bacillus thuringiensis* serovar *konkukian*. *Antonie Van Leeuwenhoek*. **53**: 125-136.

Minami, E., Kouchi, H., Carlson, R.W., Cohn, J.R., Kolli, V.K., Day, R.B., Ogawa, T., and Stacey, G. 1996. Cooperative action of lipo-chitin nodulation signals on the induction of the early nodulin, ENOD2, in soybean roots. *Mol. Plant. Microbe. Interact*. **9**: 574-583.

Minami, S., Suzuki, H., Okamoto, Y., Fujinaga, T., and Shigemasa, Y. 1998. Chitin and chitosan activate complement via the alternative pathway. *Carbohydr. Polym*. **36**: 151-155.

References

Miyashita, K., Fujii, T., and Saito, A. 2000. Induction and repression of a *Streptomyces lividans* chitinase gene promoter in response to various carbon sources. *Biosci. Biotechnol. Biochem*. **64**: 39-43.

Mizuochi, T., and Nakata, M. 1999. HIV infection and oligosaccharides: A novel approach to preventing HIV infection and the onset of AIDS. *J. Infect. Chemother*. **5**: 190-195.

Monreal, J. and Reese, E. 1969. The chitinase of *Serratia marcescens. Can. J. Microbiol*. **15**: 689-696.

Morimoto, K., Kimura, T., Sakka, K., and Ohmiya, K. 2005. Overexpression of a hydrogenase gene in *Clostridium paraputrificum* to enhance hydrogen gas production. *FEMS Microbiol. Lett*. **246**: 229-234.

Moser, F., Irwin, D., Chen, S., and Wilson, D.B. 2008. Regulation and characterization of *Thermobifida fusca* carbohydrate-binding module proteins E7 and E8. *Biotechnol. Bioeng.* **100**: 1066-1077.

Muzzarelli, R.A.A. 2010. Chitins and chitosans as immunoadjuvants and non-allergenic drug carriers. *Mar. Drugs.* **8**: 292-312.

Nakatani, H., and Monte, C. 2002. Simulation of hyaluronidase reaction involving hydrolysis, transglycosylation and condensation. *Biochem. J*. **365:** 701-705.

Neeraja, Ch., Anil, K., Purushotham P., Suma, K., Sarma, P., Moerschbacher, B.M., and Podile, A.R. 2010. Biotechnological approaches to develop bacterial chitinases as a bioshield against fungal diseases of plants. *Crit. Rev. Biotechnol*. **30**: 231-241.

Ngo, D.N., Lee, S.H., Kim, M.M., and Kim, S.K. 2009. Production of chitin oligosaccharides with different molecular weights and their antioxidant effect in RAW 264.7 cells. *J. Funct. Foods*. **1**: 188-198.

Ni, X., and Westpheling J. 1997. Direct repeat sequences in the *Streptomyces* chitinase-63 promoter direct both glucose repression and chitin induction. *Proc. Natl. Acad. Sci U.S.A* . **94**: 13116-13121.

Ohnuma, T., Numata, T., Osawa, T., Mizuhara, M., Lampela, O., Juffer, A.H., Skriver, K., and Fukamizo, T. 2011a. A class V chitinase from *Arabidopsis thaliana*: gene responses, enzymatic properties, and crystallographic analysis. *Planta*. **234**:123-137.

References

Ohnuma, T., Numata, T., Osawa, T., Mizuhara, M., Vårum, K., and Fukamizo, T. 2011b. Crystal structure and mode of action of a class V chitinase from *Nicotiana tabacum*. *Plant Mol. Biol*. **75**: 291-304.

Okada, M., Matsumura, M., and Shibuya, N. 2001. Identification of a high-affinity binding protein for N-acetylchitooligosaccharide elicitor in theplasma membrane from rice leaf and root cells. *J. Pl. Physiol*. **158**: 121-124.

Okafo, G., Langridge, J., North, S., Organ, A., West, A., Morris, M., and Camilleri, P. 1997. High performance liquid chromatographic analysis of complex N-linked glycans derivatized with 2-aminoacridone. *Anal. Chem*. **69**: 4985-4993.

Okamoto, Y., Yano, R., Miyatake, K., Tomohiro, I., Shigemasa, Y., and Minami, S. 2003. Effects of chitin and chitosan on blood coagulation. *Carbohydr. Polym*. **53**: 337-342.

Omura, S., Arai N., Yamaguchi, Y., Masuma, R., Iwai, Y., Namikashi, M., Turberg, A., Kolbl, H., and Shiomi, K. 2000. Argifin, a new chitinase inhibitor, produced by *Gliocladium* sp. FDD-0668, I. Taxonomy fermentation and biological activities. *J. Antibiot*. **53**: 603-608

Orikoshi, H., Nakayama, S., Hanato, C., Miyamoto, S., and Tsujibo, H. 2005a. Role of the N-terminal polycystic kidney disease domain in chitin degradation by chitinase A from a marine bacterium, *Alteromonas* sp. strain O-7. *J. Appl. Microbiol*. **99:** 551-557.

Orikoshi, H., Nakayama, S., Miyamoto, K., Hanato, C., Yasuda, M., Inamori, Y., and Tsujibo, H. 2005b. Roles of four chitinases (ChiA, ChiB, ChiC, and ChiD) in the chitin degradation system of marine bacterium *Alteromonas* sp. Strain O-7. *Appl. Environ. Microbiol*. **71**: 1811-1815.

Pace, C.N., Vajdos, F., Fee, L., Grimsley, G., and Gray, T. 1995. How to measure and predict the molar absorption coefficient of a protein? *Protein Sci.* **4**: 2411-2423.

Papanikolau, Y., Prag, G., Tavlas, G., Vorgias, C.E., Oppenheim, A.B., and Petratos, K. 2001. High resolution structural analyses of mutant chitinase A complexes with substrates provide new insight into the mechanism of catalysis. *Biochemistry*. **40:** 11338-11343.

Peiselt da Silva, K.M., and Pais da silva, M.I. 2004. Copper sorption from diesel oil on chitin and chitosan polymers. *Colloids. Surf. A.* **237**: 15-21.

References

Perrakis, A., Tews, I., Dauter, Z., Oppenheim, A.B., Chet, I.,Wilson, K.S., and Vorgias, C.E. 1994. Crystal structure of a bacterial chitinase at 2.3 Å resolution. *Structure*. **2**: 1169-1180.

Perugino, G., Trincone, A., Rossi, M., and Moracci, M. 2004. Oligosaccharide synthesis by glycosynthases. *Trends Biotechnol*. **22:** 31-37.

Price, N.P.J., and Naumann, T.A. 2011. A high-throughput MALDI-TOF mass spectrometry-based assay of chitinase activity. *Anal. Biochem*. 411: 94-99.

Rao F.V., Andersen, O.A., Vora, K.A., De Martino, J.A., and van Aalten. D.M. 2005. Methylxanthine drugs are chitinase inhibitors: Investigation of inhibition and binding modes. *Chem. Biol.* **12**: 973-980.

Razdan, A., and Pettersson, D. 1994. Effect of chitin and chitosan on nutrient digestibility and plasma lipid concentrations in broiler chickens. *Br. J. Nutr*. **72**: 277-288.

Rinaudo, M. 2006. Chitin and chitosan: Properties and applications. *Prog. Polym. Sci*. **31:** 603-632.

Rouvinen, J., Bergfors,T., Teeri ,T., Knowles, J.K., and Jones, T.A. 1990. Three-dimensional structure of cellobiohydrolase II from *Trichoderma reesei*. *Science*. **249:** 380-386.

Saito, A., Fujii, T., and Miyashita, K. 2003. Distribution and evolution of chitinase genes in *Streptomyces* species. involvement of gene-duplication and domain-deletion. *Antonie Van Leeuwenhoek*. **84**: 7-15.

Saito, A., Fujii, T., Yoneyama, T., and Miyashita, K. 1998. glkA is involved in glucose repression of chitinase production in *Streptomyces lividans*. *J. Bacteriol*. **180**: 2911-2914.

Saito, A., Ishizaka, M., Francisco, P.B., Fujii, T., and Miyashita, K. 2000. Transcriptional co-regulation of five chitinase genes scattered on the *Streptomyces coelicolor* A3 (2) chromosome. *Microbiology*. **146**: 2937-2946.

Saito, A., Miyashita, K., Biukovic, G., and Schrempf, H. 2001. Characteristics of a *Streptomyces coelicolor* A3(2) extracellular protein targeting chitin and chitosan. *Appl. Environ. Microbiol*. **67**: 1268-1273.

Sakaguchi, T., Horikoshi, T., and Nakajima, A. 1981. Adsorption of uranium by chitin phosphate and chitosan phosphate. *Agric. Biol. Chem*. **45**: 2191-2195.

References

Sambrook, J., and Russell, D.W. 2001. *Molecular Cloning: A Laboratory Manual*. Painview, NY: Cold Spring Harbor Laboratory Press.

Painview, NY: Cold Spring Harbor Laboratory Press.Sampei, Z., Nagao, Y., Fukazawa, T., Fukagawa, S., Matsuo, T., Endo, K., Yatsunami, R., and Nakamura, S., 2004. Gene cloning and deletion analysis of chitinase J from alkaliphilic *Bacillus* sp. strain J813. *Nucleic Acids Symp. Ser*. **48:** 167-168.

Sasaki, C., Yokoyama, A., Itoh, Y., Hashimoto, M., Watanabe, T., and Fukamizo, T. 2002. Comparative study of the reaction mechanism of family 18 chitinases from plants and microbes. *J. Biochem*. **131**: 557-564.

Schnellmann, J., Zeltins, A., Blaak, H., and Schrempf, H. 1994. The novel lectin-like protein CHB1 is encoded by a chitin-inducible *Streptomyces olivaceoviridis* gene and binds specifically to crystalline alpha-chitin of fungi and other organisms. *Mol. Microbiol*. **13**: 807-819.

Schrempf, H. 2001. Recognition and degradation of chitin by *Streptomycetes*. *Antonie Van Leeuwenhoek*. **79**: 285-289.

Seidl, V., Huemer, B., Seiboth, B., and Kubicek, C.P., 2005. A complete survey of *Trichoderma* chitinases reveals three distinct subgroups of family 18 chitinases. *FEBS J*. **272**: 5923-5939.

Shaikh, F. A., and Withers, S. G. 2008. Teaching old enzymes new tricks: engineering and evolution of glycosdiases and glycosyl transferase for improved glycoside synthesis. *Biochem. Cell Biol*. **86:** 169-177.

Shen, K.T., Chen, M.H., Chan, H.Y., Jeng, J.H., and Wang, Y.J. 2009. Inhibitory effects of chitooligosaccharides on tumor growth and metastasis. *Food Chem. Toxicol*. **47**: 1864-1871.

Songsiriritthigul, C., Lapboonrueng, S., Pechsrichuang, P., Pesatcha, P., and Yamabhai, M. 2010. Expression and characterization of *Bacillus licheniformis* chitinase (ChiA), suitable for bioconversion of chitin waste. *Bioresour. Technol*. **101:** 4096-4103.

Sørbotten, A., Horn, S.J., Eijsink, V.G., and Vårum, K.M. 2005. Degradation of chitosans with chitinase B from *Serratia marcescens*. Production of chito-oligosaccharides and insight into enzyme processivity. *FEBS J*. **272**: 538-549.

References

Suetake, T., Tsuda, S., Kawabata, S., Miura, K., Iwanaga, S., Hikichi, K., Nitta, K., and Kawano, K. 2000. Chitin-binding proteins in invertebrates and plants comprise a common chitin-binding structural motif. *J. Biol. Chem*. **275:** 17929-17932.

Suginta , W., Vongsuwan, A., Songsiriritthigul, C., Svasti, J., and Prinz, H. 2005. Enzymatic properties of wild-type and active site mutants of chitinase A from *Vibrio carchariae*, as revealed by HPLC-MS. *FEBS J*. **272:** 3376-3386.

Suginta, W., Chuenark, D., Mizuhara, M., and Fukamizo, T. 2010. Novel *β-N*-acetylglucosaminidases from *Vibrio harveyi* 650: Cloning, expression, enzymatic properties, and subsite identification. *BMC Biochemistry*. **11:** 40-51.

Suzuki, K., Sugawara, N., Suzuki, M., Uchiyama, T., Katouno, F., Nikaidou, N., and Watanabe, T. 2002. Chitinases A, B, and C1 of *Serratia marcescens* 2170 produced by recombinant *Escherichia coli*: enzymatic properties and synergism on chitin degradation. *Biosci. Biotechnol. Biochem*. **66:** 1075-1083.

Suzuki, K., Suzuki, M., Taiyoji, M., Nikaidou, N., and Watanabe, T. 1998. Chitin binding protein (CBP21) in the culture supernatant of *Serratia marcescens* 2170. *Biosci. Biotechnol. Biochem*. **62**: 128-135.

Suzuki, K., Taiyoji, M., Sugawara, N., Nikaidou, N., Henrissat, B., and Watanabe, T. 1999. The third chitinase gene (chiC) of *Serratia marcescens* 2170 and the relationship of its product to other bacterial chitinases. *Biochem. J*. **343:** 587-596.

Suzuki, K., Uchiyama, T., Suzuki,M., Nikaidou, N., Regue, M., and Watanabe, T. 2001. LysR-type transcriptional regulator ChiR is essential for production of all chitinases and a chitin-binding protein, CBP21, in *Serratia marcescens* 2170. **65:** 338-347.

Synstad, B., Gåseidnes, S., Van Aalten, D. M. F., Vriend, G., Nielsen, J. E., and Eijsink, V.G.H. 2004. Mutational and computational analysis of the role of conserved residues in the active site of a family 18 Chitinase. *FEBS J*. **271**: 253-262.

Tabudravu, J.N., Eijsink, V.A., Gooday, G.W., Jaspar, M., Komander, D., Legg, M., Synstad, B., and van Aalten, D.M., 2002. Psammaplin A, a chitinase inhibitor isolated from the Fijian marine sponge *Aplysinella rhax*. *Bioorg. Med. Chem*. **10**: 1123-1128.

References

Taghavi, S., Garafola, C., Monchy, S., Newman, L., Hoffman, A., Weyens, N., Barac, T., Vangronsveld, J., and van der Lelie1, D. 2009. Genome survey and characterization of endophytic bacteria exhibiting a beneficial effect on growth and development of poplar trees. *Appl. Environ. Microbiol*. **75:** 748-757.

Taira, T., Fujiwara, M., Dennhart, N., Hayashi, H., Onaga, S., Ohnuma, T., Letzel, T., Sakuda, S., and Fukamizo, T. 2010. Transglycosylation reaction catalyzed by a class V Chitinase from cycad, *Cycas revoluta*: A study involving site-directed mutagenesis, HPLC, and real-time ESI-MS. *Biochim. Biophys. Acta*. **1804**: 668-675.

Taira, T., Hayashi, H., Tajiri, Y., Onaga, S., Uechi, G., Taira, T., Hayashi, H., Tajiri, Y., Onaga, S., Uechi, G., Iwasaki, H., Ohnuma, T., and Fukamizo, T. 2009. A plant class V chitinase from a cycad (*Cycas revoluta*): biochemical characterization, cDNA isolation, and posttranslational modification. *Glycobiology*. **19:**1452-1461.

Tantimavanich, S., Pantuwatana, S., Bhumiratana, A., and Panbangred, W. 1998. Multiple chitinase enzymes from a single gene of *Bacillus licheniformis* TP-1. *J. Ferment. Bioeng*. **85:** 259-265.

Terwisscha van Scheltinga, A.C., Armand, S., Kalk, K.H., Isogai, A., Henrissat, B., and Dijkstra, B.W. 1995. Stereochemistry of chitin hydrolysis by a plant chitinase/lysozyme and X-ray structure of a complex with allosamidin: evidence for substrate assisted catalysis. *Biochemistry*. **34**: 15619-15623.

Terwisscha van Scheltinga, A.C., Hennig, M., and Dijkstra, B.W. 1996. The 1.8 Å resolution structure of hevamine, a plant chitinase/lysozyme, and analysis of the conserved sequence and structure motifs of glycosyl hydrolase family 18. *J. Mol. Biol*. **262**: 243-257.

Terwisscha van Scheltinga, A.C., Kalk, K.H., Beintema, J.J., and Dijkstra, B.W. 1994. Crystal structures of hevamine, a plant defence protein with chitinase and lysozyme activity, and its complex with an inhibitor. *Structure*. **2:** 1181-1189.

Tews, I., Scheltinga, A.C., Terwisscha, V., Perrakis, A., Wilson, K.S., and Dijkstra, B.W. 1997. Substrate-assisted catalysis unifies two families of chitinolytic enzymes. *J. Am. Chem. Soc*. **119**: 7954-7959.

Tharanathan, R. N., and Kittur, F. S. 2003. Chitin -The undisputed biomolecule of great potential. *Crit. Rev. Food. Sci. Nutr*. **43**: 61-87.

References

Uchiyama, T., Katouno, F., Nikaidou, N., Nonaka, T., Sugiyama, J., and Watanabe, T. 2001. Roles of the exposed aromatic residues in crystalline chitin hydrolysis by chitinase A from *Serratia marcescens* 2170. *J. Biol. Chem*. **276**: 41343-41349.

Umekawa, M., Huang, W., Li, B., Fujita, K., Ashida, H., Wang, L. X., and Yamamoto, K. 2008. Mutants of *Mucor hiemalis* Endo-β-N-acetylglucosaminidase show enhanced transglycosylation and glyco-synthase-like activities. *J. Biol. Chem*. **283**: 4469-4479.

Usui, T., Matsui, H., and Isobe, K. 1990. Enzymic synthesis of chitooligosaccharides utilizing transglycosylation by chitinolytic enzymes in a buffer containing ammonium sulfate. *Carbohydr. Res*. **203**: 65-77.

Vaaje-Kolstad, G., Bunæs, A.C., Mathiesen, G., and Eijsink, V.G. H. 2009. The chitinolytic system of *Lactococcus lactis* ssp. *Lactis* comprises a nonprocessive chitinase and a chitin-binding protein that promotes the degradation of α- and β-chitin. *FEBS J*. **276**: 2402-2415.

Vaaje-Kolstad, G., Horn, S.J., van Aalten, D.M., Synstad, B., and Eijsink, V.G. 2005a. The non-catalytic chitin-binding protein CBP21 from *Serratia marcescens* is essential for chitin degradation. *J. Biol.Chem*. **280**: 28492-28497.

Vaaje-Kolstad, G., Houston, D.R., Riemen, A.H., Eijsink, V.G.H and van Aalten, D.M., 2005b. Crystal structure and binding properties of the *Serratia marcescens* chitin binding protein CBP21. *J. Biol. Chem*. **280**: 11313–11319.

Vaaje-Kolstad, G., Vasella, A., Peter, M.G., Netter, C., Houston, D.R., Westereng, B., Synstad, B., Eijsink, V.G., and van Aalten, D.M. 2004. Interactions of a family 18 chitinase with the designed inhibitor Hm508 and its degradation product, chitobiono-δ-lactone. *J. Biol Chem*. **279**: 3612-3619.

Vaaje-Kolstad, G., Westereng, B., Horn, S.J., Liu, Z., Zhai, H., Sørlie, M., and Eijsink, G.V.H. 2010. An oxidative enzyme boosting the enzymatic conversion of recalcitrant polysaccharides. *Science*. **330:** 219-222.

van Aalten, D. M. F., Komander, D., Synstad, B., Gåseidnes, S., Peter, M. G., and Eijsink, V. G. H. 2001. Structural insights into the catalytic mechanism of a family 18 exo-Chitinase. *Proc. Natl. Acad. Sci.U.S.A*. **98**: 8979-8984.

References

van Aalten, D. M. F., Synstad, B., Brurberg, M. B., Hough, E., Riise, B. W., Eijsink, V. G. H., and Wierenga, R. K. 2000. Structure of a two-domain chitotriosidase from *Serratia marcescens* at 1.9-Å resolution. *Proc. Natl. Acad. Sci. U. S. A.* **97**: 5842–5847.

van Scheltinga, A.C.T., Kalk, K.H., Beintema, J.J., and Dijkstra, B.W.1994. Crystal-structures of hevamine, a plant defense protein with chitinase and lysozyme activity, and its complex with an inhibitor. *Structure*. **2:** 1181-1189.

Varrot, A., Frandsen, T. P., von Ossowski, I., Boyer, V., Cottaz, S., Driguez, H., Schulein, M., and Davies, G. J. 2003. Structural basis for ligand binding and processivity in cellobiohydrolase cel6a from humicola insolens. *Structure*. **11:** 855-864.

Vocadlo, D.J., Davies, G.J., Laine, R., and Withers, S.G. 2001. Catalysis by hen egg-white lysozyme proceeds *via* a covalent intermediate. *Nature*. **412**: 835-838.

Wang, S.L., Lin, H.T., Liang, T.W., Chen, Y.J., Yen, Y.H., and Guo, S.P. 2008. Reclamation of chitinous materials by bromelain for the preparation of antitumor and antifungal materials. *Bioresour. Technol*. **99**: 4386-4393.

Watanabe, T., Ito, Y., Yamada, T., Hashimoto, M., Sekine, S., and Tanaka, H. 1994. The roles of C-terminal domain and type III domains of chitinase A1 from *Bacillus circulans* WL-12 in chitin degradation. *J. Bacteriol*. **176:** 4465-4472.

Watanabe, T., Kimura, K., Sumiya, T., Nikaidou, N., Suzuki, K., Suzuki, M., Taiyoji, M., Ferrer, S. and Regue, M. 1997. Genetic analysis of the chitinase system of *Serratia marcescens* 2170. *J. Bacteriol*. **179**: 7111-7117.

Watanabe, T., Oyanagi, W., Suzuki, K., and Tanaka, H.1990. Chitinase system of *Bacillus circulans* WL-12 and importance of chitinase A1 in chitin degradation. *J Bacteriol*. **172:** 4017-4022.

Williams, S. J., and Withers, S. G. 2000. Glycosyl fluorides in enzymatic reactions. *Carbohydr. Res*. **327**: 27-46.

Xia, G., Jin, C., Zhou, J., Yang, S., Zhang, S., and Jin, C. 2001. A novel chitinase having a unique mode of action from *Aspergillus fumigatus* YJ-407. *Eur. J. Biochem*. **268:** 4079-4085.

Yamada, H., and Imoto, T. 1981. A convenient synthesis of glycolchitin, a substrate of lysozyme. *Carbohydr. Res*. **92**: 160–162.

References

Yamanoi, T., Tsutsumida, M., Oda, Y., Akaike, E., Osumi, K., Yamamamoto, K., and Fujita, K. 2004. Transglycosylation reaction of *Mucor hiemalis* endo-β-N-acetylglucosaminidase using sugar derivatives modified at C-1 or C-2 as oligosaccharide acceptors. *Carbohydr. Res.* **339**: 1403-1406.

You, Y., Park, W.H., Ko, B.M., and Min, B.M. 2004. Effects of PVA sponge containing chitooligosaccharide in the early stage of wound healing. *J. Mater. Sci. Mater. Med.* **15**: 297-301.

Zakariassen, H., Aam, B.B.,Horn, S.J., Vårum, K.M., Sørlie, M., and Eijsink, V.G. 2009, Aromatic residues in the catalytic center of chitinase A from *Serratia marcescens* affect processivity, enzyme activity, and biomass converting efficiency. *J. Biol. Chem.* **284**: 10610-10617.

Zakariassen, H., Hansen, M.C., Jøranli, M., Eijsink, G. H.V., and Sørlie, M. 2011. Mutational effects on transglycosylating activity of family 18 chitinases and construction of a hypertransglycosylating mutant. *Biochemistry*. **50**: 5693-5703.

Zeltins, A., and Schrempf, H. 1997. Specific interaction of the *Streptomyces* chitin-binding protein CHB1 with alpha-chitin - the role of individual tryptophan residues. *Eur. J. Biochem* **246:** 557-564.

Zhao, Y., Chen, G., Sun, M., Jin, Z., and Gao, C. 2006. Study on preparation of the pH sensitive hydroxyethyl chitin/poly (acrylic acid) hydrogel and its drug release property. *Sheng Wu Yi Xue Gong Cheng Xue Za Zhi*. **23**: 338-341.